Grain weight retention during terminal heat stress in hard winter wheat

by

Nicholas J. Schuh

B.S., Iowa State University, 2018

A THESIS

submitted in partial fulfillment of the requirements for the degree

MASTER OF SCIENCE

Department of Agronomy
College of Agriculture

KANSAS STATE UNIVERSITY
Manhattan, Kansas

2024

Approved by:

Co-Major Professor
Mary J. Guttieri

Approved by:

Co-Major Professor
Allan Fritz

Copyright

Abstract

Climate-resilient wheat cultivars with tolerance to high temperatures after flowering are essential to reliable wheat production in the central and southern Great Plains. Breeders have an experiential understanding of germplasm capable of maintaining test weight under terminal heat stress, yet understanding of underlying genetics is limited. In a preliminary greenhouse/growth chamber experiment to identify post-anthesis heat stress tolerance genetic resources within central and southern Great Planes germplasm, two breeding lines were identified with contrasting tolerance phenotypes: HV9W03-1596R maintained green leaf area, and TX04M410164 maintained grain weight under post-anthesis heat stress. A recombinant inbred population (208 lines) was developed from the progeny of crossing these two lines and grown in ten Kansas field environments. Traits measured were yield, plant height, flowering time, physiological maturity time, grain fill period, test weight, kernel diameter, kernel weight, and kernel hardness. Yield, plant height, flowering time, test weight, kernel diameter, and kernel weight were all found to be highly heritable. In the 2018 field season, average high temperature during the 21 days following anthesis at three trial locations was 29.1°C to 30.4°C, while the optimal temperature for wheat grain filling is reported to be 21.3°C. In three 2018 trial locations, mean test weight ranged from 652 to 758 g L^{-1}, and mean kernel weight ranged from 19.8 to 23.5 mg. In contrast, in three 2020 trial locations, mean test weight ranged from 745 to 830 g L^{-1}, and mean kernel weight ranged from 26.5 to 30.9 mg. Stress sensitivity indices (SSIs) were calculated at seven trials, using three highest yielding trials as the control environment. The SSIs for flowering time and physiological maturity had very little variation under an extreme stress environment and high variation under a moderately stressful environment. We observed the same phenomena in yield and kernel diameter SSIs. Two quantitative trait loci were found on chromosome 1B in a preliminary analysis, and SNP markers were developed. One SNP was significant for kernel diameter, kernel hardness, kernel weight, test weight, grain yield, plant height, and grain fill period length and the other was significant for kernel hardness, test weight, grain yield, plant height, and grain fill period length best linear unbiased predictors. One SNP was significant for kernel diameter and test weight stress sensitivity, and the second SNP was significant for kernel weight, grain fill period, and physiological maturity stress sensitivity. The RIL population also was segregating for the *Ppd-D1* and *Vrn-D3* genes that affect flowering

time. These flowering time genes had significant effects on stress sensitivity. Future work will isolate near isogenic lines from RILs heterozygous at one or both of the 1B regions. These lines will be evaluated for heat tolerance in controlled environments and field environments to quantify the effects of these regions on post anthesis heat stress tolerance.

Table of Contents

List of Figures

List of Tables

Chapter 1 - Literature Review

History and Importance of Wheat

Origin and Domestication

Wheat (*Triticum aestivum* L.) originated in the Tigris and Euphrates river valley, near what is present day Iraq and was domesticated around 10,000 years ago (Eckardt, 2010; U.S. National Association of Wheat Growers, 2019). *Triticum urartu* (genome A^uA^u) is thought to have originated from Einkorn (*Triticum monococcum boeoticum*, genome A^mA^m) in the mountains of southeast Turkey somewhere between 8,000 to 10,000 years ago (Heun et al., 1997). *Triticum urartu* hybridized with an extinct species most closely related to *Aegilops speltoides* (genome SS) to form *Triticum turgidum* ssp. *dicoccoides* (genome AABB)(Dvorak & Akhunov, 2005; Huang et al., 2002). According to genetic studies, domesticated AABB wheats (*Triticum dicoccum*) are most closely related to wild populations from the mountains in southeast Turkey (*Triticum dicoccoides*) (Özkan, Brandolini, Schäfer-Pregl, & Salamini, 2002). Wild emmer (*Triticum turgidum ssp. dicoccoides*, genome AABB) was domesticated by human selection to create free threshing domesticated emmer wheat (*Triticum turgidum ssp. dicoccum*, genome AABB). Domesticated emmer hybridized with a wild goatgrass species (*Aegilops tauschii*, genome DD) to form the commonly grown hexaploid bread wheat (*Triticum aestivum*, genome AABBDD)(Avni et al., 2017; Heun et al., 1997). Since the creation of hexaploid bread wheat, its cultivation has spread around the globe and is one of the most important crops grown today.

Importance

In 2019, the world produced 765,769,635 tonnes of wheat with 52,257,620 tonnes produced by The United States of America (FAOSTAT, 2021). The world population is expected

to grow to about 10 billion by the year 2050 (Food and Agriculture Organization of the United Nations, 2017). This is almost a 2 billion person increase from today's population (United Nations, 2021). Being the third most important crop in terms of global production (Shewry & Hey, 2015), wheat production will have to increase by 388 million tons/year (i.e., an increase of 1.5% more per year than the current rate of 0.9% per year) to meet the 2050 population calorie demand for wheat (Ray et al, 2013). The United Nations' Sustainable Development Goal 2 is aimed to "End hunger, achieve food security and improved nutrition and promote sustainable agriculture", and one of the steps to achieve this goal is stated in Goal 2.4; to "ensure sustainable food production systems and implement resilient agricultural practices… that strengthen capacity for adaptation to climate change, extreme weather, drought, flooding and other disasters…" by 2030 (UNIDO, 2018). Hard red winter wheat yields in the United States have stagnated since 2000 increasing only 0.008076 tons per hectare per year on average (Grassini et al, 2013; Patrignani et al, 2014). In addition to yield stagnation, wheat yields are trending more variable year to year than they were before 2000 (USDA ERS - Wheat Data, 2024). This condition of stagnant and variable yields seems more prevalent in the US Great Plains, a region where there has not been much yield improvement in varieties released in the early 2000's (Grassini et al., 2013; Graybosch & Peterson, 2010). One solution is to breed wheat that is more consistently high yielding in the current and future climate of the central Great Plains.

Climate Change and Wheat Production

The climate in the Great Plains of the United States challenges the stability of crop production. Naturally, this region is characterized by semi-arid climate in the west to sub-humid in the east (Sciarresi et al., 2019), with rainfall gradients of 400 to 1200 mm and elevation ranges from 300 to 1200 m (Lollato et al., 2020). Additionally, the weather in this region is becoming

more variable with more extreme weather events trending into the future ("Kansas Mesonet, 2017: Kansas Mesonet Historical Data," 2023). For example, the occurrence of 10 hours of compound hot-dry-windy events that are prevalent in the US Great Plains can account for 4% wheat yield loss, and the frequency of these events has been increasing in as much as 8 hours per decade in parts of the region (Zhao et al., 2022). According to the National Association of Wheat Growers, the Central and Southern Great Plains grow the most wheat area (6,902,727 hectares in 2017) out of all the growing regions in the United States (NAWG, 2024). Kansas consistently plants the most acres (3.3 million hectares in 2023) of wheat in the United States every year and produces the most winter wheat (5.5 million metric tons in 2023) every year (USDA-NASS, 2023). In 2018, Kansas had one of the hottest, driest growing seasons on record. Yet 2019 was one of the coolest and wettest growing seasons on record ("Kansas Mesonet, 2017: Kansas Mesonet Historical Data," n.d.). This highly variable climate makes selecting improved wheat varieties very difficult. From 1980-2003, there were 58 extreme weather events that have caused over one billion dollars worth in damages in the United States (Ross, Lott, & Center, 2003). Ten major (greater than one billion dollars in damages) droughts/heatwaves occurred in the United States from 1980-2002 and account for the largest percentage of weather-related monetary loss within that time. Reynolds et al., (2016) defined heat stress as "Supra-optimal temperatures occurring at any plant growth stage that can result in >=10% yield loss." In a comprehensive summary of the available literature on temperature stress for wheat, Porter & Gawith, (1999) suggested that the lethal level of heat for a wheat plant is 47.5°C, the optimum temperature for anthesis is 21°C with the maximum temperature being 31°C, the optimum temperature for grain filling is 20.7°C with the maximum temperature being 35.4°C. The reproductive stage is more sensitive to heat stress than the vegetative stage in wheat when looking at all available literature.

In Kansas, Tack, Barkley, & Nalley (2015) found that the largest associations to yield loss in wheat are freezing temperatures in the fall and extreme heat in the spring. They also found that when there are temperatures above 34°C in the spring, there are large negative yield effects on Kansas winter wheat, and the more recently released varieties are less heat tolerant than older wheat varieties for Kansas. This is hypothesized to be because newer wheat varieties in Kansas have longer grain fill periods than the older Kansas varieties and thus present a larger window for post-anthesis heat stress to damage plant yield components (Tack et al., 2015). Simulations using weather data from 1985 to 2011 in Kansas have demonstrated that a 1°C increase in average temperature throughout the growing season is associated with a wheat yield reduction of 21% (Barkley et al., 2014). Likewise, simulation of wheat yield in the US Great Plains during the 1986-2016 time frame suggested that heat stress during the reproductive stages can account for as much as 12% of the variability of simulated wheat yields (Lollato, Edwards, & Ochsner, 2017). It is clear that the environment and extreme weather events such as prolonged heat stress can severely reduce wheat yield (Barkley et al., 2014), and models have linked a 5.5% reduction in global wheat production to weather trends (relative to a counterfactual without climate trend) from 1980 to 2008 (Lobell, Schlenker, & Costa-Roberts, 2011).

Physiology of Heat and Drought Stress

Heat Stress on the Pre-Flowering and Anthesis Stages

Temperature modulates wheat development through three important related mechanisms: (i) growth rate, (ii) duration of important developmental periods, and (iii) reproductive allocation (Sadras et al., 2022). Heat stress can increase growth rates, hastening the conclusion of the vegetative stages and prompt an early reproductive stage, and reduce allocation of resources to the developing grain. Grain number is the most important yield-driving factor for wheat, and

grain weight is a finer modulator of wheat yield (Slafer et al., 2022; Slafer et al., 2014). Grain number is determined during the critical period for yield determination (20 days pre-anthesis to 10 days post-anthesis; (Fischer, 1985)) and grain weight is determined between booting and maturity (Calderini et al., 2001).

Although grain weight yield modulation is modest as compared to grain number across environments and genotypes (Slafer et al., 2022, 2014), increases in grain weight within an environment either as a function of genotype or management can significantly increase grain yield (Jaenisch et al., 2022). Grain number and weight are highly influenced by environmental factors such as temperature, moisture, and fertility. In a growth chamber study on "Chinese Spring" wheat, plants were subjected to heat stress (36/26°C day/night temperature) at randomly assigned physiological stages (ranging from 15 days before anthesis to 30 days after anthesis) and randomly assigned one of two heat stress durations (five days or two days). Five days of heat stress imposed at ten, five, or zero days before anthesis significantly reduced floret fertility, reducing grain number. Likewise, short exposure (two days) to heat stress "significantly decreased floret fertility when imposed anytime between ten days before anthesis through four days after anthesis" (Prasad & Djanaguiraman, 2014). A greenhouse experiment found that heat stress (glass canopies over pots that kept plants 4-5°C warmer than the ambient temperature and continued through maturity) imposed on the boot and heading stages of wheat resulted in more severe reduction in performance (grain weight, yield, grain number per spike, and water use efficiency) than heat stress imposed at the anthesis and grain filling stages (Nawaz, Farooq, Cheema, & Wahid, 2013).

Heat stress was shown to most negatively affect wheat, a C_3 grass crop adapted to cool environments, when the same treatment was compared to rice (*Oryza sativa*), a C_3 grass crop

adapted to warm environments or millet (*Pennisetum glaucum*), a C_4 grass crop adapted to hot environments. The extreme sensitivity of wheat to heat stress may be due to light reactions and damage to photosystem II (Al-Khatib & Paulsen, 1999). Oxidative damage occurs because of the imbalance of photosynthesis and respiration in heat stressed plants (Fitter & Hay, 2002). High temperature was found to limit the rate of photosynthesis. Under high temperatures, mesophyll conductance was less efficient at transferring CO^2 from the intracellular air space to RUBISCO, which resulted in a "very substantial limitation on photosynthesis" (Bernacchi, Portis, Nakano, Von Caemmerer, & Long, 2002). A recombinant inbred line (RIL) population from a cross between "Danbata" (heat resistant) and "Nacozari" (heat susceptible) wheat varieties had a mean yield reduction of 47% in an irrigated Mediterranean climate (heat stress) compared to the same population in a controlled non-heat stress environment (Blum, Klueva, & Nguyen, 2001). Heat stress can cause morphological abnormalities to the reproductive parts of wheat, ultimately decreasing floret fertility and reducing individual kernel weight (Prasad & Djanaguiraman, 2014).

Post Anthesis Heat Stress

Post anthesis heat stress reduces the yield and quality of wheat grain. Growth chamber studies have enabled researchers to apply heat stress at an exact physiological time. Growth chamber controlled heat stress (day/night 35/20°C) on wheat during grain filling (heat stress started 12 days after heading and continued for 15 days) had a substantial influence on the chlorophyll content, antioxidant enzyme activity and yield parameters such as significant reductions in biomass, yield, grain number, harvest index, and thousand kernel weight on the winter wheat RIL population of "Plainsman" and "MV Magma" (Balla et al., 2009). Thousand kernel weight and yield had the greatest change between heat tolerant lines and heat susceptible

lines, and demonstrated a genetic association for thousand kernel weight under post anthesis heat stress conditions (Balla et al., 2009). Even a single day of post-anthesis heat stress significantly reduced grain yield and accelerated flag leaf senescence (A. S. M. H. M. Talukder, et al., 2014). The wheat cultivar "Yecora 70" had a significant reduction in individual kernel weight when 45°C heat stress was applied 30 days after anthesis (Fischer, 1985). Heat stress has been shown to "accelerate leaf senescence during grain filling, leading to reduced photosynthesis and assimilate supply to the developing grains" (Bheemanahalli et al., 2019). Heat stress during reproductive stage negatively affects pollination and gametogenesis and negatively affects starch synthesis and causes a faster senescence in the grain filling stages (Reynolds et al., 2016). Heat stress during the post anthesis and grain filling period limits the amount of photosynthate that is accumulated in the grain (Prasad & Djanaguiraman, 2014). In a field study in Australia, Cossani and Sadras (2021) suggested that elevated temperatures during the critical period not only reduced wheat yield (-530 kg ha °C $^{-1}$), but its impacts interacted with moisture and nitrogen availability. Similarly, a growth chamber experiment showed increased male sterility in wheat when temperatures were 30°C at floret formation (Saini et al., 1984). In terms of grain weight, Dupont et al. (2006) found that wheat grain protein doubled with the addition of post anthesis N, P, K (0.1 g per day of 20, 20, 20 N, P, K liquid fertilizer) under optimal temperatures (24/17°C) but had no significant difference under post-anthesis heat stress conditions (37/28°C) Altenbach et al. (2003) performed growth chamber studies on "Butte 86" spring wheat and found that starch accumulation in the grain ceased much earlier in the high temperature treatments (6 days earlier under 37/17°C, and 16-19 days earlier under 37/28°C treatments). They concluded that the reduction of starch content under high temperatures was the result of an earlier starch accumulation cessation rather than from an inhibition of starch biosynthesis (Altenbach et al.,

2003). Likewise, under both controlled environment chambers and field-based heat tents, Bergkamp et al. (2018) suggested that prominent winter wheat varieties adapted to Kansas differed in their tolerance to heat stress, which reduces yields through lower thousand kernel weight, grain number, and harvest index (Bergkamp et al., 2018).

Drought Stress on Wheat

Drought stress conditions and heat stress conditions often are present at the same time in the Great Plains (Zhao et al., 2022). Drought stress tolerance often is associated with heat stress tolerance. Drought stress resistance strategies can be divided into escape, avoidance, and tolerance (Barnabás et al, 2008; Chaves et al., 2003; Levitt, 1972). Escape is when the plant does not experience high levels of the drought stress because it completes its life cycle before the drought stress occurs. Many wheat cultivars in Kansas are early maturing cultivars and do well because they complete their life cycle before the onset of the mid-summer drought and heat stress, and simulated evidence suggests that a shorter phyllochron, which would result in faster leaf and tillering appearance and shorter maturity, could further benefit yields in this region (Sciarresi et al., 2019). Avoidance involves minimizing water loss by closing stomata and reducing light absorbance, and maximizing water uptake by investing nutrients in root growth (Ehleringer & Dawson, 1992). Both traits (stomatal closure and deeper rooting systems) seem like promising breeding targets in the western portion of the US Great Plains from a modeling perspective (Sciarresi et al., 2019). Plant tolerance is driven by physiological adaptation that allows a plant to survive in a more stressful environment. Tolerance can include smaller plant cells or more ridged cell walls (Morgan, 2003), smaller leaf area, or thicker cuticles. Plant responses to short-term drought stress include stomatal closure, decreased carbon assimilation, multi-stress sensing, inhibition of growth, xylem hydraulic changes, and root osmotic

adjustment. Plant responses to long-term drought stress include shoot growth inhibition, reduced transpiration area, metabolic acclimation, osmotic adjustment to the stressful environment, increased root growth and increased absorption area (Chaves et al., 2003). Winter wheat cultivars adapted to the US Great Plains have varied mechanisms to adapt to drought conditions. For example, although TAM 111 and TAM 112 share similar pedigrees, TAM 112 responds to drought stress with "distinct sink strength, gas exchange, and source sink relationships via robust transcriptomic modifications and elevated ABA content" compared to TAM 111 (Reddy et al., 2014).

Previous Genetic Studies

Heat tolerance in common wheat was demonstrated to be controlled by multiple genes (Yang, Sears, Gill, & Paulsen, 2002). In rice, RNA-sequencing during reproductive heat stress suggested that reduced productivity in heat-susceptible plants may be associated with poor pollen development of poor anther production (González-Schain et al., 2016). In a controlled environment experiment, a wheat RIL population from a cross between "Halberd" (heat tolerant) and "Cutter" (heat susceptible) was subjected to heat stress 10 days after pollination for 3 days in the heat stressed environment (38°C /18°C day/night). QTL for yield components under heat stress and heat susceptibility index were found on chromosomes 1A, 2A, 2B, and 3B. These regions are commonly associated with flag leaf length, width, and visual wax content. This study also validated the use of the main spike for detection of heat tolerance QTL in wheat (Mason et al., 2010). In a RIL population created from "Ventnor" and "Karl 92", heat stress (30/25°C day/night) was applied in a growth chamber study 10 days after anthesis until maturity. Nine QTL for heat tolerance were found on chromosome 2A, two on chromosome 6A, two on chromosome 6B, and one on chromosomes 3A, 3B, and 7A (Vijayalakshmi et al., 2010). In

another growth chamber study, a RIL population of "Ventnor" and "Karl 92" was subjected to heat stress at 36/30°C (day/night) during the post anthesis stage. This study demonstrated that chromosome 2A had a QTL region associated with days to maximum senescence. SPAD chlorophyll content QTLs had been found in the same experiment on chromosome 6A, 7A, 1B, and 1D, and QTL for thylakoid membrane damage also were found on chromosome 6A, 7A, and 1D (S. K. Talukder et al., 2014). A RIL population from the cross "NW1014" by "HUW468" identified QTLs on chromosomes 2B, 7B and 7D of wheat that were associated with heat tolerance (Paliwal et al. 2012). In a growth chamber experiment, susceptible lines showed as much as 85.4% reduction in chlorophyl content after 16 days of post-anthesis heat stress (36°C day, 30°C night temperature), and some heat stress tolerant lines showed as low as 30.6% reduction in the same experiment compared to the control environment group (Fu, Bowden, Jagadish, & Gill, 2023).

Growth chamber experiments do not always translate to field trials. Field trials have more variability and less control over the environmental variables, but are more practical to breeders and producers because the trial environment is the target environment. QTL on chromosome 3B accounted for up to 22% of variance in canopy temperature and grain yield under heat stress field conditions (Bennett et al., 2012). A rye translocation (T1BL.1RS) was associated with moderate drought tolerance and decreased yield while other studies have found T1BL.1RS to increase yield (Villareal et al., 1998). QTL for drought and heat stress in wheat were also found on 1B, 2B, 3B, 4A, 4B, and 7A. They also found a QTL region on chromosome 1B that confer heat and drought stress adaptation by way of a large number of traits (Pinto et al., 2010). QTL associated with flag leaf senescence under heat stress were discovered on chromosome 2D and 2B (Verma et al., 2004). The delayed flag leaf senescence phenotype also is called the "stay green" trait. In

some field trials with spring wheat, stay-green traits have accounted for around 30% of yield variability in populations under heat stress and heat combined with drought stress (Lopes & Reynolds, 2012). Green leaf area and canopy temperature depression were significantly associated with grain yield, grain filling duration, and biomass in field experiments and suggested that the stay green trait can be used as a morphological marker in wheat to screen for heat tolerance (Kumari, et al., 2013).

Conclusions

Post-anthesis heat stress, and its combination with drought stress conditions, is becoming more common in the US Great Plains. When post-anthesis heat stress and/or drought events happen, wheat yields are reduced. The need for wheat is increasing with the global population, and solutions are needed to meet that demand. Previous research has identified many heat tolerance QTLs on 1A, 1B, 1D, 2A, 2B, 2D, 3A, 3B, 4A, 6A, 7A, and 6B. Still, there is an urgent need to identify new genes to be introgressed into wheat cultivars that mitigate the stresses imposed by the variable climate since the gene location and gene action is important for mobilizing a heat or drought tolerant phenotype in elite germplasm. Identifying stable, reliable markers associated with heat or drought tolerance enables breeders to efficiently and accurately screen breeding populations for germplasm that will be more stable in the variable climate of the central and southern great plains. The objectives of this study were to develop the phenotypic data on a population with contrasting heat tolerance. The most important phenotypes needed in wheat are heat stress tolerance and drought stress tolerance. The phenotypic data collected will eventually be used as response variables for mapping QTL associated with heat stress tolerance. The results from these studies help us understand the mechanism of heat tolerance under heat

stress that results in the phenotype of increased test weight and increased individual kernel weight under field conditions.

References

Al-Khatib, K., & Paulsen, G. M. (1999). High-temperature effects on photosynthetic processes in temperate and tropical cereals. *Crop Science*, *39*(1), 119–125. https://doi.org/10.2135/cropsci1999.0011183X003900010019x

Altenbach, S. B., DuPont, F. M., Kothari, K. M., Chan, R., Johnson, E. L., & Lieu, D. (2003). Temperature, water and fertilizer influence the timing of key events during grain development in a US spring wheat. *Journal of Cereal Science*, *37*(1), 9–20. https://doi.org/10.1006/jcrs.2002.0483

Avni, R., Nave, M., Barad, O., Baruch, K., Twardziok, S. O., Gundlach, H., … Distelfeld, A. (2017). Wild emmer genome architecture and diversity elucidate wheat evolution and domestication. *Science*, *357*(6346), 93–97. https://doi.org/10.1126/science.aan0032

Balla, K., Bencze, S., Janda, T., & Veisz, O. (2009). Analysis of heat stress tolerance in winter wheat. https://doi.org/10.1556/AAgr.57.2009.4.6

Barkley, A., Tack, J., Nalley, L. L., Bergtold, J., Bowden, R., & Fritz, A. (2014). Weather, disease, and wheat breeding effects on Kansas wheat varietal yields, 1985 to 2011. *Agronomy Journal*, *106*(1), 227–235. https://doi.org/10.2134/agronj2013.0388

Barnabás, B., Jäger, K., & Fehér, A. (2008). The effect of drought and heat stress on reproductive processes in cereals. *Plant, Cell and Environment*, *31*(1), 11–38. https://doi.org/10.1111/j.1365-3040.2007.01727.x

Bennett, D., Reynolds, M., Mullan, D., Izanloo, A., Kuchel, H., Langridge, P., & Schnurbusch, T. (2012). Detection of two major grain yield QTL in bread wheat (Triticum aestivum L.)

under heat, drought and high yield potential environments. *Theoretical and Applied Genetics*, *125*(7), 1473–1485. https://doi.org/10.1007/s00122-012-1927-2

Bergkamp, B., Impa, S. M., Asebedo, A. R., Fritz, A. K., & Jagadish, S. V. K. (2018). Prominent winter wheat varieties response to post-flowering heat stress under controlled chambers and field based heat tents. *Field Crops Research*, *222*(September 2017), 143–152. https://doi.org/10.1016/j.fcr.2018.03.009

Bernacchi, C. J., Portis, A. R., Nakano, H., Von Caemmerer, S., & Long, S. P. (2002). Temperature response of mesophyll conductance. Implications for the determination of Rubisco enzyme kinetics and for limitations to photosynthesis in vivo. *Plant Physiology*, *130*(4), 1992–1998. https://doi.org/10.1104/pp.008250

Bheemanahalli, R., Sunoj, V. S. J., Saripalli, G., Prasad, P. V. V., Balyan, H. S., Gupta, P. K., … Jagadish, S. V. K. (2019). Quantifying the impact of heat stress on pollen germination, seed set, and grain filling in spring wheat. *Crop Science*, *59*(2), 684–696. https://doi.org/10.2135/cropsci2018.05.0292

Blum, A., Klueva, N., & Nguyen, H. T. (2001). Wheat cellular thermotolerance is related to yield under heat stress. *Euphytica*, *117*(2), 117–123. https://doi.org/10.1023/A:1004083305905

Blum, A., Shpiler, L., Golan, G., & Mayer, J. (1989). Yield stability and canopy temperature of wheat genotypes under drought-stress. *Field Crops Research*, *22*(4), 289–296. https://doi.org/10.1016/0378-4290(89)90028-2

Borrás, L., Slafer, G. A., & Otegui, M. E. (2004). Seed dry weight response to source-sink manipulations in wheat, maize and soybean: A quantitative reappraisal. *Field Crops Research*, *86*(2–3), 131–146. https://doi.org/10.1016/j.fcr.2003.08.002

Calderini, D. F., Savin, R., Abeledo, L. G., Reynolds, M. P., & Slafer, G. A. (2001). The importance of the period immediately preceding anthesis for grain weight determination in wheat. *Euphytica*, *119*(1–2), 199–204. https://doi.org/10.1023/A:1017597923568

Chaves, M. M., Maroco, J. P., & Pereira, J. S. (2003). Understanding plant responses to drought - From genes to the whole plant. *Functional Plant Biology*, Vol. 30, pp. 239–264. https://doi.org/10.1071/FP02076

Chen, Y., Carver, B. F., Wang, S., Cao, S., & Yan, L. (2010). Genetic regulation of developmental phases in winter wheat. *Molecular Breeding*, *26*(4), 573–582. https://doi.org/10.1007/s11032-010-9392-6

Cruppe, G., DeWolf, E., Jaenisch, B. R., Andersen Onofre, K., Valent, B., Fritz, A. K., & Lollato, R. P. (2021). Experimental and producer-reported data quantify the value of foliar fungicide to winter wheat and its dependency on genotype and environment in the U.S. central Great Plains. *Field Crops Research*, *273*. https://doi.org/10.1016/J.FCR.2021.108300

Dvorak, J., & Akhunov, E. D. (2005). Tempos of gene locus deletions and duplications and their relationship to recombination rate during diploid and polyploid evolution in the Aegilops-Triticum alliance. *Genetics*, *171*(1), 323–332. https://doi.org/10.1534/genetics.105.041632

Eckardt, N. A. (2010). Evolution of domesticated bread wheat. *Plant Cell*, *22*(4), 993. https://doi.org/10.1105/tpc.110.220410

Ehleringer, J. R., & Dawson, T. E. (1992, December 1). Water uptake by plants: perspectives from stable isotope composition. *Plant, Cell & Environment*, Vol. 15, pp. 1073–1082. https://doi.org/10.1111/j.1365-3040.1992.tb01657.x

FAOSTAT. (2021). Retrieved February 16, 2021, from http://www.fao.org/faostat/en/#data/QC

Fischer, R. A. (1985). Number of kernels in wheat crops and the influence of solar radiation and temperature. *The Journal of Agricultural Science*, *105*(2), 447–461. https://doi.org/10.1017/S0021859600056495

Fischer, R. A., & Maurer, R. (1978). Drought resistance in spring wheat cultivars. I. Grain yield responses. *Australian Journal of Agricultural Research*, *29*(5), 897–912. https://doi.org/10.1071/AR9780897

Fitter, A., & Hay, R. K. M. (2002). *Environmental physiology of plants*. 367.

Food and Agriculture Organization of the United Nations. (2017). The Future of Food and Agriculture. *Food and Agriculture Organization of the United Nations*, (November), 1–52.

Fu, J., Bowden, R. L., Jagadish, S. V. K., & Gill, B. S. (2023). Genetic variation for terminal heat stress tolerance in winter wheat. *Crop Science*, *57*(5), 2626–2632. https://doi.org/10.2135/cropsci2016.12.0978

Giordano, N., Sadras, V. O., Correndo, A. A., & Lollato, R. P. (2024). Cultivar-specific phenotypic plasticity of yield and grain protein concentration in response to nitrogen in winter wheat. *Field Crops Research*, *306*, 109202. https://doi.org/10.1016/J.FCR.2023.109202

González-Schain, N., Dreni, L., Lawas, L. M. F., Galbiati, M., Colombo, L., Heuer, S., … Kater, M. M. (2016). Genome-wide transcriptome analysis during anthesis reveals new insights into the molecular basis of heat stress responses in tolerant and sensitive rice varieties. *Plant and Cell Physiology*, *57*(1), 57–68. https://doi.org/10.1093/pcp/pcv174

Grassini, P., Eskridge, K. M., & Cassman, K. G. (2013). ARTICLE Distinguishing between yield advances and yield plateaus in historical crop production trends. *Nature Communications*, *4*. https://doi.org/10.1038/ncomms3918

Graybosch, R. A., & Peterson, C. J. (2010). Genetic improvement in winter wheat yields in the Great Plains of North America, 1959-2008. *Crop Science*, *50*(5), 1882–1890. https://doi.org/10.2135/cropsci2009.11.0685

Heun, M., Schäfer-Pregl, R., Klawan, D., Castagna, R., Accerbi, M., Borghi, B., & Salamini, F. (1997). Site of einkorn wheat domestication identified by DNA fingerprinting. *Science*, *278*(5341), 1312–1314. https://doi.org/10.1126/science.278.5341.1312

Huang, S., Sirikhachornkit, A., Su, X., Faris, J., Gill, B., Haselkorn, R., & Gornicki, P. (2002). Genes encoding plastid acetyl-CoA carboxylase and 3-phosphoglycerate kinase of the Triticum/Aegilops complex and the evolutionary history of polyploid wheat. *Proceedings of the National Academy of Sciences of the United States of America*, *99*(12), 8133–8138. https://doi.org/10.1073/pnas.072223799

Jaenisch, B. R., de Oliveira Silva, A., DeWolf, E., Ruiz-Diaz, D. A., & Lollato, R. P. (2019). Plant population and fungicide economically reduced winter wheat yield gap in kansas. *Agronomy Journal*, *111*(2), 650–665. https://doi.org/10.2134/agronj2018.03.0223

Jaenisch, B. R., Munaro, L. B., Jagadish, S. V. K., & Lollato, R. P. (2022). Modulation of Wheat Yield Components in Response to Management Intensification to Reduce Yield Gaps. *Frontiers in Plant Science*, *13*(May), 1–18. https://doi.org/10.3389/fpls.2022.772232

Kansas Mesonet, 2017: Kansas Mesonet Historical Data. (n.d.). Retrieved October 8, 2020, from https://mesonet.k-state.edu/weather/historical/#

Kim, J., Slafer, G. A., & Savin, R. (2021). Are portable polyethylene tents reliable for imposing heat treatments in field-grown wheat? *Field Crops Research*, *271*(January), 108206. https://doi.org/10.1016/j.fcr.2021.108206

Kleinsasser, A. (2019). 2019 in Review. In *Spotter Newsletter*. https://doi.org/10.1016/s1365-

6937(19)30334-x

Knapp, M. (2019). Climate Office - Kansas weather highlights for 2018. Retrieved December 16, 2023, from https://climate.k-state.edu/news/stories/2019/01/weather_highlights/

Korzun, V., Röder, M. S., Ganal, M. W., Worland, A. J., & Law, C. N. (1998). Genetic analysis of the dwarfing gene (Rht8) in wheat. Part I. Molecular mapping of Rht8 on the short arm of chromosome 2D of bread wheat (Triticum aestivum L.). *Theoretical and Applied Genetics*, *96*(8), 1104–1109. https://doi.org/10.1007/s001220050845

Kumari, M., Pudake, R. N., Singh, V. P., & Joshi, A. K. (2013). Association of staygreen trait with canopy temperature depression and yield traits under terminal heat stress in wheat (Triticum aestivum L.). *Euphytica*, *190*(1), 87–97. https://doi.org/10.1007/s10681-012-0780-3

Levitt, J. (1972). Physiological Adaptations: Responses of Plants to Environmental Stresses. *Academic Press, New York, xiv*, 698. https://doi.org/10.1126/science.177.4051.786.a

Li, G., Boontung, R., Powers, C., Belamkar, V., Huang, T., Miao, F., … Yan, L. (2017). Genetic basis of the very short life cycle of "Apogee" wheat. *BMC Genomics*, *18*(1), 1–12. https://doi.org/10.1186/s12864-017-4239-8

Lobell, D. B., Schlenker, W., & Costa-Roberts, J. (2011). Climate trends and global crop production since 1980. *Science*, *333*(6042), 616–620. https://doi.org/10.1126/science.1204531

Lollato, R. P., Bavia, G. P., Perin, V., Knapp, M., Santos, E. A., Patrignani, A., & DeWolf, E. D. (2020). Climate-risk assessment for winter wheat using long-term weather data. *Agronomy Journal*, *112*(3), 2132–2151. https://doi.org/10.1002/agj2.20168

Lollato, R. P., Edwards, J. T., & Ochsner, T. E. (2017). Meteorological limits to winter wheat

productivity in the U.S. southern Great Plains. *Field Crops Research*, *203*, 212–226. https://doi.org/10.1016/j.fcr.2016.12.014

Lopes, M. S., & Reynolds, M. P. (2012). Stay-green in spring wheat can be determined by spectral reflectance measurements (normalized difference vegetation methylation and chromatin patterning index) independently from phenology. *Journal of Experimental Botany*, *63*(10), 3789–3798. https://doi.org/10.1093/jxb/ers071

Mason, R. E., Mondal, S., Beecher, F. W., Pacheco, A., Jampala, B., Ibrahim, A. M. H., & Hays, D. B. (2010). QTL associated with heat susceptibility index in wheat (Triticum aestivum L.) under short-term reproductive stage heat stress. *Euphytica*, *174*(3), 423–436. https://doi.org/10.1007/s10681-010-0151-x

Morgan, J. M. (2003). Osmoregulation and Water Stress in Higher Plants. *Https://Doi.Org/10.1146/Annurev.Pp.35.060184.001503*, *35*(1), 299–319. https://doi.org/10.1146/ANNUREV.PP.35.060184.001503

Munaro, L. B., Hefley, T. J., DeWolf, E., Haley, S., Fritz, A. K., Zhang, G., … Lollato, R. P. (2020). Exploring long-term variety performance trials to improve environment-specific genotype × management recommendations: A case-study for winter wheat. *Field Crops Research*, *255*(January). https://doi.org/10.1016/j.fcr.2020.107848

Nations, U. (n.d.). Population. Retrieved March 1, 2021, from un.org website: https://www.un.org/en/global-issues/population

Nawaz, A., Farooq, M., Cheema, S. A., & Wahid, A. (2013). Differential response of wheat cultivars to terminal heat stress. *International Journal of Agriculture and Biology*, *15*(6), 1354–1358.

NAWG. (2024). Wheat Production by Region. Retrieved February 4, 2024, from

https://wheatworld.org/wheat-production-regions/

Özkan, H., Brandolini, A., Schäfer-Pregl, R., & Salamini, F. (2002, October 1). AFLP analysis of a collection of tetraploid wheats indicates the origin of Emmer and hard wheat domestication in Southeast Turkey [2]. *Molecular Biology and Evolution*, Vol. 19, pp. 1797–1801. https://doi.org/10.1093/oxfordjournals.molbev.a004002

Paliwal, R., Röder, M. S., Kumar, U., Srivastava, J. P., & Joshi, A. K. (2012). QTL mapping of terminal heat tolerance in hexaploid wheat (T. aestivum L.). *Theoretical and Applied Genetics*, *125*(3), 561–575. https://doi.org/10.1007/s00122-012-1853-3

Patrignani, A., Lollato, R. P., Ochsner, T. E., Godsey, C. B., & Edwards, J. T. (2014). Yield gap and production gap of rainfed winter wheat in the Southern great plains. *Agronomy Journal*, *106*(4), 1329–1339. https://doi.org/10.2134/AGRONJ14.0011

Pinto, R. S., Reynolds, M. P., Mathews, K. L., McIntyre, C. L., Olivares-Villegas, J. J., & Chapman, S. C. (2010). Heat and drought adaptive QTL in a wheat population designed to minimize confounding agronomic effects. *Theoretical and Applied Genetics*, *121*(6), 1001–1021. https://doi.org/10.1007/s00122-010-1351-4

Porter, J. R., & Gawith, M. (1999, January 1). Temperatures and the growth and development of wheat: A review. *European Journal of Agronomy*, Vol. 10, pp. 23–36. https://doi.org/10.1016/S1161-0301(98)00047-1

Prasad, P. V. V., & Djanaguiraman, M. (2014). Response of floret fertility and individual grain weight of wheat to high temperature stress: Sensitive stages and thresholds for temperature and duration. *Functional Plant Biology*, *41*(12), 1261–1269. https://doi.org/10.1071/FP14061

Ray, D. K., Mueller, N. D., West, P. C., & Foley, J. A. (2013). Yield Trends Are Insufficient to

Double Global Crop Production by 2050. *PLoS ONE*, *8*(6), 66428. https://doi.org/10.1371/journal.pone.0066428

Reddy, S. K., Liu, S., Rudd, J. C., Xue, Q., Payton, P., Finlayson, S. A., … Lu, N. (2014). Physiology and transcriptomics of water-deficit stress responses in wheat cultivars TAM 111 and TAM 112. In *Journal of Plant Physiology* (Vol. 171). https://doi.org/10.1016/j.jplph.2014.05.005

Reynolds, M. P., Quilligan, E., Aggarwal, P. K., Bansal, K. C., Cavalieri, A. J., Chapman, S. C., … Yadav, O. P. (2016, March 1). An integrated approach to maintaining cereal productivity under climate change. *Global Food Security*, Vol. 8, pp. 9–18. https://doi.org/10.1016/j.gfs.2016.02.002

Ross, T., Lott, N., & Center, N. C. D. (2003). A climatology of 1980-2003 extreme weather and climate events. In *National Climatic Data Center Technical Report No. 2003-01*. Retrieved from http://www.ncdc.noaa.gov/ol/reports/billionz.html

Sadras, V. O., Giordano, N., Correndo, A., Cossani, C. M., Ferreyra, J. M., Caviglia, O. P., … Lollato, R. P. (2022). Temperature-Driven Developmental Modulation of Yield Response to Nitrogen in Wheat and Maize. *Frontiers in Agronomy*, *4*, 903340. https://doi.org/10.3389/FAGRO.2022.903340/BIBTEX

Saini, H. S., Sedgley, M., & Aspinall, D. (1984). Developmental anatomy in wheat of male sterility induced by heat stress, water deficit or abscisic acid. *Australian Journal of Plant Physiology*, *11*(4), 243–253. https://doi.org/10.1071/PP9840243

Sciarresi, C., Patrignani, A., Soltani, A., Sinclair, T., & Lollato, R. P. (2019). Plant traits to increase winter wheat yield in semiarid and subhumid environments. *Agronomy Journal*, *111*(4), 1728–1740. https://doi.org/10.2134/agronj2018.12.0766

Shewry, P. R., & Hey, S. J. (2015). The contribution of wheat to human diet and health. *Food and Energy Security*, Vol. 4, pp. 178–202. https://doi.org/10.1002/FES3.64

Slafer, G. A., García, G. A., Serrago, R. A., & Miralles, D. J. (2022). Physiological drivers of responses of grains per m2 to environmental and genetic factors in wheat. *Field Crops Research*, *285*(March). https://doi.org/10.1016/j.fcr.2022.108593

Slafer, G. A., Savin, R., & Sadras, V. O. (2014). Coarse and fine regulation of wheat yield components in response to genotype and environment. *Field Crops Research*, *157*, 71–83. https://doi.org/10.1016/j.fcr.2013.12.004

Tack, J., Barkley, A., & Nalley, L. L. (2015). Effect of warming temperatures on US wheat yields. *Proceedings of the National Academy of Sciences of the United States of America*, *112*(22), 6931–6936. https://doi.org/10.1073/pnas.1415181112

Talukder, A. S. M. H. M., McDonald, G. K., & Gill, G. S. (2014). Effect of short-term heat stress prior to flowering and early grain set on the grain yield of wheat. *Field Crops Research*, *160*, 54–63. https://doi.org/10.1016/j.fcr.2014.01.013

Talukder, S. K., Babar, M. A., Vijayalakshmi, K., Poland, J., Prasad, P. V. V., Bowden, R., & Fritz, A. (2014). Mapping QTL for the traits associated with heat tolerance in wheat (Triticum aestivum L.). *BMC Genetics*, *15*(1), 97. https://doi.org/10.1186/s12863-014-0097-4

Team}, {R Core. (2022). *R: A Language and Environment for Statistical Computing*. Retrieved from https://www.r-project.org/

U.S. National Association of Wheat Growers. (2019). Wheat Facts | National Association of Wheat Growers. Retrieved January 20, 2021, from https://www.wheatworld.org/wheat-101/wheat-facts/

UNIDO. (2018). Indicator 2.4.1: Proportion of agricultural area under productive and sustainable agriculture. Retrieved from https://unstats.un.org/sdgs/metadata/?Text=&Goal=&Target=2.4

USDA-NASS. (2023). USDA/NASS QuickStats. Retrieved February 3, 2024, from National Agricultural Statistics Service website: https://quickstats.nass.usda.gov/

USDA ERS. (2018). USDA ERS - Wheat Data. Retrieved December 11, 2023, from https://www.ers.usda.gov/data-products/wheat-data/

Verma, V., Foulkes, M. J., Worland, A. J., Sylvester-Bradley, R., Caligari, P. D. S., & Snape, J. W. (2004). Mapping quantitative trait loci for flag leaf senescence as a yield determinant in winter wheat under optimal and drought-stressed environments. *Euphytica*, *135*(3), 255–263. https://doi.org/10.1023/B:EUPH.0000013255.31618.14

Vijayalakshmi, K., Fritz, A. K., Paulsen, G. M., Bai, G., Pandravada, S., & Gill, B. S. (2010). Modeling and mapping QTL for senescence-related traits in winter wheat under high temperature. *Molecular Breeding*, *26*(2), 163–175. https://doi.org/10.1007/s11032-009-9366-8

Villareal, R. L., Bañuelos, O., Mujeeb-Kazi, A., & Rajaram, S. (1998). Agronomic performance of chromosomes 1B and T1BL.1RS near-isolines in the spring bread wheat Seri M82. *Euphytica*, *103*(2), 195–202. https://doi.org/10.1023/A:1018392002909

Wang, S., Wong, D., Forrest, K., Allen, A., Chao, S., Huang, B. E., … Akhunov, E. (2014). Characterization of polyploid wheat genomic diversity using a high-density 90 000 single nucleotide polymorphism array. *Plant Biotechnology Journal*, *12*(6), 787–796. https://doi.org/10.1111/pbi.12183

Wei, T., & Simko, V. (2021). *R package "corrplot": Visualization of a Correlation Matrix*.

Retrieved from https://github.com/taiyun/corrplot

Yang, J., Sears, R. G., Gill, B. S., & Paulsen, G. M. (2002). Quantitative and molecular characterization of heat tolerance in hexaploid wheat. *Euphytica*, *126*(2), 275–282. https://doi.org/10.1023/A:1016350509689

Zhao, H., Zhang, L., Kirkham, M. B., Welch, S. M., Nielsen-Gammon, J. W., Bai, G., … Lin, X. (2022). U.S. winter wheat yield loss attributed to compound hot-dry-windy events. *Nature Communications*, *13*(1). https://doi.org/10.1038/s41467-022-34947-6

Chapter 2 - Field Evaluation of Grain Yield and Kernel Traits in the HV9W03-1596R × TX04M410164 Population

Rationale and Objectives

A previous study (Fu et al., 2023) identified heat tolerant wheat germplasm by subjecting 304 winter wheat lines to a heat stress in a growth chamber (36°C day, 30°C night) ten days after anthesis. Data were compared to the same 304 winter wheat lines grown in a non-stress condition growth chamber. The plants remained in either the control or heat stressed growth chamber for 16 days. The ten most heat tolerant lines identified in this experiment, along with the three susceptible checks, then were replicated ten times per line in the same experimental conditions described above. Both experiments measured chlorophyl content with a SPAD chlorophyl meter at 0, 4, 8, 12, and 16 days of treatment, tiller shoot dry weight, whole plant seed count, and whole plant seed weight. In this experiment, HV9W03-1596R was identified as being equal to the lowest percentage loss of chlorophyl content (49.2% chlorophyl retention), having moderate seed weight per plant (41.0 g), a moderate single seed weight (48.1 mg), and a median (statistically equal to both the highest and lowest line) dry shoot weight under terminal heat stress. TX04M410164 was identified as being equal to having the highest percentage loss of chlorophyl content at treatment day 16 (10.2% chlorophyl retention), being equal to the highest seed weight per plant (50.4 g), being equal to the highest single seed weight under terminal heat stress (64.4 mg), and being equal to the lowest dry shoot weight (74.3 g).

Quantification of stress susceptibility within a population segregating for these contrasting heat tolerance traits, chlorophyll retention and grain weight retention, is necessary to characterize the genetic architecture of heat stress tolerance traits. This characterization will

enable subsequent identification of genomic regions associated with heat stress tolerance in the HV9W03-1596R × TX04M410164 population of hard winter wheat.

The objective of the field trials in this study was to quantify the difference in stress susceptibility within the population of recombinant inbred lines (RILs) of the hard winter wheat population, HV9W03-1596R x TX04M410164, for yield-related agronomic traits. Then, having quantified the stress susceptibility within the population, our objective was to assess the interrelationships among the measured agronomic traits. The relationship between stress susceptibility and performance in a control (non-stressed) environment can provide insight into the impact of breeding selection in non-stress, high-yield environments and on the agronomic fitness of lines under stress conditions. Our hypothesis is that the two observed modes of post-anthesis heat stress tolerance are genetically controlled and their effect can be quantified.

Materials and Methods

A recombinant inbred population was constructed by Dr. Jianming Fu (Kansas State University) using the two lines: HV9W03-1596R and TX04M410164 as parents. This population was advanced by single seed descent through the F_5 generation. F_5-derived seed was provided to USDA-ARS for studies to characterize the abiotic stress tolerance in this population under field conditions.

208 $F_{5:7}$ lines were increased in Yuma, AZ in 2017 for planting in field trials in fall 2017. Subsequent field trials were planted using seed harvested from the Ashland Bottoms location in the prior year.

Field trials were conducted in ten Kansas site-years resulting from the combination of locations and years (Table 2.1). Trials were sown in partially replicated incomplete block design

with replicated checks. There were 208 unique RILs and 5 replicated checks: the parents HV9W03-1596R and TX04M410164, and the commercially available wheat varieties “Everest”, “WB-4458”, and “WB-Cedar”. The varieties “Gallagher” and “Zenda” were included as filler plots in 2018 only due to seed limitations, and they were removed from statistical analysis in each location. Both parents, all checks, and all RILs were semi-dwarf in stature and early maturing. Each location had 300 plots total.

Table 2.1 Trial Designs and Trial Abbreviations

Year Location	Trial Abbreviations	Ranges Deep	Rows Wide	Blocks	Ranges per Block	Rows per Block
2018 Ashland	18 ASM	20	15	6	10	5
2018 Sumner	18 SUM	15	20	6	5	10
2018 McPherson	18 McP	20	15	6	10	5
2019 Ashland	19 ASM	15	20	6	5	10
2019 Sumner	19 SUM	15	20	6	5	10
2019 Hutchinson	19 HUM	15	20	6	5	10
2020 Ashland	20 ASM	15	20	6	5	10
2020 Kingman	20 KGM	15	20	6	5	10
2020 Hutchinson	20 HUM	15	20	6	5	10
2020 Sumner	20 SUM	15	20	6	5	10

The trials were sown with a Hege 1000 research plot drill at 60 g of seed per plot on the dates listed in Table 2.2. The planted plot area averaged 5.5 m^2, 1.524 m wide and 3.71 m long and was comprised of 6 rows spaced 19 cm apart for a planting density of 109 kg of seed ha^{-1}. The harvested area varied by location and year because alleys were cut between plots at some locations and not others. Plant height (HT) was recorded as the length from the ground to the tip of the average spikes excluding the awns. Flowering time (FT) was recorded as when 10% of the spikes had anthers extruded within the plot. Physiological maturity (PM) was recorded as the date when the chlorophyll had left the peduncle in 90% of the spikes within the plot. Grain fill period (GFP) was calculated as the physiological maturity days minus the flowering time. The

trials were harvested on the dates listed in Table 2.2 with a research plot combine when grain was approximately 13% moisture. The locations in 2018 were harvested with a Hege 140 plot combine where all the grain harvested from the plots was kept, and yield was recorded by weighing the harvested grain and weights were corrected to a 12% moisture basis. All test weight was measured gravimetrically using a Winchester bushel weight apparatus (151 Filling Hopper and Stand, Seedburo, Des Plaines, IL) and a 0.5 L grain cup. In 2019 and 2020, harvest was completed using a Zurn 150 research plot combine (Zurn 150, Zurn Harvesting, Westernhausen, Germany) where the yield and moisture were measured using a H2 grain gage (H2 Classic graingage, HarvestMaster, Logan, UT) and samples were taken from each plot to measure test weight using the Winchester bushel weight apparatus. A subsample of grain from each plot was used to determine kernel characteristics using a Single Kernel Characterization System (SKCS) (Peterson Instruments-SKCS4100). Measurements were obtained for mean kernel diameter, mean kernel weight, mean kernel moisture, and kernel hardness index. Flowering and physiological maturity were measured in the Ashland Bottoms environment.

Table 2.2 Location, planting date, and harvest date for field trials.

Year Location	Location	Planting date	Harvest date
18 ASM	39.143908, -96.630951	10/27-10/28/2017	6/15/2018
18 SUM	37.4596, -97.6279	10/18/2017	6/18/2018
18 McP	38.2635, -97.5929	10/19/2017	6/19/2018
19 ASM	39.144244, -96.633259	10/24/2018	7/2/2019
19 SUM	37.4598482, -97.62238128	11/6/2018	6/28/2019
19 HUM	37.96292681, -98.12083271	10/24/2018	6/26/2019
20 ASM	39.12795949, -96.61556051	10/18/2019	6/30/2020
20 KGM	37.53524385, -98.26593771	10/15/2019	6/18/2020
20 HUM	37.92892621, -98.02934169	10/14/2019	6/30/2020
20 SUM	37.45965276, -97.62597572	10/16/2019	6/18/2020

Genetic Markers. The Wheat iSelect 90K SNP array (Wang et al., 2014) was used to identify markers that were polymorphic between the parents when evaluated in the Hard Winter

Wheat Association Mapping Panel. Ina preliminary analysis, chromosome 1B had high LOD genomic regions associated with heat tolerance phenotypes collected during the 2018 and 2019 field trials. Markers (available https://wheat.triticeaetoolbox.org/breeders_toolbox/trial/2772). A subset of 90K SNPs and associated designed KASP assays for SNPs that have been genetically mapped and were designated as chromosome-specific was obtained from PolyMarker. The union of these two sets of SNPs provided 118 potential assays for SNPs mapping to chromosome 1B. This list was filtered to a sample of 25 assays spanning 1.4 Mb to 637 Mb on chromosome 1B.

A parent test was conducted on the RIL population using the 25 assays selected for chromosome 1B to find KASP assays that differentiated the two parents. The parent test was performed by running the 25 KASP assays on both parents' DNA separately and on a synthetic heterozygote DNA. This synthetic heterozygote was created by mixing the two parental DNA pools in equal parts so that half of the DNA was from each parent. The results of this parent test showed us which of the 25 KASP assays would reliably tell the parental DNA apart as well as identify the heterozygote.

Two assays (BS_060270_51 and Kukric44369_131) reliably distinguished parental DNA and heterozygote DNA. These two assays were applied to the entire RIL population and the results were used in statistical analysis.

Both parents also were previously screened with 17 common physiology and pathology markers. HV9W03-1569R was found to have the late release from vernalization allele (Vrn-D3b-Late observed in the cultivar 2174) of the *Vrn-D3* gene and TX04M410164 was found to have the early release from vernalization allele (Vrn-D3a-Early observed in the cultivar "Jagger") of the *Vrn-D3* gene. The Vrn-D3-KASP marker was used to identify the alternate alleles of the *Vrn-D3* gene, which is an important gene influencing the timing of the release from vernalization and

is located on chromosome 7D (Chen et al., & Yan, 2010). HV9W03-1569R was found to have the long day insensitive allele (Ppd-D1a observed in cultivar 2174) of the *Ppd-D1* gene and TX04M410164 was found to have the long day sensitive allele (Ppd-D1b observed in Jagger). The MAS00026 marker was used to identify the alternate alleles of the *Ppd-D1* gene. The *Ppd-D1* gene is an important gene for initiation of anthesis based on long day photoperiod sensitivity and is located on chromosome 2D (Chen et al., 2010; Li et al., 2017).

Statistical analysis. Phenotypic data were analyzed in JMP Genomics 9.0 (SAS Institute, Inc., Cary, NC) using the augmented design structure of the partially replicated design. Check entries and environments were fit as fixed effects. Blocks and RILs were fit as random effects. Intercept-centered best linear unbiased predictors (BLUPs) in each environment and across environments were calculated in JMP Genomics. We calculated BLUPs instead of best linear unbiased estimates (BLUEs) because we are calculating solutions based off the fixed effects of this model. Broad-sense heritability (H^2) was estimated on an entry-mean basis:

Equation 2.1 Broad-sense heritability equation.

$$H^2 = \frac{\sigma_g^2}{\sigma_g^2 + \frac{\sigma_{ge}^2}{E} + \frac{\sigma_{error}^2}{E * r}}$$

where σ_g^2 is genotypic variance, σ_{ge}^2 is the genotype-by-environment variance, σ_{error}^2 is the residual error variance, E is the number of environments, and *r* is the average replication of RILs within an environment (Equation 2.1).

The three highest-yielding trial environments (2020 Kingman, 2020 Sumner, and 2019 Hutchinson) were combined to create the synthetic high yield environment (least heat-stressed), and the analysis of variance described above was repeated for these three environments to calculate BLUPs for all RILs in the synthetic high yield environment.

Table 2.3 Traits measured at each location.

Location	Yield	Height	Flowering time	Physiological maturity	Grain fill period	Test weight	Kernel diameter	Kernel weight	Kernel hardness
18 ASM	x	x	x	X	x	x	x	x	x
18 SUM	x	x				x	x	x	x
18 McP	x	x				x	x	x	x
19 ASM	x	x	x	X	x	x	x	x	x
19 SUM	x	x				x	x	x	x
19 HUM	x	x				x	x	x	x
20 ASM	x	x	x	X	x	x	x	x	x
20 KGM	x					x	x	x	x
20 HUM	x					x	x	x	x
20 SUM	x					x	x	x	x

Growing degree days were calculated by averaging the daily high and low temperatures (in Celsius). If the daily low temperature was below 0 degrees Celsius, the daily low temperature was recorded as 0 for the calculation. For this experiment, growing degree days are an accrued measurement starting at January 1st and ending at physiological maturity.

The environmental stress index (ESI) was calculated on a location basis to quantify the stress intensity in each environment:

Equation 2.2 Environmental stress index equation.

$$ESI_j = 1 - \left(\frac{BLUE_j}{BLUE_C}\right)$$

where $BLUE_j$ is the best linear unbiased estimate of the jth environment, $BLUE_C$ is the best linear unbiased estimate of the control environment (Equation 2.2).

The stress sensitivity index (SSI) for the ith genotype in the jth environment was estimated using the Fischer and Maurer susceptibility index (Blum, Shpiler, Golan, & Mayer, 1989; Fischer & Maurer, 1978) on a location-genotype basis:

Equation 2.3 Stress sensitivity index equation.

$$SSI_{ij} = \frac{1 - \left(\frac{BLUP_{ij}}{BLUP_{ic}}\right)}{ESI_j}$$

where $BLUP_{ij}$ is the best linear unbiased predictor of the ith genotype in the jth environment, $BLUP_{ic}$ is the best linear unbiased predictor of the ith genotype in the control environment, ESI_j is the environmental stress index of the jth environment (Equation 2.3). Stress sensitivity indices (SSIs) were calculated in Excel. All correlation analyses were done in R statistical software (v4.2.2; R Core Team, 2022) using the corrplot package (Wei & Simko, 2021).

Results

Trial environments. The average grain yield in the ten trial environments ranged from 1936 kg ha^{-1} at 18 ASM to 4846 kg ha^{-1} at 20 KGM. The three highest yielding environments were 20 KGM, 20 SUM, and 19 HUM (Table 2.7). These three environments also had the highest mean kernel weight. Kernel weight ranged from 21.0 mg in 18 ASM to 30.9 mg in 20 KGM. Grain fill period was 9.2 days shorter in the lowest yielding environment (18 ASM: 23.3 days) than it was in the highest yielding environment where flowering notes were recorded (20 ASM: 32.5 days), resulting in a 39.5% reduction in the grain fill period. Yield in the 18 ASM trial was 35.7% lower than in 20 ASM.

Weather. Kansas in 2018 was one of the hottest, driest years on record with April setting a record for the coldest average temperature since 1895 and then May nearly set the record as the hottest average temperature since 1895 (Knapp, 2019). Kansas in 2019 was one of the coolest, wettest years on record accumulating 508-762 mm above normal precipitation statewide. This large diversity in growing environments had interesting and large effects on many of the

measured traits. The mean grain fill period was May 10 through June 2 at Ashland in 2018, May 13 through June 12 at Ashland in 2019, May 18 through June 19 at Ashland in 2020.

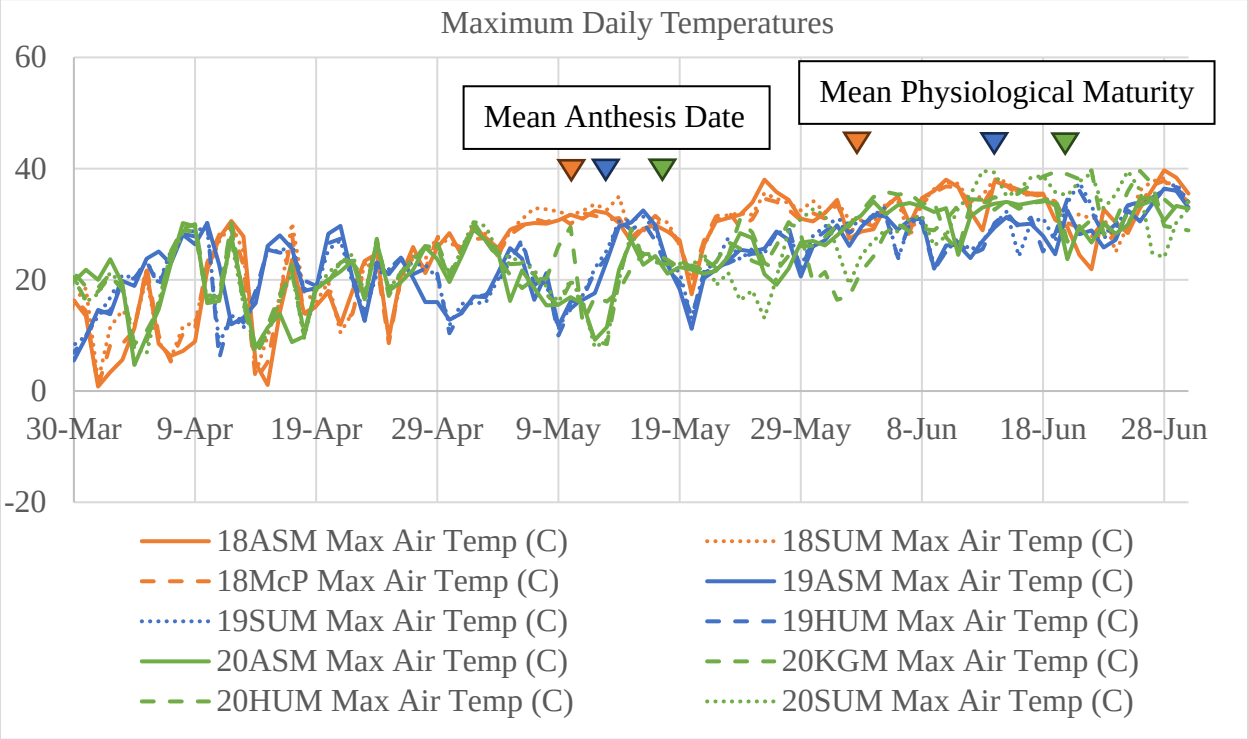

Figure 2.1 Daily maximum air temperature in Celsius for all locations.

The max daily temperatures for 18 McP, 18 ASM, and 18 SUM were greater than the other locations (Figure 2.1) when most of the wheat lines were flowering and starting grain fill (May 1st through May 15th). With the exception of a few days around May 20th, 18 McP, 18 ASM, and 18 SUM had the warmest max daily temperature from May 4th to June 2nd which includes the grain filling period.

Table 2.4 Average maximum temperature in °C during the grain fill period based on flowering and physiological maturity dates of ASM in each year.

	2018			2019			2020			
	ASM	SUM	McP	ASM	SUM	HUM	ASM	KGM	HUM	SUM
Temperature	30.6	31.2	30.3	26.1	26.7	26.0	28.4	29.3	27.6	27.9

The three 2018 locations were the warmest during grain fill, and the 2019 locations were the coolest during grain fill (Table 2.4). 18 SUM was the most heat stressed during grain fill and 19 HUM was the least stressed during grain fill (Table 2.4).

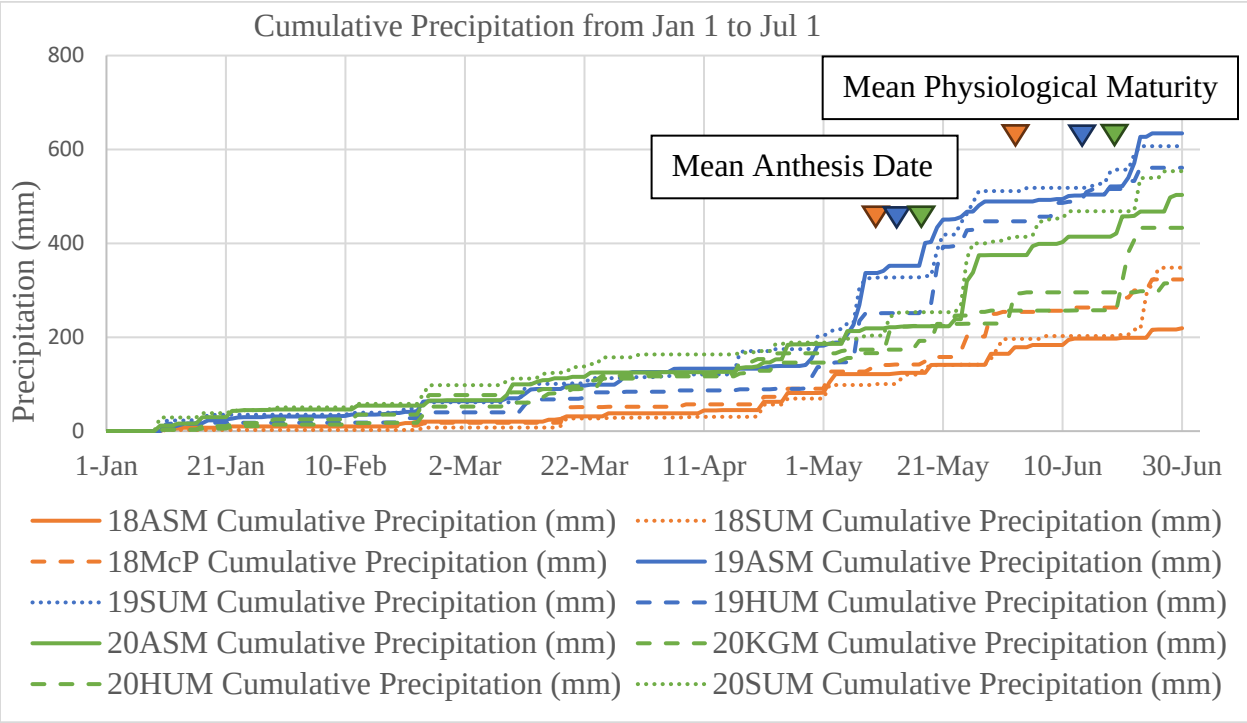

Figure 2.2 Cumulative precipitation from Jan 1 to Jul 1 in mm for all locations.

The 18 ASM environment had the least precipitation with 197 mm, while 19 ASM had the most precipitation with 504 mm. The 2019 locations received most of the precipitation around the start of anthesis through the physiological maturity stage (Figure 2.2). All of the 2019 locations received 75 to 100 mm of precipitation in the first week following anthesis, and two of the locations in 2020 received more than 100 mm in the week following the start of anthesis.

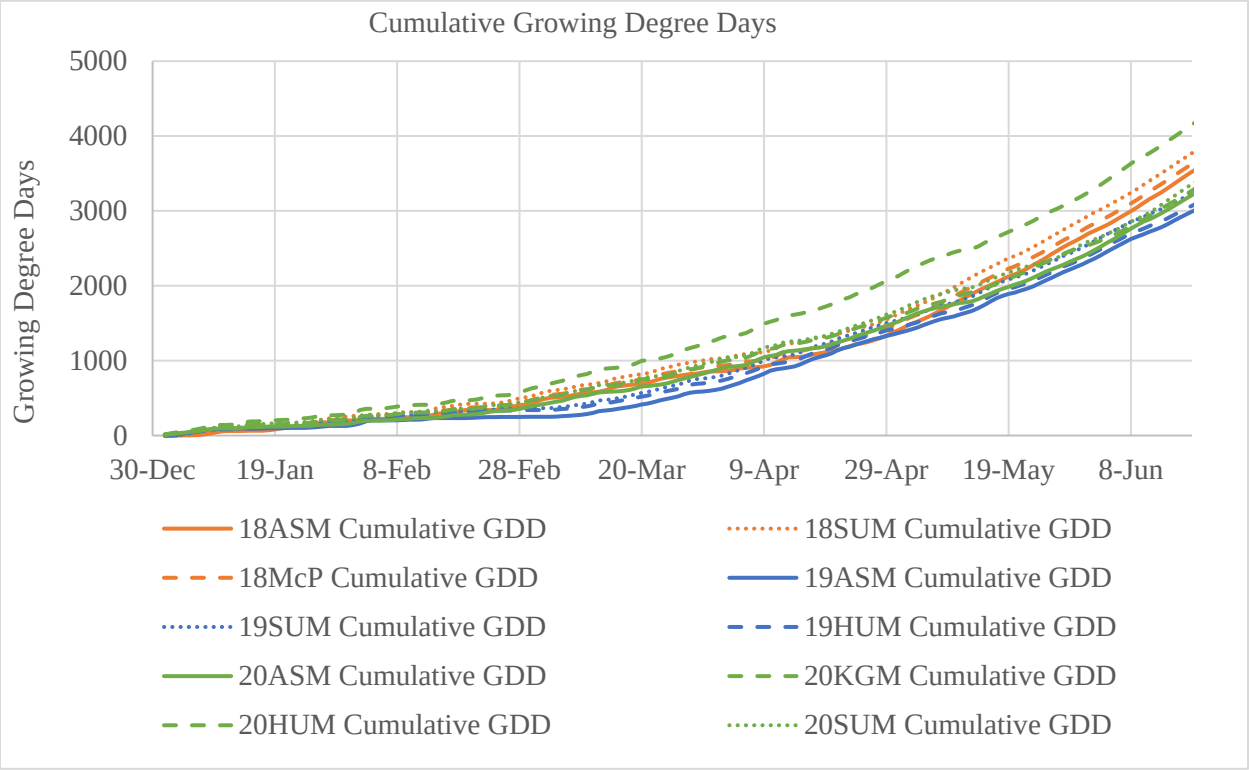

Figure 2.3 Cumulative growing degree days for all locations from Jan 1 through Jun 15.

The growing degree days accumulated varied by location. 20 KGM had the most growing degree days accumulated (3986 GDD) and 19 ASM had the least growing degree days accumulated (2867 GDD) from Jan 1 through Jun 15 (Figure 2.3).

Table 2.5 Means of the response variables in each environment.

Environment	Yield (kg ha^{-1})	Yield Rank	Height (cm)	Flowering Time (Julian days)	Physio-logical Maturity (Julian days)	Grain Fill Period (days)	Test Weight (g L^{-1})	Kernel Diameter (mm)	Kernel Weight (mg)	Kernel Hardness
18 ASM	1936	10	65.4	130.0	153.3	23.3	657	2.37	21.0	66.2
18 McP	3160	6	54.0				765	2.57	25.3	74.7
18 SUM	2968	8	57.0				726	2.48	23.7	78.8
19 ASM	3702	5	67.8	133.5	164.4	30.9	786	2.85	30.0	71.0
19 HUM	4521	3	73.0				785	2.87	30.4	74.6
19 SUM	2966	9	69.1				750	2.65	25.6	60.8
20 ASM	3013	7	67.7	137.7	170.2	32.5	773	2.83	28.9	72.9
20 HUM	3832	4					745	2.65	26.5	61.8
20 KGM	4846	1					830	2.79	30.2	78.8
20 SUM	4825	2					804	2.83	30.9	76.1
Std. Err	134		1.4	0.5	0.5	0.4	6	0.03	0.6	1.1
F-value (env.)	86.0***		78.8***	316.4***	924.8***	392.8***	246.9***	281.3***	234.7***	161.4***

Check Performance. The effect of check genotype was significant for yield and kernel weight, but non-significant for all other traits (Table 2.6). The two highest yielding checks (WB-4458 and HV9W03-1596R) also had the two longest grain fill periods (29.7 days and 29.1 days respectively and the population mean was 28.6 days). The environmental effect was highly significant for every trait. However, there was no significant interaction between check and environment for any trait; the checks responded similarly to the environments. The TX04M410164 parent had the smallest kernel weight and the lowest yield.

Parent Performance. The yield and plant height of the parents were not significantly different in our ten trial environments. Flowering time was not significantly different between the parents in 18 ASM or 20 ASM, but was significant in 19 ASM (Table 2.7). At 18 ASM, TX04M410164 had a shorter grain fill period than HV9W03-1596R. But TX04M410164 had a longer grain fill period than HV9W03-1596R at 19 ASM and statistically the same grain fill period at 20 ASM.

Table 2.6 Means of fixed effects of checks and the population of recombinant inbred lines across environments and tests of fixed effects**.**

Check Genotype	Yield (kg ha^{-1})	Height (cm)	Flowering Time (Julian Days)	Physiological Maturity (Julian Days)	Grain Fill Period (Julian Days)	Test Weight (g L^{-1})	Kernel Weight (mg)	Kernel Diameter (mm)	Kernel Hardness
Population	3313	63.6	134.1	162.7	28.6	754.5	25.8	2.64	71.3
TX04	3122	60.3	133.4	162.2	28.8	761.3	24.9	2.62	71.2
HV9W03	3909	67.5	133.9	163.0	29.1	759.4	27.5	2.74	72.6
Everest	3640	66.7	133.6	162.4	28.8	772.0	27.6	2.70	71.7
WB-4458	3809	68.9	134.3	164.0	29.7	767.2	28.4	2.76	71.6
WB-Cedar	3661	62.1	133.1	161.5	28.4	758.4	29.4	2.67	71.2
Max Std Err	234.9	3.1	1.1	1.1	0.75	12.5	1.4	0.06	2.5
					F-ratio				
Check	3.13*		0.273ns	0.673ns	0.471ns	0.704ns	2.76*	1.76ns	0.0696ns
Environment	38.2***		93.6***	316.1***	126.6***	75.2***	85.4***	106.8***	32.1***
Check X Env.	0.766ns		0.519ns	0.781ns	1.30ns	0.973ns	0.95ns	0.990ns	0.869ns

*,**,*** indicate significance at $P < 0.05, 0.01, 0.001$, respectively; ns, non-significant. HV9W03 indicates HV9W03-1596R and TX04 indicates TX04M410164.

Table 2.7 Mean yield, plant height, flowering time, physiological maturity, and grain fill period of parents (TX04 = TX04M40164, HV9W03 = HV9W03-1596R) in each trial environment.

Environment	Yield (kg ha^{-1})		Height (cm)		Flowering Time (Julian Days)		Physiological Maturity (Julian Days)		Grain Fill Period (Julian Days)	
	TX04	HV9W03	TX04	HV9W03	TX04	HV9W03	TX04	HV9W03	TX04	HV9W03
18 ASM	2070	1866	65.8	65.4	130.2	130.1	152.7	154.4	22.6	24.2
18 McP	3135	3281	54.0	54.9						
18 SUM	3026	2866	56.3	56.5						
19 ASM	3586	3612	67.2	67.5	132.8	134.1	164.4	163.7	31.6	29.8
19 HUM	4438	4457	73.9	73.5						
19 SUM	3071	2951	69.5	69.3						
20 ASM	2890	2709	67.1	66.8	138.3	137.0	170.7	169.7	32.5	32.6
20 HUM	3466	4230								
20 KGM	4962	5068								
20 SUM	5124	4728								
Std.Err	268.1	268.1	3	3	1.06	1.06	1	1	0.7	0.7

Table 2.8 Mean test weight, kernel weight, kernel diameter, and kernel hardness of parents (TX04=TX04M40164, HV9W03=HV9W03-1596R) in each trial environment.

Environment	Test weight (g L^{-1})		Kernel weight (mg)		Kernel diameter (mm)		Kernel hardness	
	TX04	HV9W03	TX04	HV9W03	TX04	HV9W03	TX04	HV9W03
18 ASM	654	658	2.36	2.35	21.2	20.6	67.4	67.4
18 McP	752	769	2.53	2.56	24.7	25.0	72.5	75.6
18 SUM	717	715	2.47	2.48	24.0	23.7	74.7	80.3
19 ASM	791	786	2.88	2.86	30.2	30.5	71.0	71.3
19 HUM	792	782	2.90	2.86	31.0	30.8	73.5	73.4
19 SUM	764	754	2.67	2.67	26.3	26.1	62.8	56.8
20 ASM	773	774	2.82	2.81	28.7	28.4	74.5	74.6
20 HUM	748	750	2.65	2.66	26.6	26.2	60.5	62.5
20 KGM	831	830	2.79	2.79	29.6	30.2	81.0	78.4
20 SUM	800	803	2.80	2.84	30.2	31.1	78.1	75.5
Std.Err	12.1	12.1	0.06	0.06	1.3	1.3	2.4	2.4

Looking at average temperature during the grain fill period, the trend shows that the warmer the average temperature during the grain fill period the lower the average yield. We also see a sharp reduction in yield once the average temperature during the grain fill period is over 23°C (Figure 2.4).

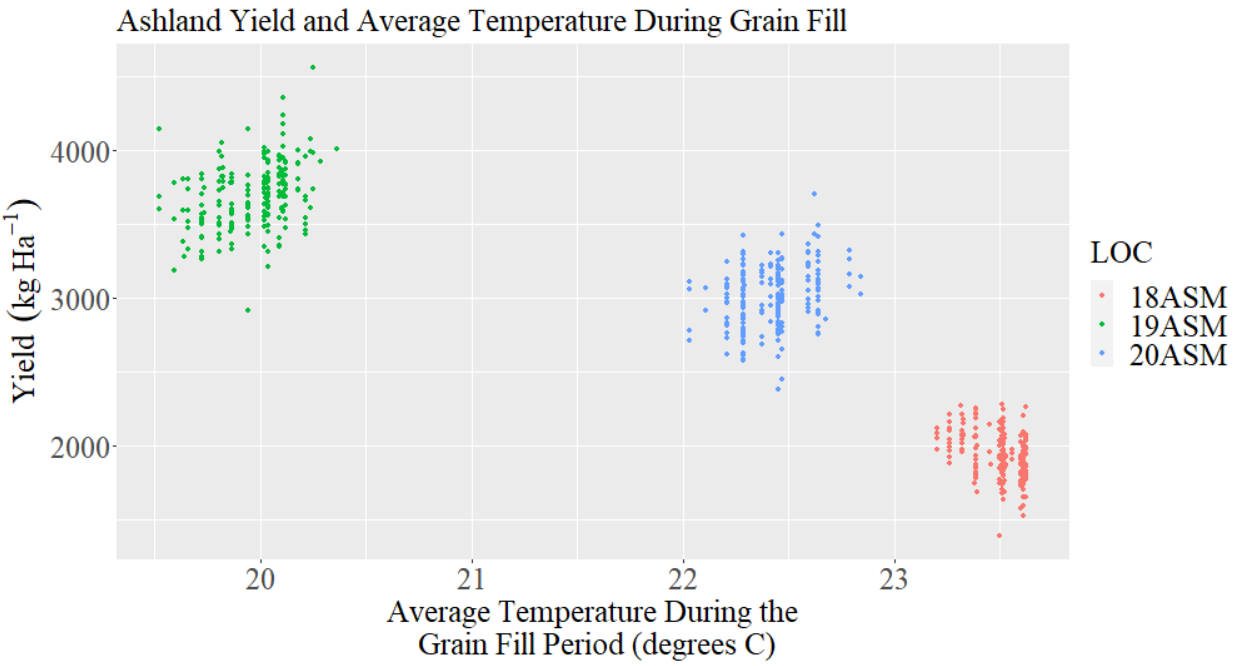

Figure 2.4 Scatter plot of yield and average temperature during the grain fill period for every RIL for every year at Ashland Bottoms.

Analysis of the recombinant inbred line population.

Variance components for recombinant inbred lines. Genetic variance for yield, plant height, flowering time, physiological maturity, grain fill period, test weight, kernel diameter, kernel weight, and kernel hardness were all significant, and all response variables had a σ^2_g Wald *P*- value of $P \leq 0.0001$, except for grain fill period, which had a significance of $P \leq 0.01$ (P =0.005). The genotype × environment interaction variance also was significant for all response variables. All response variables have a $\sigma^2_{g\times e}$ Wald *P*-value of $P \leq 0.0001$ except for plant height which had a significance of $P \leq 0.05$ (p=0.011) (Table 2.9).

Table 2.9 Components of genetic variance in multi-year analysis of variance. Genetic variance (σ^2_g), genotype-by-environment interaction variance ($\sigma^2_{g\times e}$), entry-mean heritability (H^2), ratio of genetic variance to genotype-by-environment interaction variance were calculated with mixed effects analysis of variance.

Response variable	Environments	σ^2_g	$\sigma^2_{g\times e}$	H^2	$\sigma^2_g/\sigma^2_{g\times e}$
Yield	10	43975***	61310***	0.66	0.717
Plant Height	7	9.02***	1.47*	0.86	6.13
Flowering Time	3	1.03***	0.696***	0.75	1.49
Physiological Maturity	3	0.715***	0.913***	0.57	0.783
Grain Fill Period	3	0.248**	0.690***	0.32	0.359
Test Weight	10	143***	103***	0.88	1.39
Kernel Diameter	10	0.00357***	0.00104***	0.94	3.43
Kernel Weight	10	1.88***	0.483***	0.94	3.89
Kernel Hardness	10	5.10***	7.89***	0.80	0.647

*, **, *** indicate significance at $P < 0.05, 0.01, 0.001$, respectively; ns, non-significant.

Grain yield (H^2=0.66), plant height (H^2=0.86), flowering time (H^2=0.75), test weight (H^2=0.88), kernel diameter (H^2=0.94), kernel weight (H^2=0.94), and kernel hardness (H^2=0.80) were highly heritable. Grain fill period was weakly heritable (H^2=0.32). Physiological maturity (H^2=0.57) was moderately heritable. Plant height, kernel diameter, and kernel weight all had a high ratio (>3) of $\sigma^2_g/\sigma^2_{g\times e}$. Yield, physiological maturity, grain fill period, and kernel hardness had low ratios (<1) of $\sigma^2_g/\sigma^2_{g\times e}$ (Table 2.9).

Best linear unbiased predictors.

Correlations between BLUPs. Across all environments and RILs, the pairwise correlation of height and yield was low (r = 0.24, $P < 0.001$) (Table 2.10). Height had a low correlation with every other trait except for flowering time (r = 0.57, $P < 0.001$) and physiological maturity (r = 0.49, $P < 0.001$). Yield and test weight were highly correlated (r = 0.81, $P < 0.001$). Yield was highly correlated with kernel weight (r = 0.76, $P < 0.001$) and kernel diameter (r = 0.69, $P < 0.001$). Flowering time was not correlated with yield (r = 0.06, P =

0.212) or with kernel hardness (r = -0.07, P = 0.133). Flowering time was weakly correlated with test weight (r = 0.19, P < 0.001) and moderately correlated with kernel weight (r = 0.35, P < 0.001). Flowering time was highly correlated with physiological maturity (r = 0.91, P < 0.001) and grain fill period (r = 0.66, P < 0.001), as expected. Grain fill period was correlated with kernel diameter (r = 0.87, P < 0.001), test weight (r = 0.77, P < 0.001), and kernel weight (r = 0.80, P < 0.001) but had a low correlation with kernel hardness (r = 0.25, P < 0.001) (Table 2.10).

Table 2.10 Correlations of best linear unbiased predictors (BLUPs) over all environments for all traits measured in study. Values above the diagonal are Pearson correlation coefficients and the values below the diagonal are the test of significance (P-values) for the correlations.

	Yield	Plant Height	Test Weight	Kernel Weight	Kernel Diameter	Kernel Hardness	Flowering Time	Physiological Maturity	Grain Fill Period
Yield		0.24	0.81	0.76	0.69	0.39	0.06	0.30	0.55
Plant Height	<.0001		0.06	0.32	0.40	-0.42	0.57	0.49	0.33
Test Weight	<.0001	0.026		0.83	0.80	0.44	0.19	0.51	0.77
Kernel Weight	<.0001	<.0001	<.0001		0.97	0.29	0.35	0.61	0.80
Kernel Diameter	<.0001	<.0001	<.0001	<.0001		0.21	0.50	0.74	0.87
Kernel Hardness	<.0001	<.0001	<.0001	<.0001	<.0001		-0.07	0.09	0.25
Flowering Time	0.212	<.0001	<.0001	<.0001	<.0001	0.133		0.91	0.66
Physiological Maturity	<.0001	<.0001	<.0001	<.0001	<.0001	0.028	<.0001		0.91
Grain Fill Period	<.0001	<.0001	<.0001	<.0001	<.0001	<.0001	<.0001	<.0001	

Height BLUPs. The high-yield site (the average of the three highest-yielding locations: 20 KGM, 20 SUM, and 19 HUM) had a much smaller interquartile range (0.762 cm) than all seven stress environments (18 ASM: 3.87cm, 18 McP: 3.92, 18 SUM: 3.69, 19 ASM: 4.08, 19 HUM: 4.29, 19 SUM: 4.08, 20 ASM: 3.90) for plant height (Figure 2.5). Excluding the high-yield site, the interquartile range and range for the seven field sites were similar, expectedly since the *P*-value was less than 0.05 but greater than 0.01 for the genotype environment interaction variance for plant height. It is expected that 18 McP and 18 SUM have the shortest average plant heights of all the locations because they were two of the three most stressed environments in the experiment. 19 HUM was one of the highest yielding locations in the experiment and had, on average, the greatest average plant height.

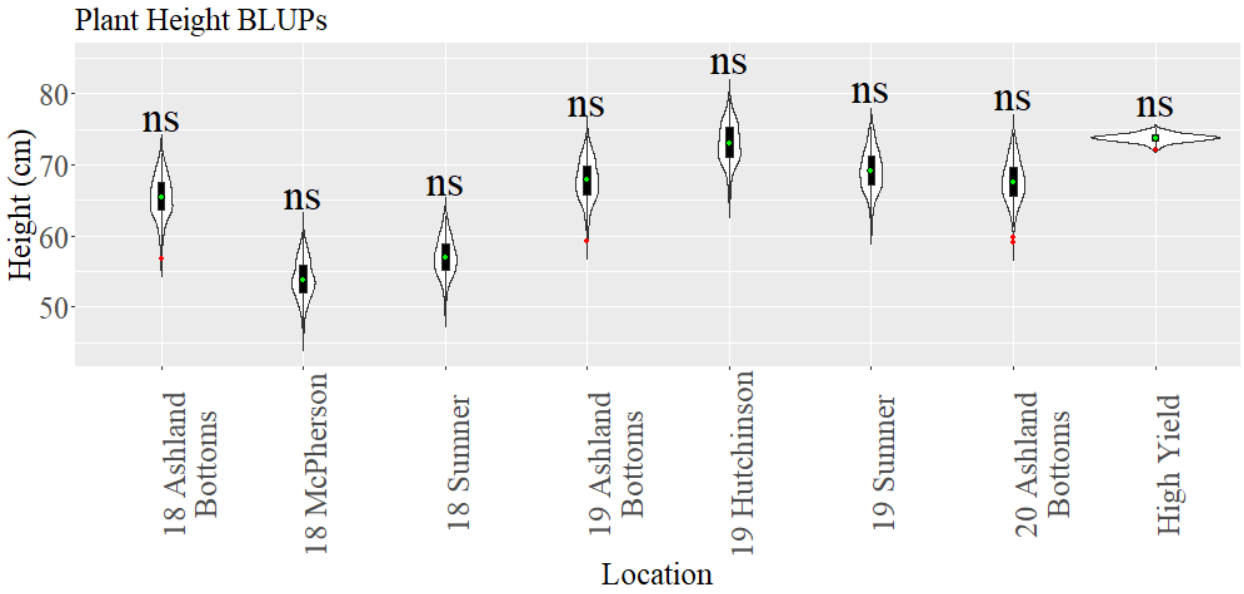

Figure 2.5 Distribution of best linear unbiased predictors for plant height in each of seven environments and in the combined analysis of the three high yield sites (High Yield). The median is indicated by a green diamond. The ends of boxes indicate the first and third quartile of the distribution. Whiskers extend to the most extreme values of the distribution, no further than 1.5 times the interquartile range from the hinge. Data beyond the whiskers are identified as outliers with red dots. Locations that are not normally distributed will have *, **, *** above the graph indicating 0.05, 0.01, and 0.001 respectively. Normally distributed locations will have a "ns" above it. Normality was calculated by using the Shapiro-Wilk Test.

Kernel diameter BLUPs. Kernel diameter BLUP distributions show two peaks at 18 ASM, 18 McP, 20 KGM, and 20 SUM suggesting two genotype groups with two different means as a response to the environment, but all these distributions are statistically normal. 18 ASM and 18 McP were high stress sites and 20 KGM and 20 SUM were low stress, high yielding sites. The remaining locations do not have as pronounced two-peak distributions.

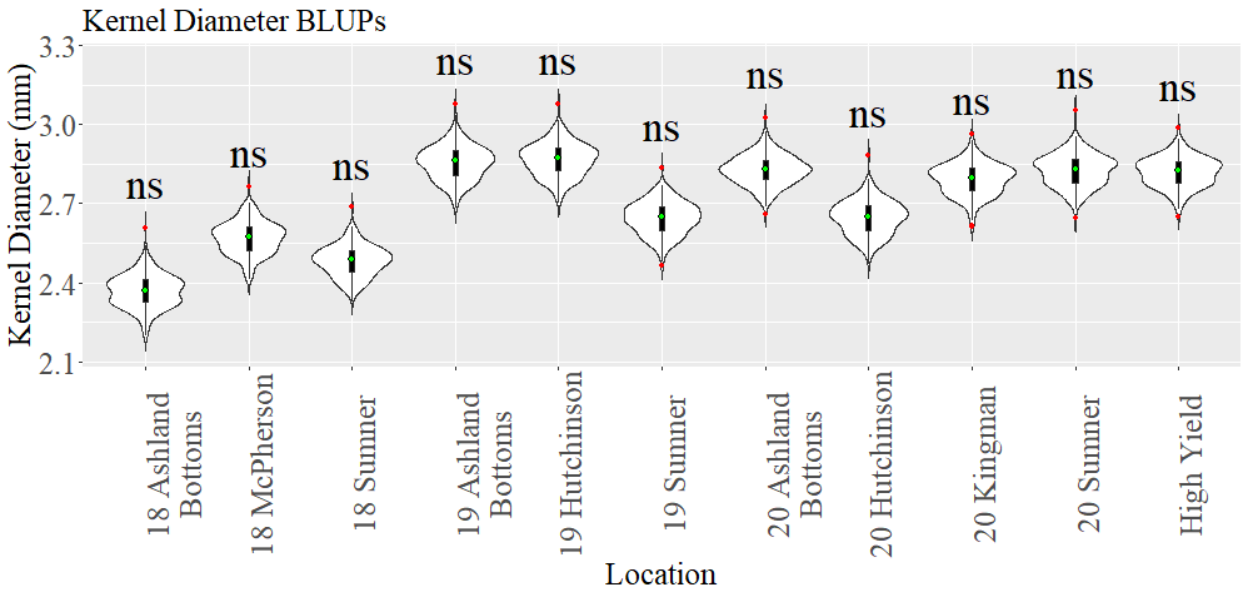

Figure 2.6 Distribution of best linear unbiased predictors for kernel diameter in each of ten environments and in the combined analysis of the three high yield sites (High Yield). The median is indicated by a green diamond. The ends of boxes indicate the first and third quartile of the distribution. Whiskers extend to the most extreme values of the distribution, no further than 1.5 times the interquartile range from the hinge. Data beyond the whiskers are identified as outliers with red dots. Locations that are not normally distributed will have *, **, *** above the graph indicating 0.05, 0.01, and 0.001 respectively. Normally distributed locations will have a "ns" above it. Normality was calculated by using the Shapiro-Wilk Test.

Test weight BLUPs. 18 ASM was a stressed environment and had a large reduction in test weight compared to the 2019 and 2020 seasons (Figure 2.7). The distribution for test weight at 18 ASM skewed lower at test weights lower than the bottom 25 percent interquartile range marking, suggesting a group of RILs that handled the heat and drought stress better (higher test weight), and a group of RILs that dropped off quickly with the stress (lower test weight). These

distributions are also not normal. The distribution among the ten environments had noticable variation while the population means also varied consistant with a large effect from environment as well as a large effect from genotype, and possibly genotype x environment interaction. The analysis of variance in Table 2.9 indicates that genotypic variance and the genotype-by-environment interaction variance were both highly significant for test weight.

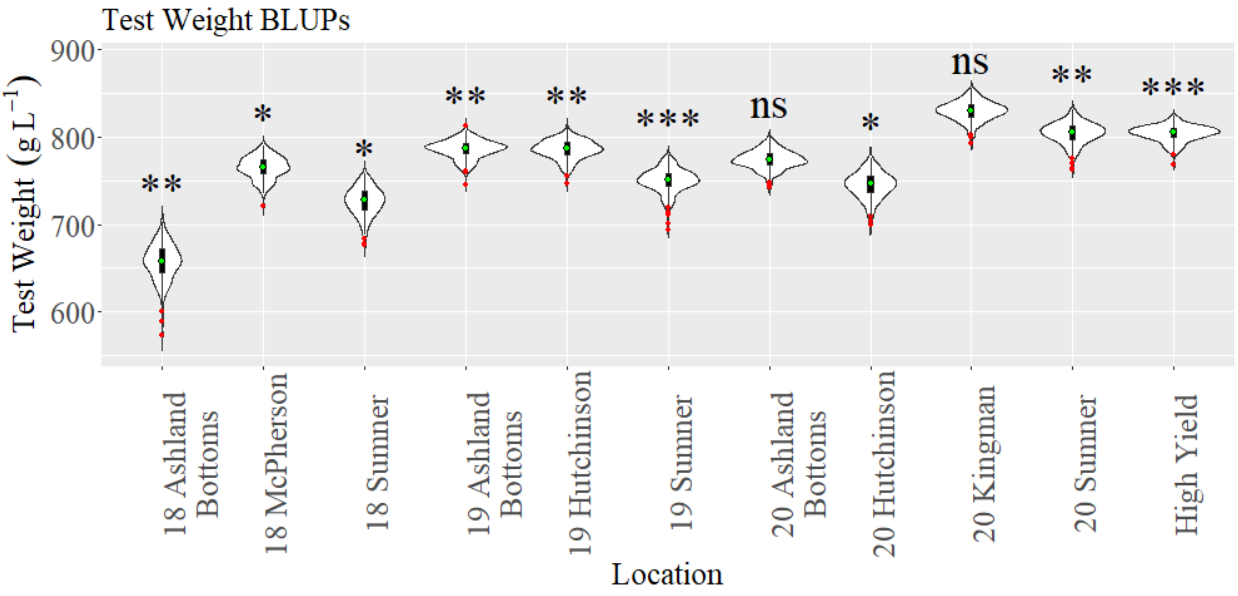

Figure 2.7 Distribution of best linear unbiased predictors for test weight in each of ten environments and in the combined analysis of the three high yield sites (High Yield). The median is indicated by a green diamond. The ends of boxes indicate the first and third quartile of the distribution. Whiskers extend to the most extreme values of the distribution, no further than 1.5 times the interquartile range from the hinge. Data beyond the whiskers are identified as outliers with red dots. Locations that are not normally distributed will have *, **, *** above the graph indicating 0.05, 0.01, and 0.001 respectively. Normally distributed locations will have a "ns" above it. Normality was calculated by using the Shapiro-Wilk Test.

Yield BLUPs. Yield was highly affected by the environment. This is very evident when comparing the yield at 18 ASM with the high yield site. 18 ASM had a mean yield of 1937.4 kg ha^{-1}, and the high yield site had a mean yield of 4719.7 kg ha^{-1}. 20 HUM had the widest distribution of all the locations (IQR of 436.0). 19 ASM and 19 SUM had significant water-

logged soils in 2019 and may account for the majority of the large reduction in yield (Figure 2.8).

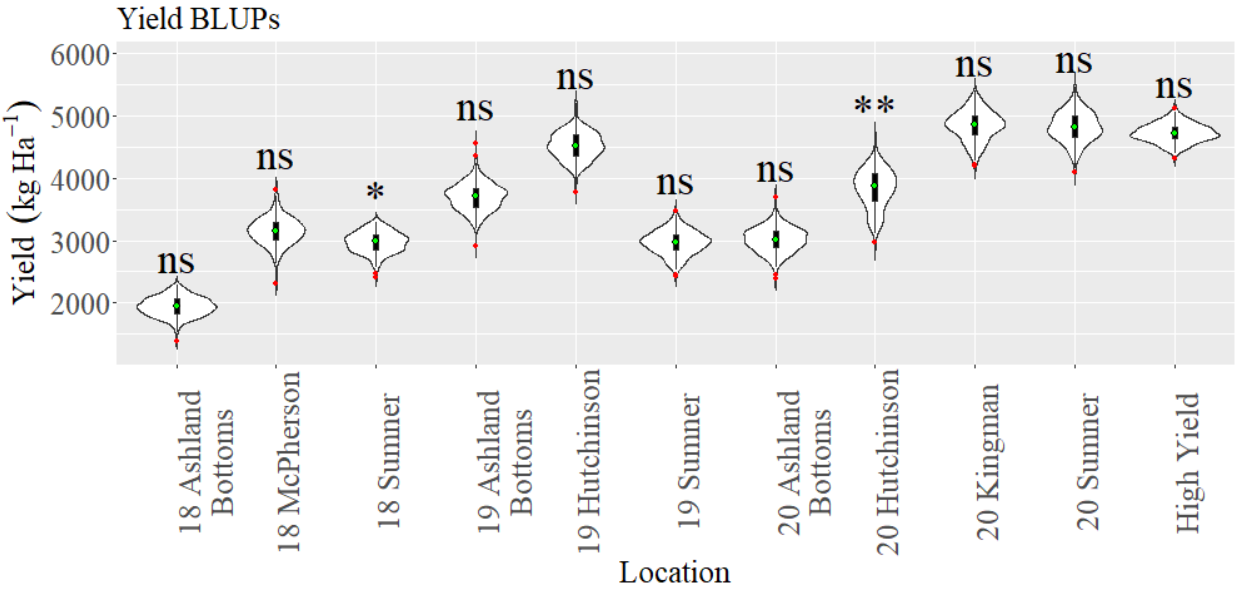

Figure 2.8 Distribution of best linear unbiased predictors for yield in each of ten environments and in the combined analysis of the three high yield sites (High Yield). The median is indicated by a green diamond. The ends of boxes indicate the first and third quartile of the distribution. Whiskers extend to the most extreme values of the distribution, no further than 1.5 times the interquartile range from the hinge. Data beyond the whiskers are identified as outliers with red dots. Locations that are not normally distributed will have *, **, *** above the graph indicating 0.05, 0.01, and 0.001 respectively. Normally distributed locations will have a “ns” above it. Normality was calculated by using the Shapiro-Wilk Test.

Kernel hardness BLUPs. The kernel hardness trait was measured using a SKCS instrument, which records a hardness index based on the seed crushing profile where harder kernels have a higher index number. 19 SUM and 20 HUM had the lowest mean harness index (60.7 and 61.9 respectively). Part of 19 SUM's poor performance is probably attributed to the water-logged soils for long periods of time and it rained for five days right before harvest. It rained a total of 66.5 mm from Jun 1 through Jun 4 at 20 HUM and the wheat was harvested on Jun 26 so the weathered wheat could account for low hardness. 18 ASM had the smallest IQR (3.41). Four of these locations appear to have a bimodal distribution (18 McP, 18 SUM, 19 SUM, 20 SUM, as does the high yield site) (Figure 2.9). There are no obvious factors in common with the bimodal distributed locations and the non-bimodal distributed locations (Figure 2.9).

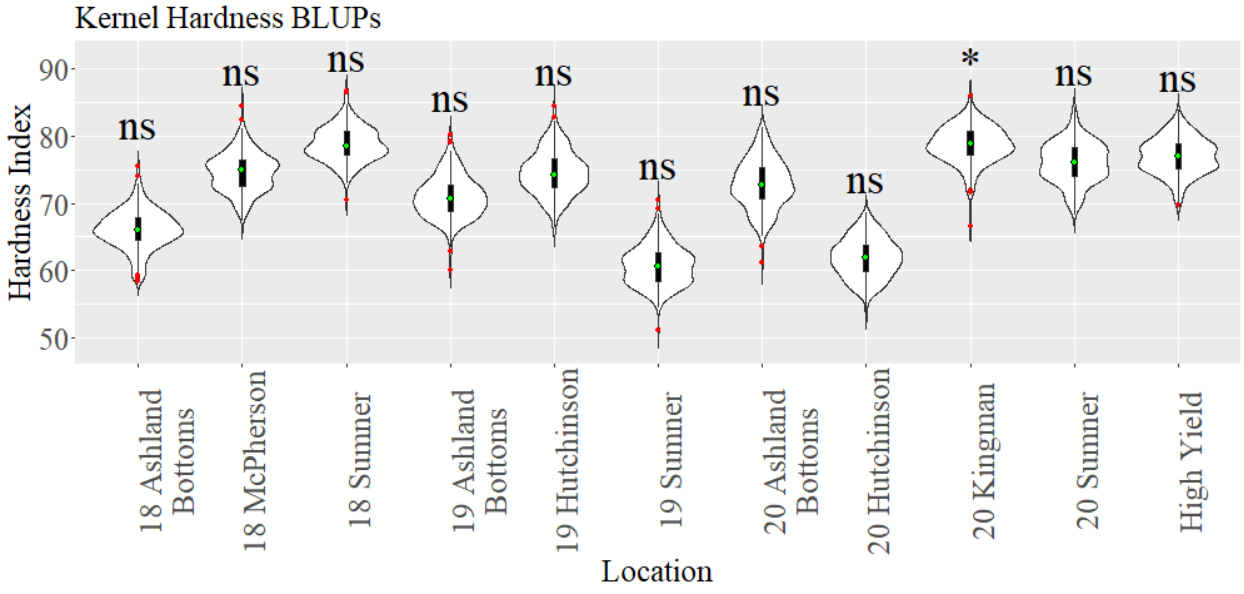

Figure 2.9 Distribution of best linear unbiased predictors for kernel hardness in each of ten environments and in the combined analysis of the three high yield sites (High Yield). The median is indicated by a green diamond. The ends of boxes indicate the first and third quartile of the distribution. Whiskers extend to the most extreme values of the distribution, no further than 1.5 times the interquartile range from the hinge. Data beyond the whiskers are identified as outliers with red dots. Locations that are not normally distributed will have *, **, *** above the

graph indicating 0.05, 0.01, and 0.001 respectively. Normally distributed locations will have a "ns" above it. Normality was calculated by using the Shapiro-Wilk Test.

Kernel weight BLUPs. Individual kernel weight was measured with the SKCS. Kernel weight was highly variable across environments. 20 SUM and 19 HUM had the highest mean kernel weight by location with 30.8 mg kernel^{-1} and 30.3 mg kernel^{-1} respectively. The lowest mean kernel weight was at 18 ASM with 20.9 mg kernel^{-1} (Figure 2.10).

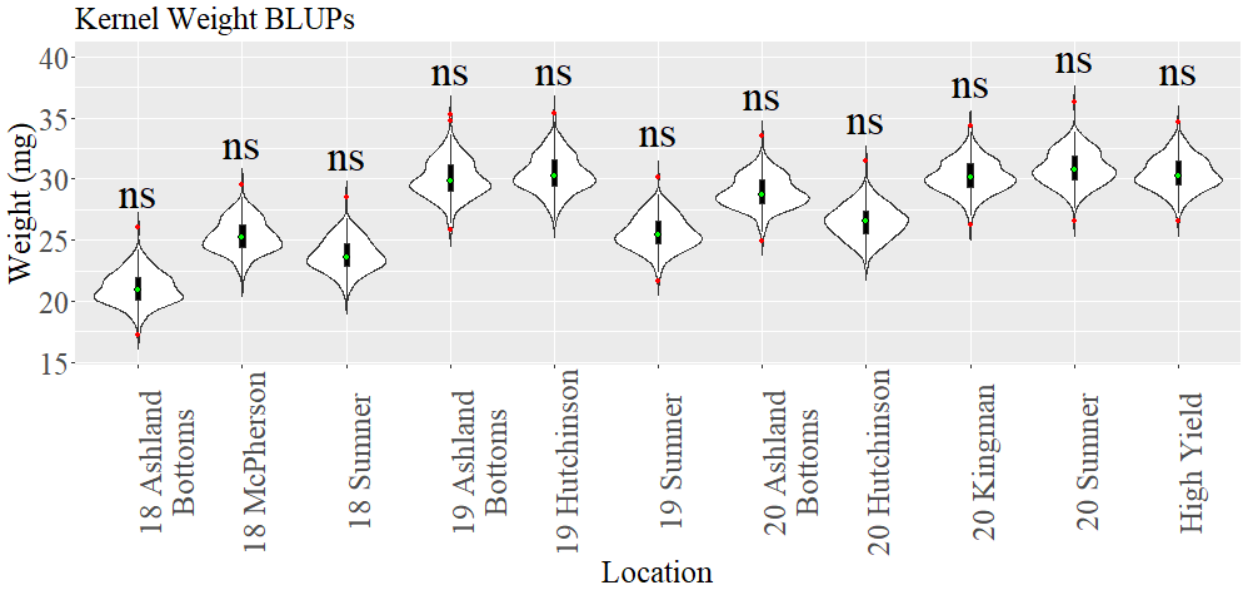

Figure 2.10 Distribution of best linear unbiased predictors for kernel weight in each of ten environments and in the combined analysis of the three high yield sites (High Yield). The median is indicated by a green diamond. The ends of boxes indicate the first and third quartile of the distribution. Whiskers extend to the most extreme values of the distribution, no further than 1.5 times the interquartile range from the hinge. Data beyond the whiskers are identified as outliers with red dots. Locations that are not normally distributed will have *, **, *** above the graph indicating 0.05, 0.01, and 0.001 respectively. Normally distributed locations will have a "ns" above it. Normality was calculated by using the Shapiro-Wilk Test.

Growing degree days and solar radiation accumulated during the grain fill period BLUPs. 18 ASM had the least growing degree days accumulated during the grain fill period and also was not normally distributed. 19 ASM and 20 ASM were normally distributed and accumulated more growing degree days (Figure 2.11).

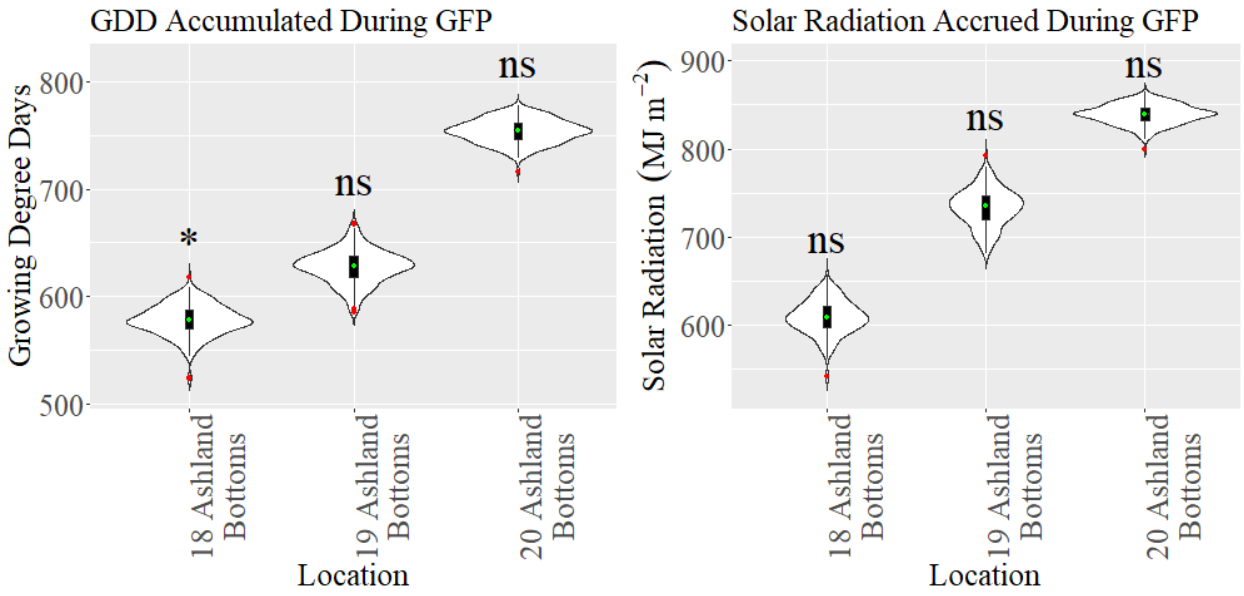

Figure 2.11 Distribution of best linear unbiased predictors for growing degree days accumulated during the grain fill period in each of three environments on the left and solar radiation accumulated during the grain fill period in each of three environments on the right. The median is indicated by a green diamond. The ends of boxes indicate the first and third quartile of the distribution. Whiskers extend to the most extreme values of the distribution, no further than 1.5 times the interquartile range from the hinge. Data beyond the whiskers are identified as outliers with red dots. Locations that are not normally distributed will have *, **, *** above the graph indicating 0.05, 0.01, and 0.001 respectively. Normally distributed locations will have a "ns" above it. Normality was calculated by using the Shapiro-Wilk Test.

Reproductive phenology trait BLUPs. The combination of heat and drought stress in 2018 hastened flowering and maturity and shortened grain fill period. The mean grain fill period was shortened by 9.2 days (or 4.4 days per one degree increase in average grain fill period temperature), physiological maturity was shortened by 16.9 days (or 8.0 days per one degree increase in average grain fill period temperature), and flowering time was shortened by 7.6 days (or 3.6 days per one degree increase in average grain fill period temperature) when comparing 18 ASM with 20 ASM (Figure 2.12). 18 ASM and 19 ASM flowering time had a larger range of days than 20 ASM flowering time. The IQR of 18 ASM, 19 ASM, and 20 ASM for flowering time was 1.44, 2.13, and 0.925 respectively (Table 2.11). The IQR of 18 ASM, 19 ASM, and 20 ASM for physiological maturity was 1.53, 1.63, and 1.01 respectively (Table 2.11).

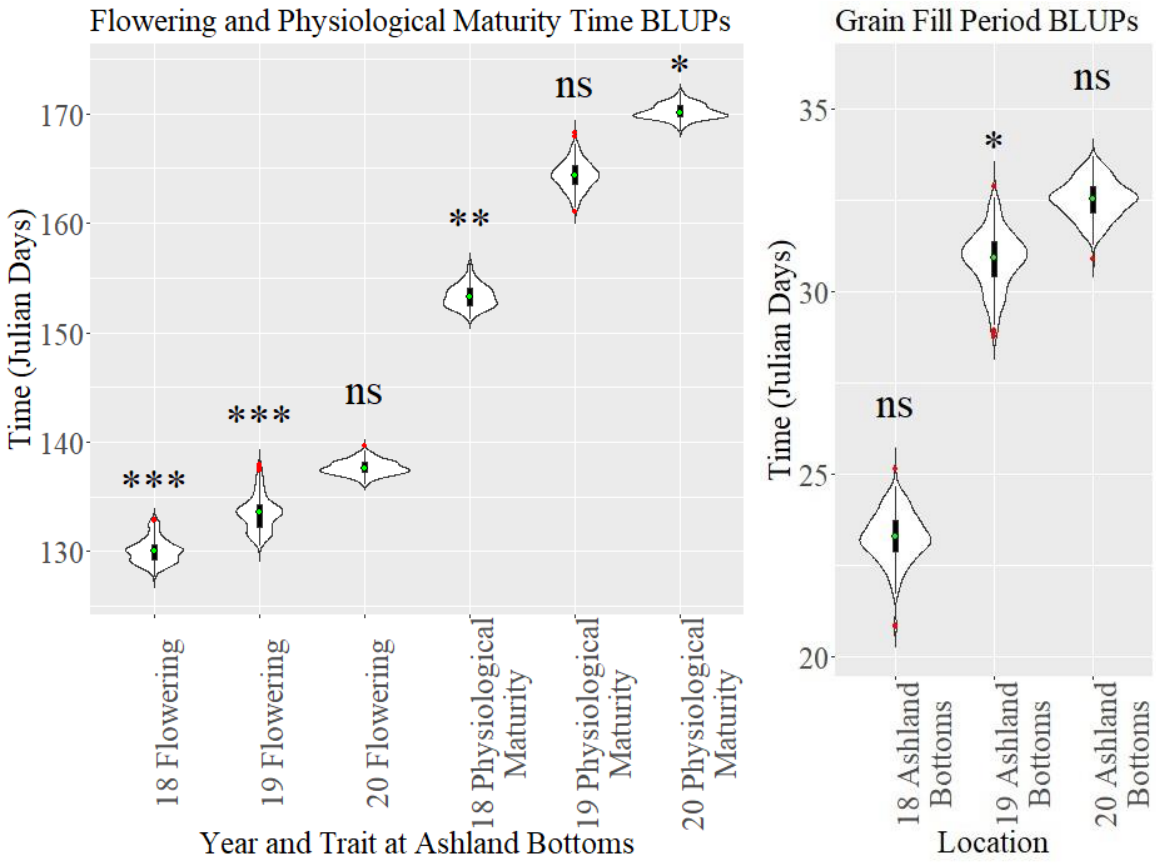

Figure 2.12 Distribution of best linear unbiased predictors for flowering time, physiological maturity time, and grain fill period in each of three environments. The median is indicated by a green diamond. The ends of boxes indicate the first and third quartile of the distribution. Whiskers extend to the most extreme values of the distribution, no further than 1.5 times the interquartile range from the hinge. Data beyond the whiskers are identified as outliers with red dots. Locations that are not normally distributed will have *, **, *** above the graph indicating 0.05, 0.01, and 0.001 respectively. Normally distributed locations will have a "ns" above it. Normality was calculated by using the Shapiro-Wilk Test.

Table 2.11 Table of quartile values and interquartile ranges (IQR) for flowering time, physiological maturity, and grain fill period BLUPs of the population at Ashland Bottoms.

	Flowering Time (Julian Days)				Physiological Maturity Time (Julian Days)				Grain Fill Period (Julian days)			
	25%	50%	75%	IQR	25%	50%	75%	IQR	25%	50%	75%	IQR
18 ASM	129.2	130.0	130.6	1.44	152.5	153.2	154	1.53	22.9	23.3	23.7	0.847
19 ASM	132.2	133.5	134.3	2.13	163.6	164.4	165.2	1.63	30.4	30.9	31.4	0.965
20 ASM	137.2	137.6	138.1	0.925	169.7	170.1	170.7	1.01	32.2	32.5	32.9	0.702

Stress sensitivity.

Environmental stress intensity. Yield was the most sensitive to stress at every location when compared to height, test weight, kernel diameter, or kernel weight (Table 2.12). The stress of an environment did not have the same effect on every trait (Table 2.12). The high yield site used in the ESI calculation was calculated in a combined analysis using the three highest yielding sites (19 HUM, 20 KGM, and 20 SUM) for every trait. Grain fill period consistently had a higher environmental stress intensity than flowering time and physiological maturity time. In a higher stress environment (18 ASM), physiological maturity environmental stress intensity increased much more than the flowering time environmental stress intensity. And likewise, significantly increased the grain fill period environmental stress intensity because the grain fill period is calculated by subtracting flowering time from physiological maturity. If the ESI for a trait x environment was less than 0.02, then that environment was counted as a non-stress environment for the trait and was excluded from the calculation of SSI. An ESI smaller than 0.02 causes small changes to have a much larger effect on the SSI for a RIL to the point that it is not useful. At 19 ASM, there was no environmental stress for kernel diameter (-0.00957) or kernel weight (0.0181) (Table 2.12) even though 19 ASM ranked fifth in yield (Table 2.5). The locations and traits that had a non-stressful environment were kernel hardness at 18 SUM (-0.0232), kernel diameter at 19 ASM (-0.00957), kernel diameter at 20 ASM (-0.000206), and kernel weight at 19 ASM (0.0181).

Table 2.12 Environmental stress intensity for each trait in each test environment. Negative stress intensities indicate there was no environmental stress for that location for that trait.

	Environmental Stress Intensity								
Environment	Height	Test Weight	Kernel Diameter	Kernel Hardness	Kernel Weight	Yield	Flowering Time	Physiological Maturity	Grain Fill Period
18 ASM	0.113	0.182	0.160	0.142	0.309	0.590	0.0555	0.0992	0.284
18 McP	0.269	0.0485	0.0886	0.0305	0.168	0.333			
18 SUM	0.227	0.0968	0.119	-0.0232	0.219	0.372			
19 ASM	0.0811	0.0224	-0.00957	0.0776	0.0181	0.217	0.0303	0.0342	0.0507
19 SUM	0.0633	0.0671	0.0602	0.207	0.156	0.373			
20 ASM	0.0827	0.0375	-0.000206	0.0598	0.0538	0.363			
20 HUM		0.0738	0.0588	0.192	0.126	0.192			

Stress sensitivity indices. Stress sensitivity indices are reported for the trait x environment combinations with ESI values > 0.02.

Plant height SSI. The height SSI had a small interquartile range at 18 SUM (0.185) but a much larger interquartile range in the 19 SUM (0.712) location. 18 McP and 18 SUM had a much narrower distribution than 19 ASM, 19 SUM, and 20 ASM because the ESI for height at 18 McP and 18 SUM were much higher than the other locations for height. 18 ASM, 18 McP, and 18 SUM were the three most stressed environments, but the distribution of 18 ASM is more similar to the distributions of SSIs in 2019 and 2020 locations with narrower distributions (Figure 2.13).

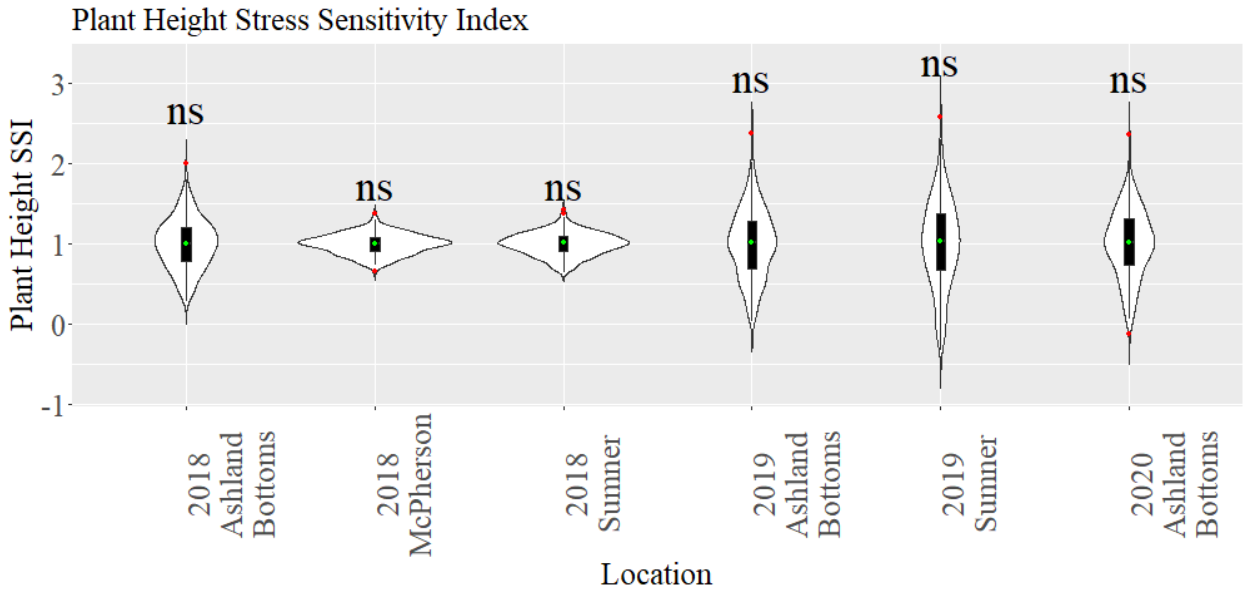

Figure 2.13 Distribution of the stress sensitivity indices for plant height in six environments, calculated relative to the best linear unbiased predictors across three high yield environments. The median is indicated by a green diamond. The ends of boxes indicate the first and third quartile of the distribution. Whiskers extend to the most extreme values of the distribution, no further than 1.5 times the interquartile range from the hinge. Data beyond the whiskers are identified as outliers with red dots. Locations that are not normally distributed will have *, **, *** above the graph indicating 0.05, 0.01, and 0.001 respectively. Normally distributed locations will have a "ns" above it. Normality was calculated by using the Shapiro-Wilk Test.

Test weight SSI. 19 ASM had the largest interquartile range for test weight SSI (0.377) where as 18 ASM had the smallest interquartile range in test weight SSI (0.132). 19 ASM also

had the lowest test weight ESI (0.0224) making it the least stressed location (Table 2.12). 18 ASM (0.132), 18 SUM (0.203), 19 SUM (0.207), and 20 HUM (0.222) had narrower IQRs. 18 McP (0.284), 19 ASM (0.377), 20 ASM (0.294) had broader IQRs (Figure 2.14).

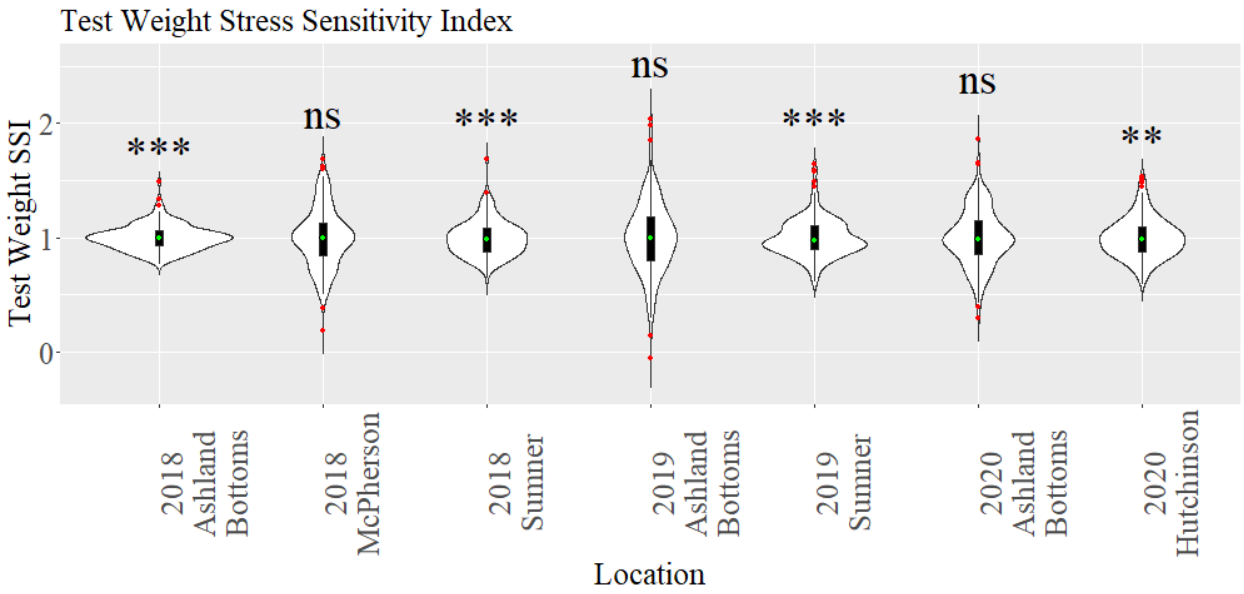

Figure 2.14 Distribution of the stress sensitivity indices for test weight in seven environments, calculated relative to the best linear unbiased predictors across three high yield environments. The median is indicated by a green diamond. The ends of boxes indicate the first and third quartile of the distribution. Whiskers extend to the most extreme values of the distribution, no further than 1.5 times the interquartile range from the hinge. Data beyond the whiskers are identified as outliers with red dots. Locations that are not normally distributed will have *, **, *** above the graph indicating 0.05, 0.01, and 0.001 respectively. Normally distributed locations will have a "ns" above it. Normality was calculated by using the Shapiro-Wilk Test.

Kernel diameter SSI. Kernel diameter SSI for the three 2018 locations had narrow distributions (IQR <0.2). 19 SUM and 20 HUM had 3 to 5 outliers that extended more than one SSI away from the mean and had broad distributions (IQR >0.2). The 19 ASM and 20 ASM trials were not included in this figure because the environmental stress intensity from kernel diameter in this environment was <0.02 (Figure 2.15).

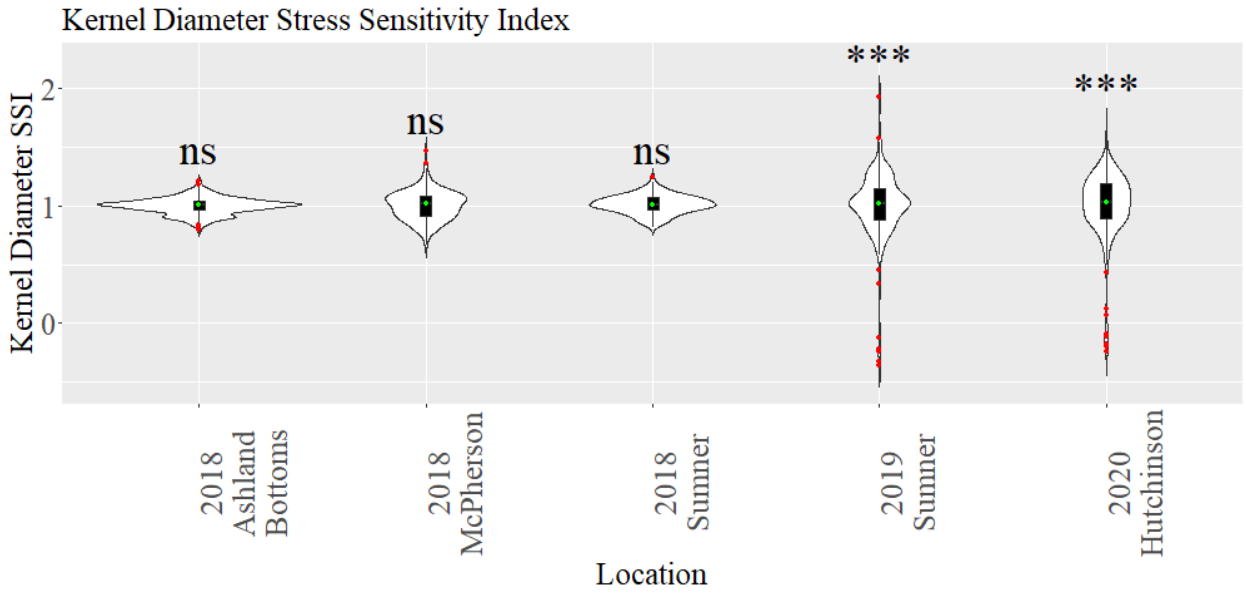

Figure 2.15 Distribution of the stress sensitivity indices for kernel diameter in six environments, calculated relative to the best linear unbiased predictors across three high yield environments. The median is indicated by a green diamond. The ends of boxes indicate the first and third quartile of the distribution. Whiskers extend to the most extreme values of the distribution, no further than 1.5 times the interquartile range from the hinge. Data beyond the whiskers are identified as outliers with red dots. Locations that are not normally distributed will have *, **, *** above the graph indicating 0.05, 0.01, and 0.001 respectively. Normally distributed locations will have a "ns" above it. Normality was calculated by using the Shapiro-Wilk Test.

Kernel hardness SSI. 18 McP and 20 ASM had much broader distributions (>1.0) broad distribution compared to the rest of the locations (IQRs <0.5). The 18 SUM environment was excluded from this analysis because the ESI for kernel hardness was < 0.02 (Figure 2.16).

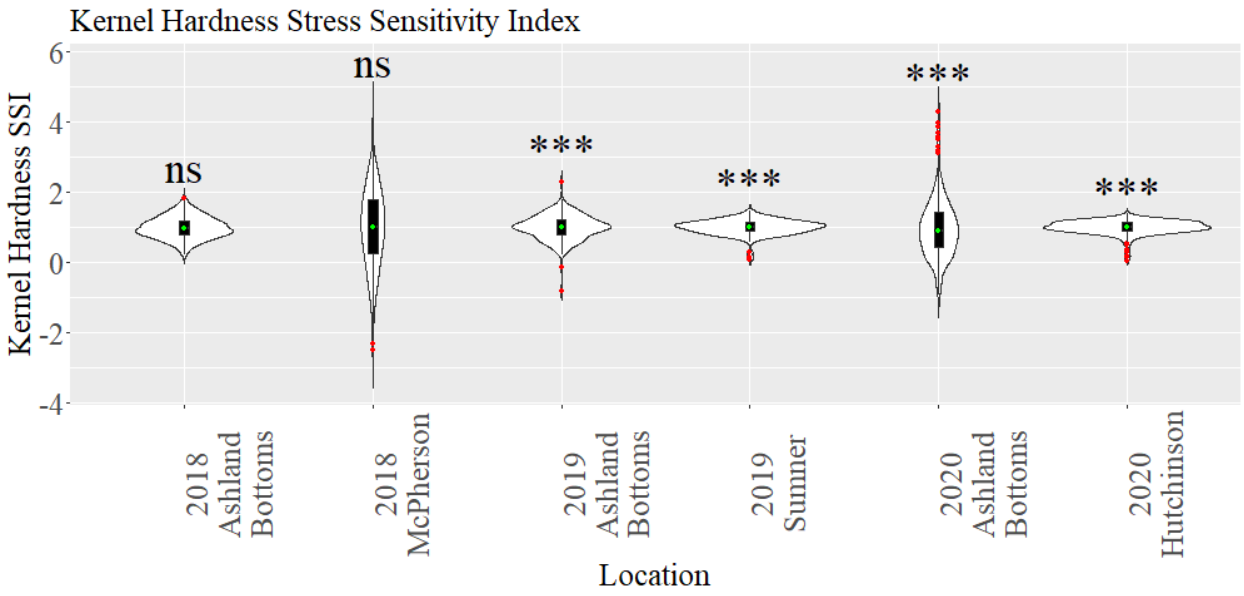

Figure 2.16 Distribution of the stress sensitivity indices for kernel hardness in six environments, calculated relative to the best linear unbiased predictors across three high yield environments. The median is indicated by a green diamond. The ends of boxes indicate the first and third quartile of the distribution. Whiskers extend to the most extreme values of the distribution, no further than 1.5 times the interquartile range from the hinge. Data beyond the whiskers are identified as outliers with red dots. Locations that are not normally distributed will have *, **, *** above the graph indicating 0.05, 0.01, and 0.001 respectively. Normally distributed locations will have a "ns" above it. Normality was calculated by using the Shapiro-Wilk Test.

Individual kernel weight SSI. 20 ASM had a very broad distribution (IQR of 0.603) compared to the rest of the locations (IQR < 0.22) for individual kernel weight SSI. 18 ASM has the most narrow distribution in individual kernel weight SSI (IQR of 0.0942) and also had the greatest ESI (0.309) (Table 2.12). 19 ASM was excluded from this analysis because the ESI was <0.02 (Figure 2.17).

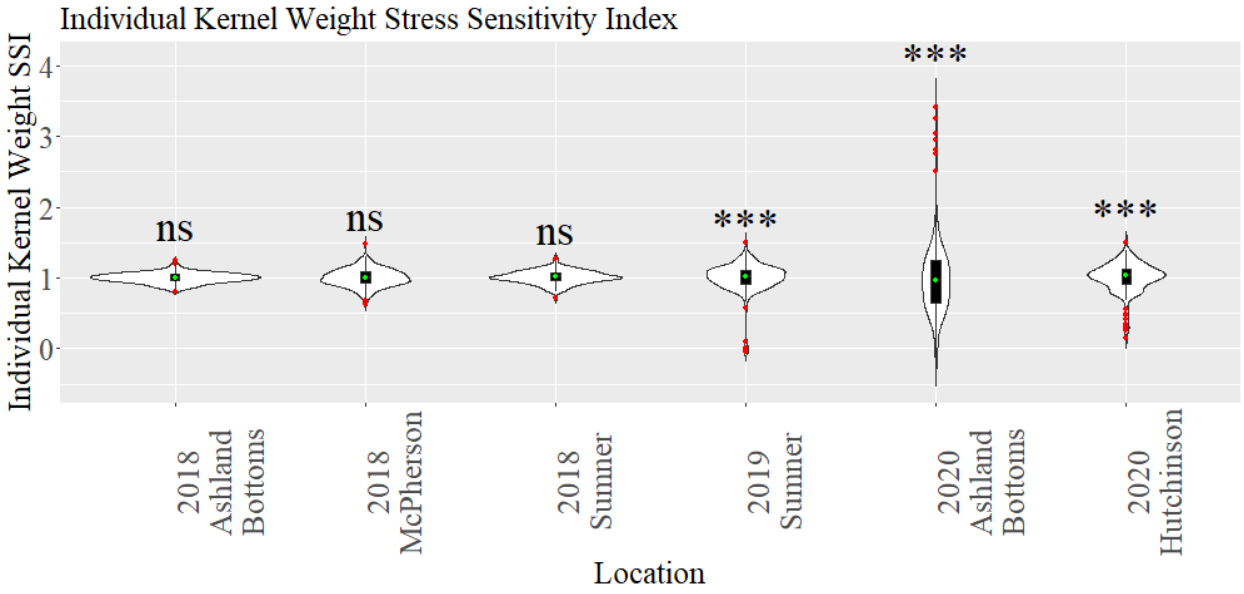

Figure 2.17 Distribution of the stress sensitivity indices for individual kernel weight in six environments, calculated relative to the best linear unbiased predictors across three high yield environments. The median is indicated by a green diamond. The ends of boxes indicate the first and third quartile of the distribution. Whiskers extend to the most extreme values of the distribution, no further than 1.5 times the interquartile range from the hinge. Data beyond the whiskers are identified as outliers with red dots. Locations that are not normally distributed will have *, **, *** above the graph indicating 0.05, 0.01, and 0.001 respectively. Normally distributed locations will have a "ns" above it. Normality was calculated by using the Shapiro-Wilk Test.

Yield SSI. 20 HUM had the largest IQR (0.472) for the yield SSI and 18 ASM had the smallest IQR (0.0576) for the yield SSI and the greatest ESI for yield (0.590) (Figure 2.18, Table 2.12).

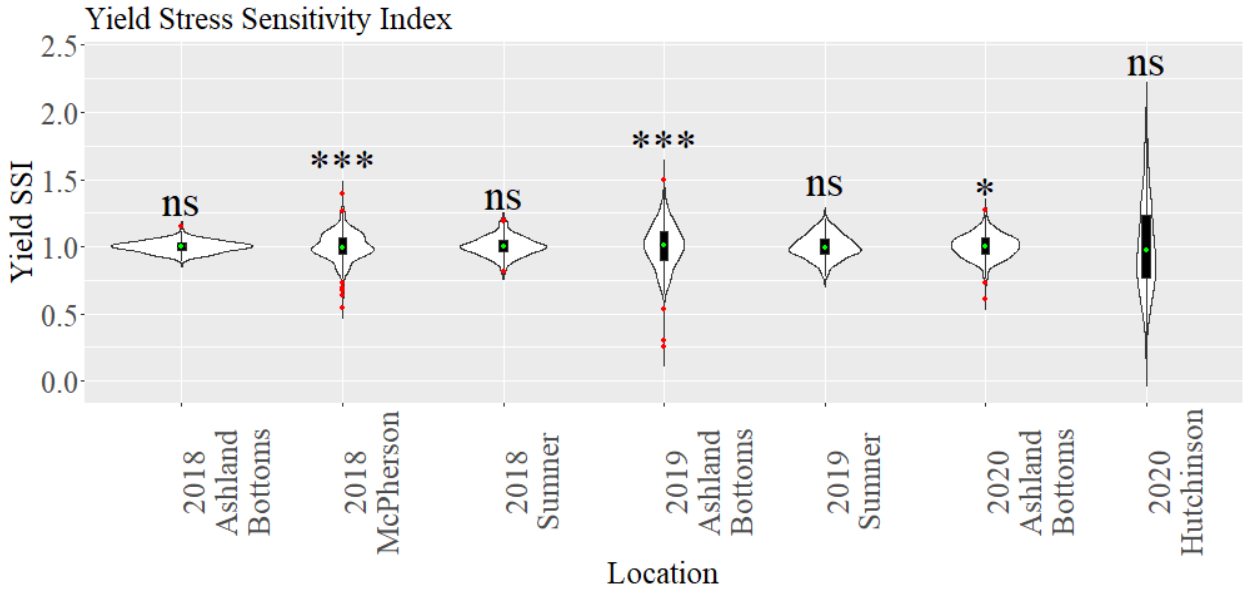

Figure 2.18 Distribution of the stress sensitivity indices for yield in seven environments, calculated relative to the best linear unbiased predictors across three high yield environments. The median is indicated by a green diamond. The ends of boxes indicate the first and third quartile of the distribution. Whiskers extend to the most extreme values of the distribution, no further than 1.5 times the interquartile range from the hinge. Data beyond the whiskers are identified as outliers with red dots. Locations that are not normally distributed will have *, **, *** above the graph indicating 0.05, 0.01, and 0.001 respectively. Normally distributed locations will have a "ns" above it. Normality was calculated by using the Shapiro-Wilk Test.

Reproductive phenology traits SSI. 20 ASM was used as the reference environment for the three reproductive phenology traits collected because these traits were only recorded at Ashland Bottoms in all three years. For all three reproductive phenology traits, 19 ASM had a much broader SSI distribution than 18 ASM (Figure 2.19). 19 ASM had a much lower ESI than 18 ASM for all three traits (Table 2.12).

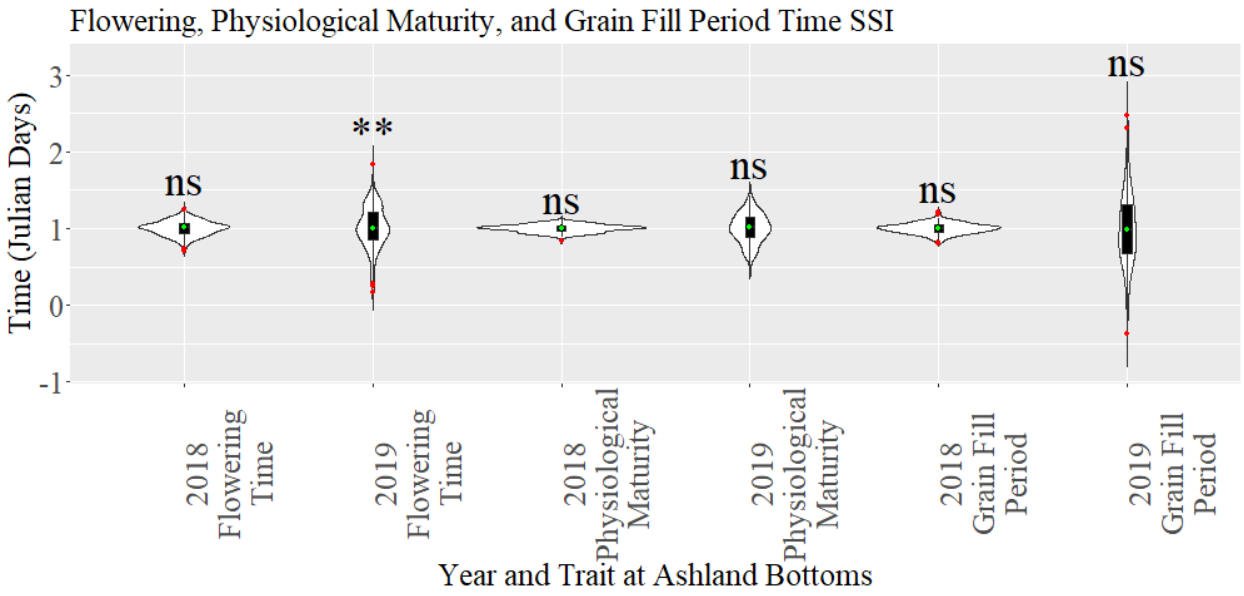

Figure 2.19 Distribution of the stress sensitivity indices for flowering time, physiological maturity time, and grain fill period in each of two environments, calculated relative to the best linear unbiased predictors across the high yield environment (20 ASM). The median is indicated by a green diamond. The ends of boxes indicate the first and third quartile of the distribution. Whiskers extend to the most extreme values of the distribution, no further than 1.5 times the interquartile range from the hinge. Data beyond the whiskers are identified as outliers with red dots. Locations that are not normally distributed will have *, **, *** above the graph indicating 0.05, 0.01, and 0.001 respectively. Normally distributed locations will have a "ns" above it. Normality was calculated by using the Shapiro-Wilk Test.

SSI correlation. The environmental stress indices for the yield component traits were highly correlated with one another. Test weight SSI (Figure 2.20B) was positively correlated between all pairs of environments. The weakest correlation was between 18 ASM and 20 ASM. The highest correlation was between 18 ASM and 18 SUM for the test weight SSI. All the 2018 locations were strongly, positively correlated with each other for the mean kernel diameter SSI (Figure 2.20C). The 2019 locations were weakly correlated with 18 ASM and 18 McP for the mean kernel diameter SSI. The strongest negative correlation for the mean kernel diameter SSI was between 18 SUM and 19 ASM. 20 ASM and 19 ASM had a strong positive correlation for the mean kernel diameter SSI.

Weak correlations generally were found for the kernel hardness SSI (Figure 2.20D). Strong negative correlations were found between 18 SUM and 18 ASM and 18 SUM and 18 McP for the kernel hardness SSI. 20 HUM and 19 ASM had a moderately strong, positive correlation for the kernel hardness SSI. The 2018 locations were positively correlated with all locations for the mean kernel weight SSI. The 2019 and 2020 locations were weakly to moderately correlated to the rest of the 2019 and 2020 locations for the mean kernel weight SSI (Figure 2.20E).

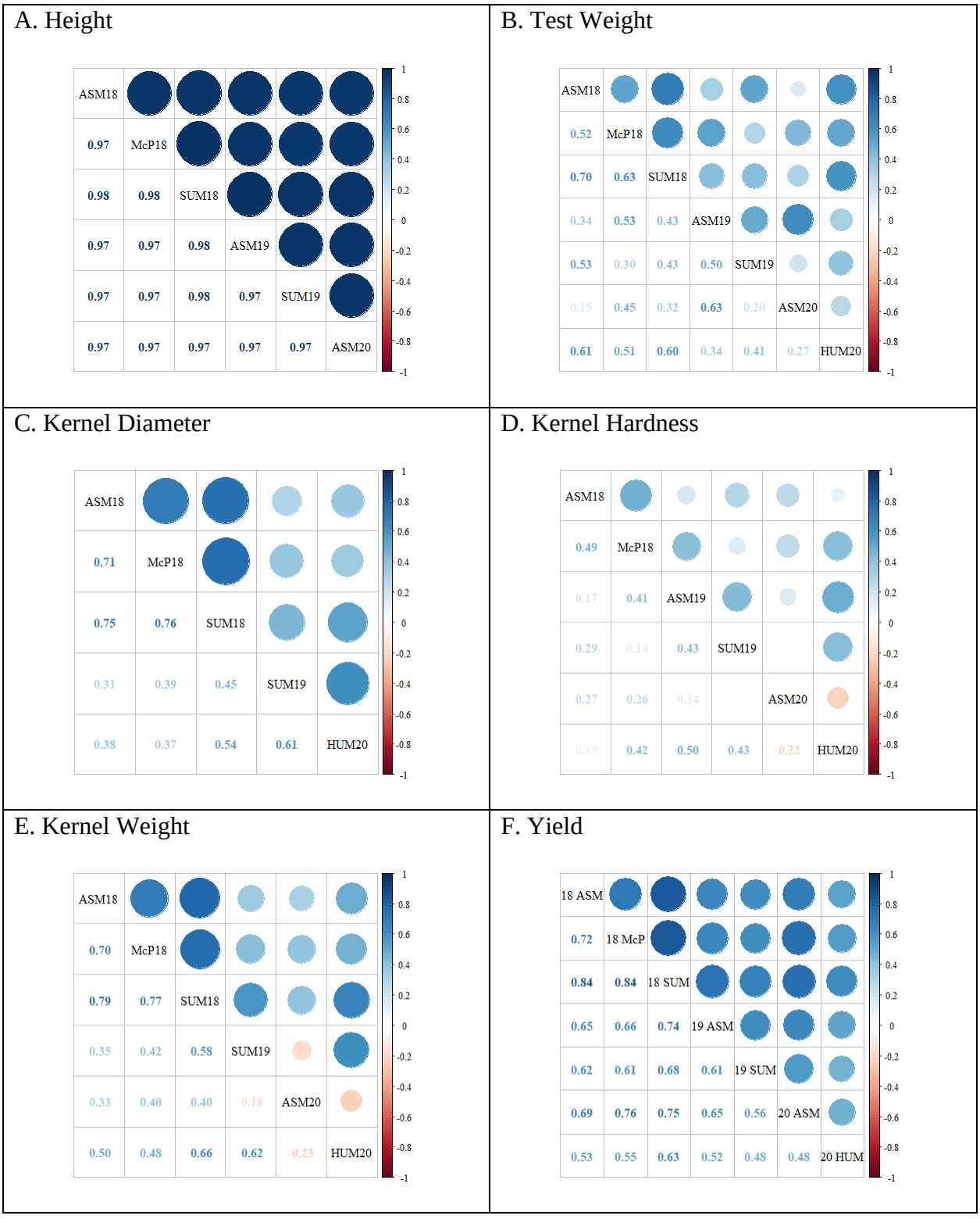

Figure 2.20 SSI Pairwise correlation. This was based on the SSI Pairwise correlations of stress sensitivity indices calculated at each environment for each response variable for the population of RILs.

Reproductive phenology trait SSI correlations. Flowering time SSI at 18 ASM was highly positively correlated with flowering time SSI at 19 ASM, but highly negatively correlated with the 18 ASM and 19 ASM grain fill period SSIs respectively. The flowering time SSIs at 18 ASM and 19 ASM were moderately positively correlated with the 18 ASM and 19 ASM physiological maturity time SSIs.

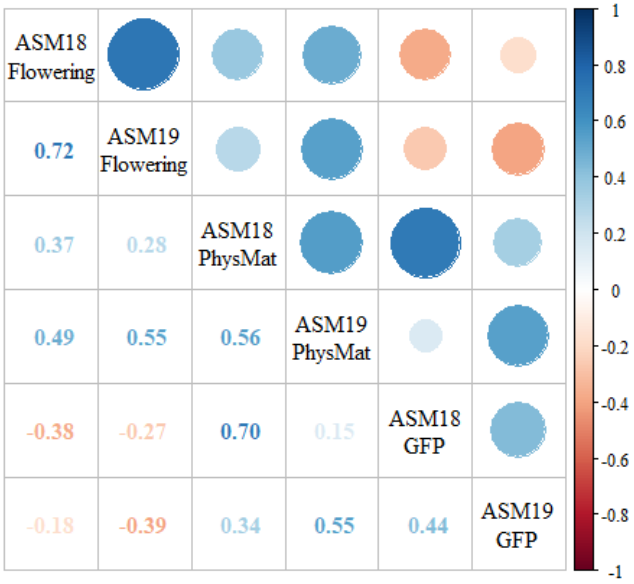

Figure 2.21 Pairwise correlation of stress sensitivity indices for reproductive phenology traits measured in the population of RILs at Ashland Bottoms in 2018 and 2019.

Correlation of SSI with control environment BLUPs. Calculating the SSI of a trait with the BLUP of a trait will show if having a higher value for a specific trait increases the stress sensitivity of a trait. Plant height SSIs in every environment were negatively correlated with BLUPs for height in the control environment (Table 2.13). This correlation indicates that the taller RILs were less sensitive to environmental stress as measured by reduction in plant height. Kernel diameter had small correlations for 18 ASM, 19 ASM, and 19 HUM. This low correlation indicates that kernel diameter in high yield environments is not predictive of response to stress. High yield site BLUP kernel weight had a small negative correlation for 18McP, 18 SUM, 19 ASM, and a moderate negative correlation with 18 ASM SSI. These low negative correlations suggest that RILs with smaller kernels in high yield environments may be better able to retain

kernel weight in stress environments. High yield site BLUP test weight was moderately and highly correlated with the 18 ASM, 18 SUM, 19 HUM,19 SUM, and 20 ASM SSIs. This indicates that RILs with high test weight in the high yield environments were less sensitive to environmental stress as measured by test weight. High yield site BLUP for yield had a small to moderate correlation with all the locations except for 19 ASM. This weak relationship indicates that yield in high yield environments is a poor predictor of tolerance to environmental stress as measured by yield. High yield site BLUP kernel hardness was moderately to highly positively correlated to all the locations' SSIs except for 18 SUM, with which it was highly negatively correlated. There is a negative relationship between these SSI by high yield BLUPs correlation and the ESI values for the respective traits at each location (Table 2.12, Table 2.13). In general, he higher the ESI, the lower the SSI correlation with high yield BLUPs.

Table 2.13 SSI by high yield best linear unbiased predictor (BLUP) correlations. The correlation between the SSI in each environment with the BLUP in the control environment for every trait.

Environment	Plant Height	Kernel Diameter	Test Weight	Yield	Kernel Hardness	Kernel Weight
18 ASM	-0.554***	-0.234***	-0.441***	-0.377***	0.516***	-0.316***
18 McP	-0.536***	-0.033ns	0.0801ns	-0.197**	0.401***	-0.0384ns
18 SUM	-0.549***	-0.117ns	-0.263***	-0.225**		-0.204**
19 ASM	-0.547***		0.00904ns	-0.128ns	-0.002ns	
19 HUM	-0.698***	0.148*	-0.257***	-0.193**	0.229***	0.0194ns
19 SUM	-0.525***	-0.0377ns	0.165*	-0.239***	0.219**	0.0596ns
20 ASM	-0.518***		-0.213**	-0.0281ns	0.0358ns	0.0382ns

*, **, *** indicate significance at $P < 0.05, 0.01, 0.001$, respectively; ns, non-significant.

Regression analysis. To further examine the relationship between stress sensitivity and performance in a control environment, we conducted linear regression analysis of the SSIs for selected trait × environment combinations on the high yield (control) BLUPs for the trait. Using the most stressful environment as an example (18 ASM), the stress sensitivity index for height decreased as the height in the control environment increased (Figure 2.22; $R^2 = 0.307$); the stress sensitivity index for test weight decreased as the test weight in the control environment increased (Figure 2.23; r^2=0.194); there was a low association between a reduction in stress sensitivity index for kernel diameter and higher kernel diameter (Figure 2.24; r^2=0.0546); and a reduction in stress sensitivity index for yield predicted a higher yield (Figure 2.25; r^2 =0.142).

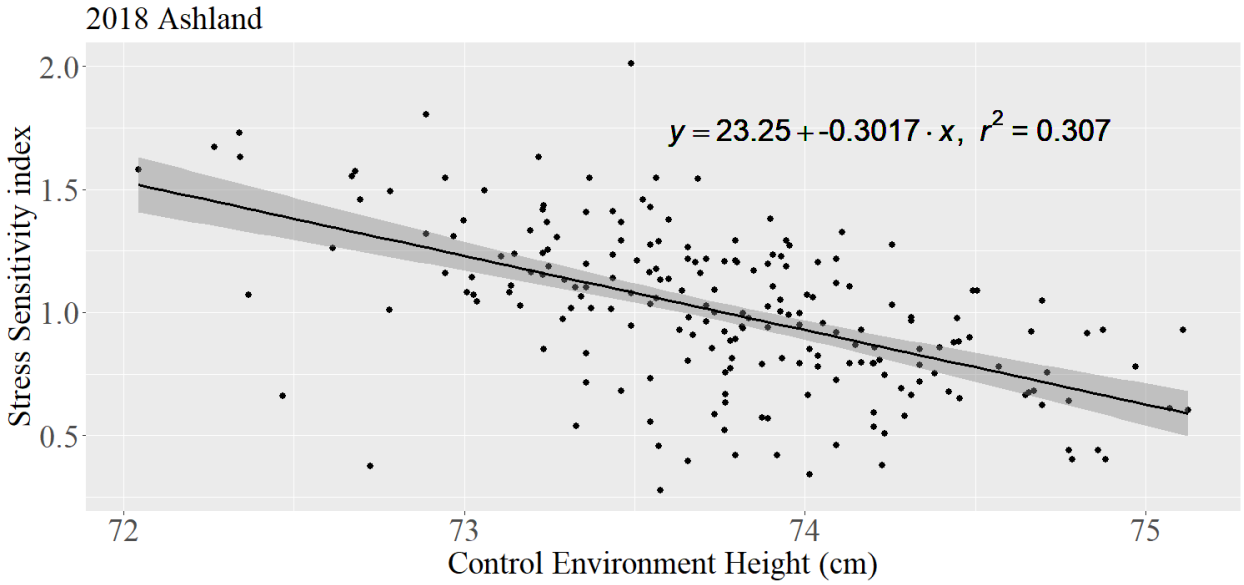

Figure 2.22 Stress sensitivity index for height of RILs at 18 ASM versus the best linear unbiased predictors of height in the control environment.

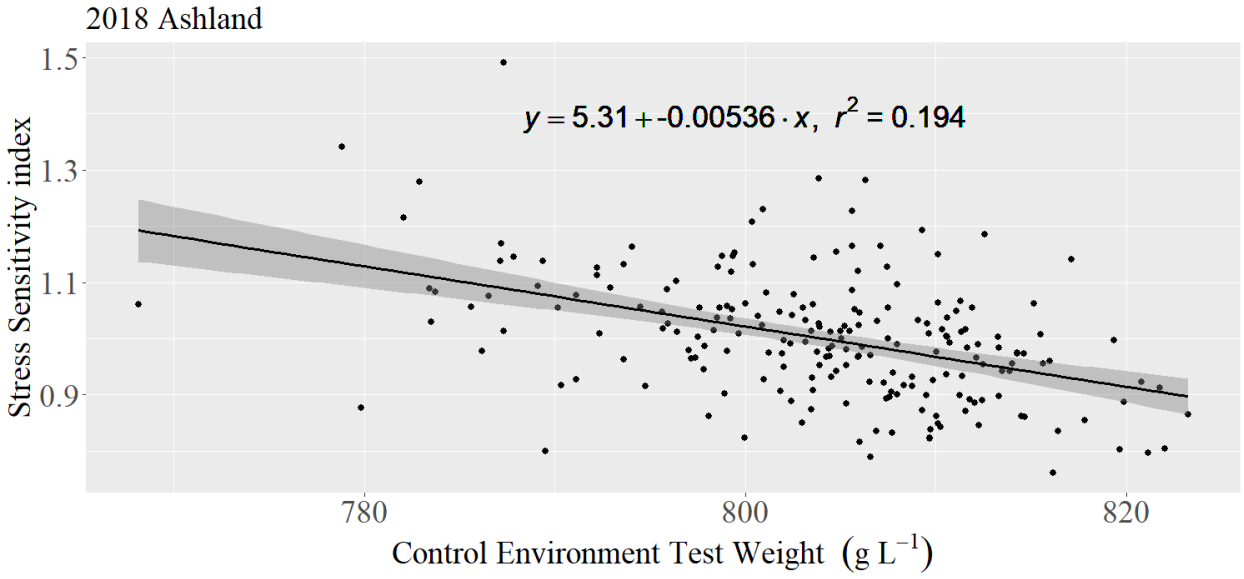

Figure 2.23 Stress sensitivity index for test weight of RILs at 18 ASM versus the best linear unbiased predictors of test weight in the control environment.

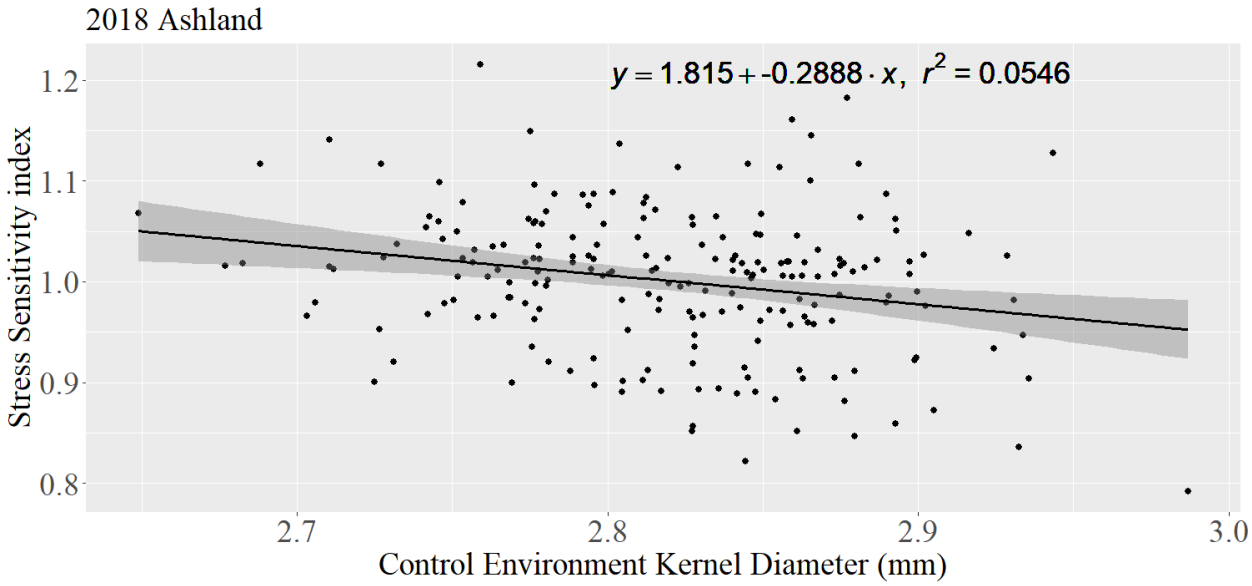

Figure 2.24 Stress sensitivity index for kernel diameter of RILs at 18 ASM versus the best linear unbiased predictors of kernel diameter in the control environment.

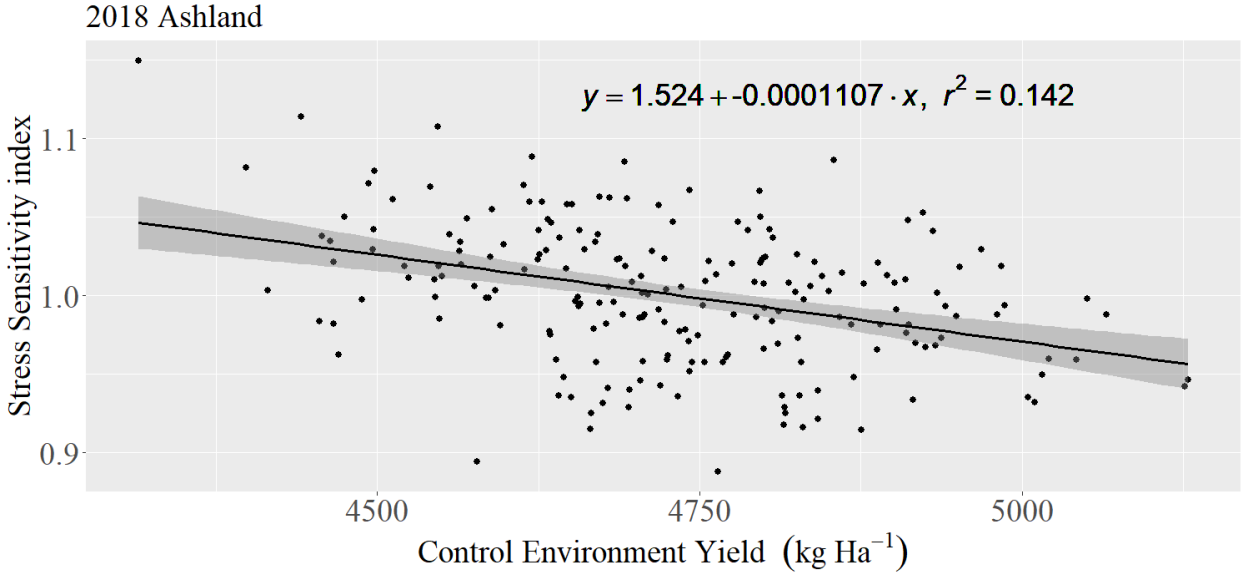

Figure 2.25 Stress sensitivity index for yield of RILs at 18 ASM versus the best linear unbiased predictors of yield in the control environment.

Genetic markers. KASP markers Vrn-D3-KASP, wMAS00026, BS_060270_51, and Kukric44369_131 were used to characterize the RIL population. Vrn-D3-KASP is associated with the *Vrn-D3* gene which has early release from vernalization and late release from vernalization phenotypes. The wMAS00026 marker is associated with the *Ppd-D1* gene which

has long day sensitive and long day insensitive phenotypes. HV9W03-1596R was characterized as having the late release from vernalization allele for the *Vrn-D3* gene and the long day insensitive allele for the *Ppd-D1* gene. TX04M410164 was characterized as having the early release from vernalization allele for the *Vrn-D3* gene and the long day sensitive allele for the *Ppd-D1* gene. Both of these genes affect the timing of anthesis initiation (Chen et al., 2010). BS_060270_51 and Kukric44369_131 are chromosome 1B markers putatively associated with heat tolerance in the segregating RIL population based on association mapping with this population and a successful parent test (to prove different marker calls for the two parents).

The Vrn-D3-KASP marker had significant associations with every trait BLUP except for grain fill period. The wMAS00026 marker had highly significant associations with every trait BLUP. The HV9W03-1596R allele of the BS_060270_51 marker had an average increase in kernel diameter BLUP of 0.00353 mm. The HV9W03-1596R allele of the BS_060270_51 marker had an average increase of test weight BLUP by 1.56 g L^{-1} and an average decrease in kernel weight by 0.0647 mg across all environments. The HV9W03-1596R allele of the Kukric44369_131 marker increased test weight BLUP by 0.584 g L^{-1}, yield BLUP by 21.6 kg ha^{-1}, and the grain fill period BLUP was decreased by 0.0975 days. The alleles of the *Vrn-D3* and *Ppd-D1* markers generally had a larger effect than the alleles of the BS_060270_51 or Kukric44369_131 markers (Table 2.14).

Table 2.14 Response of BLUPs to marker alleles estimated by regression analysis across all environments. Slope is expressed as the effect of the HV9W03-1596R allele. wMAS, Vrn-D3, Kukric44369, and BS_060270 are shortened and represent wMAS00026, Vrn-D3-KASP, Kukric44369_131, and BS_060270_51 respectively.

		Estimated slope			
Index	Units	Vrn-D3	wMAS	BS_060270	Kukric44369
Kernel diameter	Mm	-1.37E-02 ***	1.54E-02 ***	3.53E-03 **	-1.59E-03 ns
Kernel hardness		6.40E-01 ***	-3.07E-01 ***	2.37E-01 ***	-4.61E-01 ***
Kernel weight	mg	-4.15E-0 ***	2.54E-0 ***	-6.47E-02 *	-2.35E-02 ns
Test weight	g L^{-1}	-3.33E+00 ***	1.93E+00 ***	1.56E+00 ***	5.84E-01 *
Grain yield	kg ha^{-1}	6.24E+01 ***	-5.77E+01 ***	-2.20E+01 ***	2.16E+01 ***

Plant height	cm	1.28E-01 *	-1.23E+00 ***	1.58E-01 *	1.30E-01 *
Flowering time	Jd	4.80E-01 ***	-6.48E-01 ***	4.76E-02 ns	6.69E-02 ns
Grain fill period	Jd	5.70E-04 Ns	1.10E-01 ***	-6.05E-02 *	-9.75E-02 ***
Physiological maturity	Jd	4.20E-01 ***	-4.15E-01 ***	-4.30E-02 ns	-6.86E-02 ns

Linear model estimates are on top and the p-values are directly below where *, **, *** indicate significance at $P < 0.05, 0.01, 0.001$, respectively; ns, non-significant.

When locations were analyzed individually in the analysis, we could see where marker trait interactions were not significant and where they were significant. The only trait BLUP locations that were significant for the BS_060270_51 marker was test weight BLUP at 18 ASM (estimate = 4.57 g L^{-1}), 18 McP, 18 SUM, 20 HUM, Kernel hardness at 18 SUM, 19 SUM, 20 ASM, and 20 HUM (Table 2.16, Appendix A Table A. 1), yield at the high yield site (estimate = 20.5 kg ha^{-1}) (Table 2.15). The Vrn-D3-KASP marker was significant for every BLUP trait location shown except for the grain fill period BLUP and the height BLUP at every location as well as the kernel diameter BLUP at 20 ASM. The Kukric44369_131 marker was only significant for the physiological maturity BLUP at 19 ASM and the grain fill period BLUP at 18 ASM and 19 ASM. The wMAS00026 marker was significant for every trait at 18 ASM, every trait at the high yield synthetic site and all three reproductive traits at every location shown.

Table 2.15 Response of BLUPs across the high yield environment to marker alleles estimated by regression analysis. Slope is expressed as the effect of the HV9W03-1596R allele. wMAS, Vrn-D3, Kukric44369, and BS_060270 are shortened and represent wMAS00026, Vrn-D3-KASP, Kukric44369_131, and BS_060270_51 respectively.

		Estimated slope			
Index	Units	Vrn-D3	wMAS	BS_060270	Kukric44369
Kernel diameter	mm	1.39E-02 ***	-1.60E-02 ***	3.44E-03 ns	-2.01E-03 ns
Kernel hardness		-6.37E-01 ***	6.44E-01 ***	-1.05E-01 ns	-2.25E-01 ns
Kernel weight	mg	4.25E-01 ***	-2.86E-01 **	-1.08E-01 ns	-5.59E-02 ns
Test weight	g L^{-1}	2.87E+00 ***	-1.60E+00 *	-2.84E-03 ns	5.03E-01 ns

Grain yield	kg ha^{-1}	-4.71E+01 ***	4.32E+01 ***	-2.05E+01 *	1.96E+01 ns
Plant height	cm	-2.27E-02 ns	1.63E-01 ***	6.95E-03 ns	2.41E-02 ns

Linear model estimates are on top and the p-values are directly below where *, **, *** indicate significance at $P < 0.05, 0.01, 0.001$, respectively; ns, non-significant.

The Kukric44369_131 marker was only significant for the physiological maturity BLUP at 19 ASM and the grain fill period BLUP at 18 ASM and 19 ASM. The wMAS00026 marker was significant for every trait at 18 ASM, every trait at the high yield synthetic site and all three reproductive traits at every location shown (Table 2.16).

Table 2.16 Response of BLUPs by location to marker alleles estimated by regression analysis within each environment where reproductive trait data was recorded. Slope is expressed as the effect of the HV9W03-1596R allele. wMAS, Vrn-D3, Kukric44369, and BS_060270 are shortened and represent wMAS00026, Vrn-D3-KASP, Kukric44369_131, and BS_060270_51 respectively.

	Estimated slope								
Location Marker	Kernel diameter Mm	Kernel hardness	Kernel weight mg	Test weight g L^{-1}	Grain yield kg ha^{-1}	Plant height Cm	Flowering time Jd	Grain fill period Jd	Physiological maturity Jd
18_ASM	1.45E-02	-2.56E-01	4.03E-01	6.09E+00	-3.89E+01	-1.86E-01	-5.20E-01	2.87E-02	-4.21E-01
Vrn-D3	**	ns	***	***	***	Ns	***	ns	***
19_ASM	1.77E-02	-1.05E+00	5.23E-01	1.69E+00	-7.81E+01	-1.03E-01	-7.02E-01	-2.59E-03	-6.11E-01
Vrn-D3	***	***	***	*	***	Ns	***	ns	***
20_ASM	7.43E-03	-5.45E-01	2.80E-01	1.74E+00	-7.33E+01	-2.28E-01	-2.16E-01	-2.74E-02	-2.26E-01
Vrn-D3	ns	*	**	*	***	Ns	***	ns	***
18_ASM	4.67E-03	2.46E-02	1.70E-02	4.57E+00	-1.45E+01	1.15E-01	-4.49E-03	-6.53E-02	-8.89E-02
BS_060270	ns	ns	ns	**	ns	Ns	ns	ns	ns
19_ASM	-1.27E-03	3.41E-01	-1.77E-01	-4.50E-01	-2.28E+01	2.48E-01	9.66E-02	-6.57E-02	-1.08E-02
BS_060270	ns	ns	ns	ns	ns	Ns	ns	ns	ns
20_ASM	-2.71E-03	5.42E-01	-1.80E-01	-1.33E-01	-2.33E+01	2.35E-01	5.06E-02	-5.08E-02	-2.97E-02
BS_060270	ns	*	ns	ns	ns	Ns	ns	ns	ns
18_ASM	-8.61E-04	-6.89E-01	1.66E-02	1.19E+00	1.63E+01	1.51E-01	1.11E-01	-1.34E-01	-7.71E-02
Kukric4436	ns	**	ns	ns	ns	Ns	ns	**	ns
19_ASM	-1.63E-03	-4.82E-01	-1.37E-02	6.47E-01	2.52E+01	1.81E-01	7.25E-02	-1.70E-01	-1.61E-01
Kukric4436	ns	*	ns	ns	ns	Ns	ns	**	*
20_ASM	-7.92E-04	-4.07E-01	8.39E-03	4.25E-01	2.18E+01	1.81E-01	1.71E-02	1.11E-02	3.19E-02
Kukric4436	ns	ns	ns	ns	ns	Ns	ns	ns	ns
18_ASM	-1.88E-02	-6.38E-01	-2.72E-01	-5.93E+00	3.40E+01	1.45E+00	6.29E-01	-1.19E-01	3.91E-01
wMAS	***	**	**	***	**	***	***	*	***
19_ASM	-1.74E-02	6.40E-01	-2.69E-01	-8.70E-01	8.41E+01	1.42E+00	9.59E-01	-1.34E-01	6.40E-01
wMAS	***	**	*	ns	***	***	***	*	***

20_ASM wMAS	-8.75E-03 *	3.93E-01 ns	-1.18E-01 ns	8.72E-01 ns	6.40E+01 ***	1.40E+00 ***	3.57E-01 ***	-7.70E-02 *	2.14E-01 ***

Linear model estimates are on top and the p-values are directly below where *, **, *** indicate significance at $P < 0.05$, 0.01, 0.001, respectively; ns, non-significant.

Marker effects on SSIs. Kernel hardness SSI had no significant associations with any of the markers. Yield SSI was highly associated with the Vrn-D3-KASP and wMAS00026 markers but not significantly associated with the two chromosome 1B markers. The Vrn-D3-KASP and wMAS00026 markers had highly significant associations with flowering time SSI and physiological maturity SSI, but were not significantly associated with the grain fill period SSI. Kukric44369_131 marker was highly associated for the grain fill period SSI and physiological maturity SSI, but not for flowering time SSI. The BS_060270_51 marker was significant for kernel diameter SSI, test weight SSI, and plant height SSI (Table 2.17).

Table 2.17 Response of stress sensitivity indices to marker alleles estimated by regression analysis across all environments in which stress sensitivity was > 0.02. Slope is expressed as the effect of the HV9W03-1596R allele.

		Estimated slope			
Index		Vrn-D3-KASP	wMAS00026	BS_060270_51	Kukric44369_131
Kernel diameter	Estimate	1.30E+00	-6.53E-01	-2.22E+00	1.39E+00
	Pr(>|t|)	ns	ns	*	ns
Kernel hardness	Estimate	-3.35E-02	3.53E-03	1.39E-02	3.03E-03
	Pr(>|t|)	ns	ns	ns	ns
Kernel weight	Estimate	2.54E-02	-1.26E-02	2.58E-02	-5.72E-02
	Pr(>|t|)	ns	ns	ns	*
Test weight	Estimate	-3.43E-03	1.07E-02	-2.87E-02	-2.35E-03
	Pr(>|t|)	ns	ns	***	ns
Grain yield	Estimate	-2.07E-02	1.91E-02	3.11E-03	-5.72E-03
	Pr(>|t|)	***	***	ns	ns
Plant height	Estimate	-1.93E-02	1.67E-01	-2.40E-02	-1.78E-02
	Pr(>|t|)	ns	***	*	ns
Flowering time	Estimate	-7.95E-02	9.21E-02	-2.22E-03	-1.27E-02
	Pr(>|t|)	***	***	ns	ns
Grain fill period	Estimate	9.26E-03	-2.19E-02	6.88E-03	6.25E-02
	Pr(>|t|)	ns	ns	ns	***
Physiological maturity	Estimate	-4.01E-02	4.31E-02	2.85E-04	1.96E-02
	Pr(>|t|)	***	***	ns	**

***, **, *** indicate significance at *P* < 0.05, 0.01, 0.001, respectively; ns, non-significant.**

When locations were analyzed individually in the analysis, we could see where marker trait interactions were not significant and where they were significant. The BS_060270_51 marker only had a significant effect on kernel diameter SSI at 20 ASM. The Vrn-D3-KASP and

wMAS00026 markers were significant for flowering time and physiological maturity SSIs at every location where the traits were measured but had no significant effect on the grain fill period. The *Vrn-D3* gene controls the timing of release from vernalization and the *Ppd-D1* gene is for sensitivity or not to initiate flowering based on if the long day requirement is met so neither of these genes should have an effect on the grain fill period. The only marker that had an effect on the grain fill period SSI at any location was the Kukric44369_131 marker at both locations measured (Table 2.18, Table 2.19).

Table 2.18 Response of stress sensitivity indices by location to marker alleles estimated by regression analysis across all environments in which reproductive traits were recorded and stress sensitivity was > 0.02. Slope is expressed as the effect of the HV9W03-1596R allele. wMAS, Vrn-D3, Kukric44369, and BS_060270 are shortened and represent wMAS00026, Vrn-D3-KASP, Kukric44369_131, and BS_060270_51 respectively. Linear model estimates are on top and the p-values are directly below where *, **, *** indicate significance at P < 0.05, 0.01, 0.001, respectively; ns, non-significant.

		Estimated Slope		
Marker	Location	Flowering time	Grain fill period	Physiological maturity
Vrn-D3	18 ASM	-4.04E-02	5.06E-03	-1.26E-02
		***	ns	***
Vrn-D3	19 ASM	-1.18E-01	1.31E-02	-6.74E-02
		***	ns	***
wMAS	18 ASM	3.72E-02	-7.09E-03	1.14E-02
		***	ns	**
wMAS	19 ASM	1.46E-01	-3.63E-02	7.45E-02
		***	ns	***
BS_060270	18 ASM	7.52E-03	3.16E-03	3.91E-03
		ns	ns	Ns
Kukric44369	18 ASM	-1.16E-02	1.52E-02	6.52E-03
		ns	**	Ns
Kukric44369	19 ASM	-1.33E-02	1.09E-01	3.30E-02
		ns	**	**

Table 2.19 Response of stress sensitivity indices by location to marker alleles estimated by regression analysis across all environments in which stress sensitivity was > 0.02. Slope is expressed as the effect of the HV9W03-1596R allele. wMAS (*Ppd-D1*), Vrn-D3, Kukric44369, and BS_060270 are shortened and represent wMAS00026, Vrn-D3-KASP, Kukric44369_131, and BS_060270_51 respectively. Linear model estimates are on top and the p-values are directly below where *, **, *** indicate significance at P < 0.05, 0.01, 0.001, respectively; ns, non-significant.

		Estimated Slope				
Marker	Location	Kernel diameter	Kernel weight	Test weight	Grain yield	Plant height
Vrn-D3	18 ASM	6.47E-03	1.17E-02	2.59E-02	-7.25E-03	-2.04E-02
		ns	*	***	*	ns
Vrn-D3	19 ASM	-1.56E-01	1.93E-01	-5.99E-02	-4.14E-02	-1.43E-02
		ns	ns	*	***	ns
Vrn-D3	20 ASM	9.07E+00	-5.94E-02	-3.44E-02	-2.56E-02	-3.46E-02
		ns	ns	*	***	ns
wMAS	18 ASM	-1.24E-02	-8.32E-03	-3.19E-02	6.46E-03	1.58E-01
		*	ns	***	*	***
wMAS	19 ASM	2.34E-01	-1.32E-01	3.89E-02	4.89E-02	2.12E-01
		ns	ns	ns	***	***
wMAS	20 ASM	-4.47E+00	3.71E-02	8.07E-02	2.14E-02	2.05E-01
		ns	ns	***	***	***
BS_060270	18 ASM	-3.93E-03	-1.00E-02	-3.11E-02	2.13E-03	-1.33E-02
		ns	ns	***	ns	ns
BS_060270	20 ASM	-1.48E+01	7.64E-02	4.13E-03	6.10E-03	-3.78E-02
		*	ns	ns	ns	ns
Kukric44369	18 ASM	-1.58E-03	-5.64E-03	-5.00E-03	-3.15E-03	-1.56E-02
		ns	ns	ns	ns	ns
Kukric44369	19 ASM	2.79E-01	-2.95E-01	-8.65E-03	-8.84E-03	-2.67E-02
		ns	ns	ns	ns	ns
Kukric44369	20 ASM	9.10E+00	-8.32E-02	2.06E-03	-5.69E-03	-2.59E-02
		ns	*	ns	ns	ns

Marker combination effects on BLUPs. The effect of combinations of *Vrn-D3* and *Ppd-D1* alleles was evaluated by analysis of variance using the four combinations of markers as a fixed effect (0_0 = TX04M410164 alleles at *Vrn-D3* and *Ppd-D1;* 2_2 =HV9W03-1596R alleles at both loci). The marker combination of (2_0) resulted in the highest yield, latest maturity, hardest kernels, and tied for the tallest plants at all locations where these traits were recorded. This combination of alleles also resulted in the worst test weight, kernel diameter, and kernel weight.

There is a clear genotypic effect and environmental effect but very little genotype by environment effect for these marker combinations (Table 2.20).

Table 2.20 Response of BLUPs by location to marker allele combinations for the flowering time physiology traits estimated by regression analysis across all environments where reproductive trait data was recorded.

Marker Combination	Location	Kernel Diameter	Test Weight	Yield	Kernel Hardness	Kernel Weight	Height	Grain Fill Period	Flowering Time	Physiological Maturity
Vrn_Ppd		mm	g L^{-1}	kg ha^{-1}		mg	cm	Jd	Jd	Jd
0_0	18_ASM	2.36	658.86	1954.71	65.72	21.13	66.69	23.11	130.26	153.28
0_2	18_ASM	2.40	661.19	1805.02	65.03	21.79	63.95	23.36	128.97	152.50
2_0	18_ASM	2.34	651.15	2058.90	66.87	20.44	66.68	23.21	131.20	154.23
2_2	18_ASM	2.37	656.85	1959.19	66.58	20.88	64.69	23.37	129.95	153.35
0_0	18_McP	2.56	766.46	3172.52	74.37	25.40	55.22			
0_2	18_McP	2.60	768.79	3022.83	73.68	26.06	52.49			
2_0	18_McP	2.54	758.75	3276.71	75.52	24.71	55.21			
2_2	18_McP	2.57	764.45	3177.00	75.23	25.15	53.22			
0_0	18_SUM	2.48	727.80	2981.88	78.45	23.84	58.25			
0_2	18_SUM	2.51	730.14	2832.18	77.76	24.51	55.51			
2_0	18_SUM	2.45	720.10	3086.06	79.60	23.16	58.23			
2_2	18_SUM	2.48	725.79	2986.35	79.31	23.59	56.24			
0_0	19_ASM	2.85	787.51	3718.74	70.67	30.12	69.06	30.69	133.73	164.33
0_2	19_ASM	2.89	789.84	3569.04	69.98	30.78	66.32	30.94	132.44	163.54
2_0	19_ASM	2.83	779.80	3822.92	71.82	29.44	69.04	30.79	134.67	165.28
2_2	19_ASM	2.86	785.49	3723.21	71.53	29.87	67.05	30.95	133.41	164.40
0_0	19_HUM	2.86	787.04	4532.04	74.33	30.51	74.18			
0_2	19_HUM	2.90	789.37	4382.34	73.64	31.17	71.44			
2_0	19_HUM	2.84	779.33	4636.22	75.48	29.82	74.17			
2_2	19_HUM	2.87	785.03	4536.52	75.19	30.26	72.17			
0_0	19_SUM	2.64	751.53	2980.98	60.39	25.67	70.35			
0_2	19_SUM	2.68	753.86	2831.28	59.70	26.33	67.61			
2_0	19_SUM	2.62	743.82	3085.16	61.55	24.99	70.33			
2_2	19_SUM	2.65	749.52	2985.46	61.26	25.42	68.34			

0_0	20_ASM	2.82	775.43	3025.77	72.59	29.02	68.94	32.35	137.86	170.12
0_2	20_ASM	2.86	777.76	2876.07	71.90	29.68	66.21	32.60	136.57	169.34
2_0	20_ASM	2.80	767.72	3129.95	73.74	28.33	68.93	32.45	138.79	171.07
2_2	20_ASM	2.83	773.42	3030.25	73.45	28.76	66.94	32.61	137.54	170.19
0_0	20_HUM	2.64	745.97	3851.42	61.64	26.57				
0_2	20_HUM	2.68	748.30	3701.72	60.96	27.23				
2_0	20_HUM	2.62	738.26	3955.60	62.80	25.88				
2_2	20_HUM	2.65	743.96	3855.89	62.51	26.31				
0_0	20_KGM	2.79	831.28	4862.57	78.50	30.28				
0_2	20_KGM	2.83	833.62	4712.87	77.81	30.94				
2_0	20_KGM	2.77	823.58	4966.75	79.65	29.60				
2_2	20_KGM	2.80	829.27	4867.04	79.36	30.03				
0_0	20_SUM	2.82	805.90	4834.60	75.79	30.95				
0_2	20_SUM	2.86	808.24	4684.90	75.10	31.61				
2_0	20_SUM	2.80	798.19	4938.78	76.94	30.26				
2_2	20_SUM	2.83	803.89	4839.07	76.65	30.70				
0_0	HYD	2.81	805.47	4738.24	76.76	30.51	74.95			
0_2	HYD	2.85	807.80	4588.54	76.07	31.18	72.21			
2_0	HYD	2.79	797.76	4842.42	77.92	29.83	74.93			
2_2	HYD	2.82	803.46	4742.71	77.63	30.26	72.94			

Discussion

Winter wheat yields vary drastically due in part to the environment. This is evident in the field trials where we had more than 2.5 times higher yield in the highest yielding environment compared to the lowest yielding environment (Table 2.5), which is typical for wheat yield variability across environments in this region (e.g., Cruppe et al., 2021; Giordano et al., 2024; Jaenisch et al., 2019; Munaro et al., 2020).

The combined analysis of performance in the three highest yielding environments for our high yield environment was done to minimize any outlier effect that the single highest yielding location may have had on any of the traits measured. We could have planted trials in areas more likely to get heat stress and areas more likely to be non-heat stress environments by planting trials farther northwest and farther south but we would have had other factors become more significant, for instance our wheat might be more adapted to Oklahoma and less adapted to Nebraska and our results would suffer. Broadened or shortened day length would have played a larger role especially because our population is segregating for reproductive phenology traits like the photoperiod sensitivity trait: wMAS (*Ppd-D1*) or the early release from vernalization trait, *Vrn-D3*. We attempted to create a range in heat stress conditions by establishing the trials at a latitudinal gradient spanning from southern locations (Sumner, Hutchinson) to northern locations (Ashland Bottoms) since this naturally results in different temperature regimes (Lollato et al., 2020). Another reason we didn't plant trials farther northwest and farther south is that would have been inconvenient to the breeding program to plant at locations outside our normal farms. If we were working with spring-planted crops, we could have manipulated the environment for heat stress by planting later, but we cannot do that in winter wheat because planting later has other

effects on the winter wheat's physiology such as reduced tillering and other confounding effects that affect yield. Also, winter wheat has genes affecting release from vernalization timing that would minimize the effect of planting date. Planting this trial over three years also helped us obtain heat stressed (2018) and non-heat stressed environments (2019 and 2020). The three environments with the coolest temperature during the grain fill period were the three 2019 locations (Table 2.4, Figure 2.1, Figure 2.4). Only one of the three coolest temperature environments were included in the high-yield environment (19 HUM). Planting over multiple years proved more effective at obtaining heat stressed environments and non-heat stressed environments than the planting locations did. This is the most vulnerable time for wheat yield potential. Heat stress post anthesis limits the photosynthate potential by shortening the grain fill period (Bheemanahalli et al., 2019; Prasad & Djanaguiraman, 2014). In the future, we could also conduct a study with our results based on drought stress by using the weather data to select drought stressed and non-drought stressed environments and see if there are any of the same associations to the current study. It is important to note that this population was created by crossing two parents screened for two different mechanisms of heat stress tolerance. There was no screening of drought stress tolerance ever conducted for the parents or the RIL population itself. We could also have irrigated trials across different temperature environments to minimize the effect of water/ drought on our results.

The weather in 2018 was cooler in mid to late April but turned very warm for almost all of May during the grain fill period. By contrast, weather in 2019 was warmer for March and April, and much cooler in May during grain fill. We suspected this weather pattern would lengthen the grain fill period, which it did from 2018, but 2020 still had a significantly longer grain fill period than 2018 and 2019 for our field trials at Ashland (Table 2.6). This may be due

in part to 19 ASM receiving most of its rainfall during the grain fill period (Figure 2.2). 19 ASM had significantly higher test weight than 20 ASM (786 g L^{-1} and 773 g L^{-1} respectively) and 19 ASM had significantly higher kernel weight than 20 ASM (30.0 and 28.9 respectively) (Table 2.6). Weather for the three years seemed to be “hot and dry” or “cool and wet” (Figure 2.1, Figure 2.2) Because of this, we may have confounded tolerance to drought stress and tolerance to heat stress.

The importance of a long grain fill period was highlighted by the two highest yielding checks that also had the longest grain fill period. Our correlations also showed that flowering time was negatively corelated with the grain fill period (Figure 2.21) meaning our earlier flowering lines had longer grain fill periods. This is a common heat tolerance by avoidance strategy. This should provide merit to breeding for longer grain fill periods in wheat lines. The parents TX04M410164 and HV9W03-1596R having different grain fill periods as the result of genotype by environment interaction (Table 2.7) are supported by Fu et al., (2023) where HV9W03-1596R was identified as having a heat tolerance mechanism described as low percentage loss of chlorophyl content under post anthesis heat stress and TX04M410164 was identified as having a large percentage loss of chlorophyl content under terminal heat stress. Our results are consistent with the results of (Fu et al., 2023), where TX04M410164 was described as having a high seed weight per plant (not statistically significant from HV9W03-1596R) and a high single seed weight under terminal heat stress (not statistically significant from HV9W03-1596R) and HV9W03-1596R was described as being moderate for both of these traits (Table 2.6, Table 2.7, Table 2.8).

All the yield traits, kernel traits, and flowering time were highly heritable, and physiological maturity and grain fill period were not (Table 2.9), which may be a consequence of

these traits being measured in the fewest environments. Plant height, kernel diameter, and kernel weight all had high ratio of $\sigma^2_g/\sigma^2_{g\times e}$, suggesting these traits are controlled by genetics much more than a genotype x environment interaction. This does not mean that genetics control the expression of these traits more than the environment by itself, rather, it means that differences among genotypes are relatively consistent across environments. Yield, physiological maturity, grain fill period, and kernel hardness were controlled by the genotype x environment interaction more than by genetics alone.

Our results showed the pairwise correlation of height and yield was low. This does not support the results of (Fischer & Maurer, 1978) where they found that shorter wheats had higher yield potential. This was thought to be because of the plants allocating more photosynthate to grain filling and number rather than allocating it to plant biomass.

The non-normal distribution in some of the BLUPs could be due to the population's segregating for a limited number of genomic regions that have an effect on test weight, yield, kernel diameter, kernel hardness, individual kernel weight, the reproductive traits or the SSIs of those traits under terminal heat stress (Figure 2.7, Figure 2.8, Figure 2.6, Figure 2.9, Figure 2.10, Figure 2.12). 18 ASM was a location that experienced heat stress at the flowering and grain fill period (Table 2.4) so we should see the highest chance of seeing a non-normal distribution for kernel diameter, test weight, and kernel weight from the plants grown in this location. We only saw a non-normal distribution from the test weight BLUPs trait (Figure 2.7).

The increase in kernel diameter does not seem to translate to increased test weight (Table 2.10). This could be due to larger diameter kernels being less dense. We did see very similar results from the kernel weight BLUPs graph (Figure 2.10). A difference is that the kernel diameter BLUPs skewed slightly larger in diameter, while the kernel weight BLUPs skewed

slightly lower in weight. The shape of the yield BLUP distributions at each location varied. We can attribute this to yield being highly dependant on environment and genotype x environment interaction (Figure 2.8). Kernel hardness BLUPs were interesting because the high yield site, 20 SUM, 19 SUM, 18 SUM, and 18 McP all seemed to have bimodal distributions, but only 20 KGM was statistically non-normal (Figure 2.9). This does not seem to have a reasonable explanation because the second average hardest kernel location and the softest kernel location both have bimodal distributions, but the second softest kernel location and the hardest kernel location do not have a bimodal distribution. This might have something to do with the specific field conditions and timing of harvest. Our RIL population was segregating for physiological maturity and had population maturity windows of 7 days to 9 days in the locations in which we recorded physiological maturity (Figure 2.12). This large window might make the later maturing wheats softer if harvest was too close to physiological maturity. Some locations also received rain or were very humid or were very hot and dry in the week before harvest and up to harvest. If the wheat in a trial matures and dries down to harvest moisture and stays in the field too long, the weathering of the kernels can also decrease hardness. All these factors affect wheat kernel hardness. The kernel hardness trait demonstrated a large genotype x environment effect as evidenced by how different the distributions were. Flowering time BLUPs were heavily dependent on the environment and 2018 and 2019 had a non-normal distribution, probably due to the RIL population segregating for a vernalization gene (*Vrn-D3*) and a photoperiod requirment gene (*Ppd-D1*), both genes affect flowering time. The 2019 flowering time trait at Ashland Bottoms had a much longer distribution than in 2018 and 2020. 2019 was the least heat stressed year at Ashland Bottoms, which may have led to the broader range of flowering times within the population. Oddly enough, 2020 flowering time had the shortest distribution but the latest

average flowering time. 20 ASM was neither the highest nor lowest yielding location, and it was neither the most stressed nor least stressed location. 20 ASM also accumulated growing degree days at a similar rate to 18 ASM and more than 19 ASM, so that would not account for the late flowering time. 20 ASM had the longest mean grain fill period BLUPs. Temperature was warmer at the start of flowering at 20 ASM (30°C) and got much cooler through grain fill (10°C) while 19 ASM started cool (14.3°C) and ended warm (29°C). 18 ASM was warm during the entire time the plants were flowering and filling grain (28.4 °C to 31.5°C). The hot temperatures of the 2018 growing season shortened the time to physiological maturity, consequently shortening the grain fill period. The mean grain fill period was only two or three days apart from 2019 to 2020, consistant with the similar tempratures in the grain fill period. However, 18 ASM had much warmer temperatures during the grain fill period than 19 ASM and 20 ASM. This resulted with 18 ASM having the shortest grain fill period by about 7.5 days. 18 ASM had the lowest kernel weight BLUPs, followed by 18 SUM and 18 McP, indicating that the heat stress of the 2018 growing season negatively affected kernel weight. Test weight BLUPs had more variability across locations than individual kernel weight BLUPs. One would think that 19 ASM would have had the longest grain fill period because it was roughly 2°C cooler than 20 ASM during flowering and grain fill.

Yield was the most sensitive to environmental stress intensity with the largest ESI values (Table 2.12). This is probably due to yield having the longest timeframe when it can be affected among of all the traits measured. Also, there are more genes that affect yield than any of the other traits we measured. Stress primarily harms the plant's efficiency to turn water, CO^2, and sunlight into photosynthates. Some traits may not have been affected by the environmental stress because the stress was applied at a time when the physiology of the plant was not contributing to

the formation of that trait. For instance, 19 ASM ranked 5th in yield but had no environmental stress for kernel diameter (-0.00957) or kernel weight (0.0181) (Table 2.12, Table 2.5). This is stress tolerance by avoidance. Yield forming factors include plants per area, tillers per plant, heads per tiller, seeds per head, and average seed weight. Kernel weight is heavily influenced by the source sink interaction during the grain fill period. Yield is mostly sink limited in wheat (Borrás et al., 2004; Jaenisch et al., 2022) and thus the sum of the yield components must be sink limited. The window for environmental stress to affect yield is the whole growing season, starting at planting. The window for environmental stress to affect kernel weight is effectively between booting and maturity (Calderini et al., 2001; Jaenisch et al., 2022). The environment for 19 ASM was warmer than most locations in April, received a moderate amount of precipitation in April while receiving significantly more precipitation during the grain fill stage while simultaneously being cooler than most other locations (Figure 2.1, Figure 2.2). We can infer that yield forming factors tillers per plant would be negatively affected by the early season stress but the grain fill period had cool temperatures and plenty of precipitation to supply more photosynthates to the fewer kernels that remained after the early season stress.

Test weight, kernel diameter, individual kernel weight (with the exception of 20 ASM) SSI distributions all had very similar shaped distributions, while plant height, yield, flowering, physiological maturity, grain fill period time, and kernel hardness SSI distributions did not. This suggests that test weight, kernel diameter, and individual kernel weight are affected by heat stress in a similar way by sharing a lot of the same physiological pathways. For instance, heat stress in the vegetative stage would not affect these traits nearly as much as post anthesis heat stress. Our results support this idea because these three trait BLUPs (test weight, kernel diameter, and individual kernel weight) were highly correlated with each other (Table 2.10). All three traits

measure photosynthate accumulation into the wheat kernel. Thus, times of stress would affect all three of these traits fairly similarly because these traits are actively forming at the same time. Increasing temperature has been shown to reduce the yield response to nitrogen and is associated with a shorter critical period and a lower rate of assimilation per physiological time of wheat in the late season (Sadras et al., 2022). Plant height is constantly affected by environmental factors such as wind, soil moisture, and fertility, and it is also affected by manageable factors such as genetics and plant population density (Jaenisch et al., 2019; Korzun et al., 1998; Pinto et al., 2010). Yield is affected by the same factors that affect plant height, but stress at any stage limits yield in different ways. Stress during the early vegetative stages limits yield by reducing the number of tillers per plant. Stress during late vegetative stages limits yield by reducing the number of spikelets per tiller and florets per spikelet. Stress during the reproductive stages limits yield by increasing kernel abortion and reducing individual seed weights. It was interesting that 18 ASM had the least amount of variation for the flowering SSI, and 19 ASM had the most variation for flowering SSI. 18 ASM was clearly a more stressed environment than 19 ASM (Table 2.11, Table 2.12, Figure 2.19), so we would expect to see 18 ASM to have the highest amount of variation for the flowering SSI if the heat tolerance genes have an effect on flowering date under terminal heat stress unless the stress is so great, it overcomes the minor mechanisms of tolerance. In other words, the heat stress of 18 ASM could have been so extreme that the heat tolerance genes could not even keep up. Even with heat tolerance genes, wheat is still a C3 grass and was never adapted for such extreme heat. The same phenomenon was true for the grain fill period SSI where 18 ASM had much less variation than 19 ASM when we would expect the opposite (especially if the population has segregated for a stay green phenotype). The differences in most trait SSI variances being so different between 18 SUM and 18 McP and the rest of the

locations is probably due to 2018 being extremely hot and dry but 18 SUM and 18 McP being even drier than 18 ASM. This made four similar environmental groups; the control group (19 HUM, 20 KGM, 20 SUM) with the least stressed growing conditions, the most stressed group (18 ASM, 18 SUM and 18 McP), and the intermediate group (19 ASM, 20 HUM, 19 SUM) (Table 2.12).

Past research showing "accelerated leaf senescence during grain filling, leading to reduced photosynthesis and assimilate supply to the developing grains" (Bheemanahalli et al., 2019), can provide an explanation for the reduction in kernel diameter, test weight and individual kernel weight but further research is needed for us to say that accelerated leaf senescence during grain filling is what led to the reduction in these traits under more stressful environments.

The SSI correlations for test weight make sense because the growing conditions at the time test weight would have been affected by the environment the most were similar amongst the locations that were highest correlated. For example, 18 ASM was very dry and hot during reproductive stages, while 20 ASM was wet and cool during reproductive stages, and we see that 18 ASM and 20 ASM have the weakest correlation for test weight SSI. Conversely, 18 SUM was very hot and dry during reproductive stages and was more highly correlated with 18 ASM than any other location. All the 2018 locations had similar environments during the grain fill period. We see highly positive correlations for the 2018 locations for kernel diameter SSI trait. 2018 and 2019 had the most different growing seasons out of the three years, and kernel diameter SSIs were weakly correlated. Kernel diameter SSI seemed to be impacted the most by the environment. Kernel weight SSI was also highly impacted by the environment. The 2020 locations for kernel weight SSI were highly variable, and this variability might be due to very similar kernel weights in the environments used to calculate the SSI. This would make the

correlations between SSIs variable as well. Flowering time SSI and grain fill period SSI were negatively correlated, suggesting the higher stress susceptibility of flowering time, the lower stress susceptibility of the grain fill period. For future QTL mapping, plant height, test weight, yield, and the three reproductive traits appear to have predictable phenotypes across environments, and thus using the average SSI across all locations would be informative. Kernel diameter, kernel hardness, and kernel weight had less predictable phenotypes across environments and QTL mapping should be done on a per location basis.

We found that the taller wheat is, the lower the stress sensitivity index is at a rate of -0.302 SSI cm^{-1}. This finding is supported by the findings of Fischer and Maurer. Fischer and Maurer found that the shorter plants of various small grains (bread wheats, durum wheats, triticales, and barleys) had a higher yield potential than the taller plants, but the shorter small grains lost a much higher percentage of yield in the drought environments when compaired to the nonstress environment (Fischer & Maurer, 1978). This finding is similar with the findings of this experiment where the shorter plants experienced the highest negative effects on yield in the stress environments (Table 2.10). Fischer and Maurer found that the tallest bread wheats (mean height of 120 cm) kept an average of 51.7% of the yield potential while the shortest bread wheats (mean height of 53 cm) kept an average of 37.6% of the yield potential (Fischer & Maurer, 1978) (Table 6). Kernel diameter and test weight SSIs did not have high correlations with the respective BLUPs. This is probably because these traits are heavily influenced by the environment. Another trait in the plant would have to tolerate the stress in the environment to increase test weight or kernel diameter such as plant height or flowering time. This finding is also supported by Tack et al. where Kansas verieties from the 1960's are less sensitive to temperatures above 34°C (Tack et al., 2015).

One of the biggest challenges of heat stress field trials is controlling the inherent variability in field trials. Usually, researchers replicate within a location to account for field variability and apply treatments in a randomized fashion. It is very difficult to apply heat stress to a field trial in a replicated fashion. A common way to test the effect of post anthesis heat stress alone would be to use heat tents deployed around a "heat stressed group" while a "control group" would be grown in the same field in the same year. While a number of experimental methods are available for this objective (Kim, Slafer, & Savin, 2021), they are mostly unpractical for an experiment such as ours since we had 208 RILs and five check lines to test in a replicated trial which would require too much space for a heat tent trial and the labor needed to achieve this design would be immense. Irrigation can be used to mitigate drought stress and does not require much more labor, but we did not have access to irrigated fields. Future work will utilize genetic markers to identify genomic regions associated with these heat tollerance phenotypes.

Plants that had the HV9W03-1596R allele for the Kukric44369_131 marker had an estimated increase in test weight by 0.584 g L^{-1}, an increase in yield of 21.6 kg ha^{-1}, an increase in height by 0.13 cm, and an increase in flowering time by 0.0669 days. Plants that had the TX04M410164 allele for the Kukric44369_131 marker had an estimated increase in kernel grain fill period by 0.0975 days. Plants that had the HV9W03-1596R allele for the BS_060270_51 marker had an estimated increase in kernel diameter of 0.00353 mm, an increase in test weight of 1.56 g L^{-1}, and an increase in height of 0.158 cm. Plants that had the TX04M410164 allele for the BS_060270_51 marker had an estimated increase in kernel weight of 0.0647 mg, an increase in yield of 22.0 kg ha^{-1}, and an increase in the grain fill period of 0.0605 days. Plants that had the HV9W03-1596R allele for the wMAS00026 marker (*Ppd-D1*) had an estimated increase in kernel diameter of 0.0154 mm, an increase in kernel weight of 0.254 mg, an increase in test

weight of 1.93 g L^{-1}, and an increase in the grain fill period of 0.11 days. Plants that had the TX04M410164 allele for the wMAS00026 marker (*Ppd-D1*) had an estimated increase in yield of 57.7 kg ha^{-1}, an increase in plant height of 1.23 cm, an increase in flowering time of 0.648 days, an increase in grain fill period of 0.11 days, and an increase in physiological maturity of 0.415 days. Plants that had the HV9W03-1596R allele for the Vrn-D3-KASP marker had an estimated increase in yield of 62.4 kg ha^{-1}, an increase in height of 0.128 cm, an increase in flowering time of 0.48 days, and an increase in physiological maturity of 0.42 days. Plants that had the TX04M410164 allele for the Vrn-D3-KASP marker had an estimated increase in kernel diameter by 0.0137 mm, an increase in kernel weight of 0.415 mg, and an increase in test weight of 3.33 g L^{-1} (Table 2.14).

Plants that had the HV9W03-1596R allele for the Vrn-D3-KASP marker had an estimated increase in BLUPs of yield at 18 ASM, 19 ASM, 20 ASM, and the high yield site (38.9, 78.1, 73.3, and 47.1 kg ha-1 respectively), flowering time at 18 ASM, 19 ASM, and 20 ASM (0.52, 0.702, 0.216 days respectively), and physiological maturity at 18 ASM, 19 ASM and 20 ASM (0.421, 0.611, and 0.226 days respectively). Plants that had the TX04M410164 allele for the Vrn-D3-KASP marker had an estimated increase in BLUPs of kernel diameter at 18 ASM, 19 ASM and the high yield site (0.0145, 0.0177, 0.0139 mm respectively), kernel weight at 18 ASM, 19 ASM, 20 ASM, and the high yield site (0.403, 0.523, 0.28, and 0.425 mg respectively), and test weight at 18 ASM, 19 ASM, 20 ASM, and the high yield site (6.09, 1.69, 1.74, and 2.87 g L-1 respectively). Plants that had the HV9W03-1596R allele for the wMAS00026 marker had an estimated increase in BLUPs of kernel diameter at 18 ASM, 19 ASM, 20 ASM, and the high yield site (0.0188, 0.0174, 0.00875, and 0.016 mm respectively), kernel weight at 18 ASM, 19 ASM, and the high yield site (0.272, 0.269, and 0.286 mg

respectively), test weight at 18 ASM and the high yield site (5.93 and 1.6 g L-1 respectively) and grain fill period at 18 ASM, 19 ASM, and 20 ASM (0.119, 0.134, and 0.0770 days respectively). Plants that had the TX04M410164 allele for the wMAS00026 marker had an estimated increase in BLUPs of yield at 18 ASM, 19 ASM, 20 ASM, and the high yield site (34.0, 84.1, 64.0, and 43.2 kg ha-1 respectively), height at 18 ASM, 19 ASM, 20 ASM, and the high yield site (1.45, 1.42, 1.40, and 1.63 respectively), flowering time at 18 ASM, 19 ASM, and 20 ASM (0.629, 0.959, and 0.357 days respectively), and physiological maturity at 18 ASM, 19 ASM, and 20 ASM (0.391, 0.64, 0.214 days respectively). Plants that had the HV9W03-1596R allele for the BS_060270_51 marker had an estimated increase in BLUPs of test weight at 18 ASM by 4.57 g L-1 and plants that had the TX04M410164 allele for the BS_060270_51 marker had an estimated increase in BLUPs of yield at the high yield site by 20.5 kg ha-1. Plants that had the TX04M410164 allele for the Kukric44369_131 marker had an estimated increase in BLUPs of grain fill period at 18 ASM (0.134 days) and 19 ASM (0.170 days) and for physiological maturity at 19 ASM by 0.161 days (Table 2.16).

Yield SSI was highly associated with the vernalization and photoperiod sensitivity markers. Plants that had the HV9W03-1596R allele for the Vrn-D3-KASP marker, indicating a late release from vernalization, lost an average of 0.0207 in yield SSI and plants that had the wMAS00026 marker, indicating photoperiod sensistivity (late flowering), gained 0.0107 in yield SSI which means the plants that had the HV9W03-1596R allele for the Vrn-D3-KASP marker were less affected by the stressful environment than the rest of the population for the yield trait. RILs that had the HV9W03-1596R allele for the Vrn-D3-KASP marker had lower SSI values (0.0795) for flowering time and (a=0.0401) for physiological maturity. This means the plants that had the HV9W03-1596R allele for the Vrn-D3-KASP marker were more positively affected

by stressful environments for the traits flowering time and physiological maturity time compared to the location averages. Plants that had the HV9W03-1596R allele for the wMAS00026 marker (*Ppd-D1*) had heigher SSI values (*a*=0.0921) for flowering time and (*a*=0.0431) for physiological maturity. This means the plants that had the HV9W03-1596R allele for the wMAS00026 marker (*Ppd-D1*) were more negatively affected by stressful environments for the traits flowering time and physiological maturity time compared to the location averages. A lower SSI means the RIL was less sensitive to the stress for the trait. Plants that had the HV9W03-1596R allele for the BS_060270_51 marker had negative test weight (*a*=-0.0287) and kernel diameter (*a*=-2.22) SSIs which means the plants with this marker had much higher resistance to the shrinking of kernel diameter than the rest of the population in the stress environments. Plants that had the HV9W03-1596R allele for the Kukric44369_131 marker handled stress better than the rest of the population with kernel weight (*a*=-0.0572) and plants that had the TX04M410164 allele for the Kukric44369_131 marker had a longer grain fill period SSI than the rest of the population (*a*=-0.0625) and also had a smaller physiological maturity time SSI (*a*=-0.0196) (Table 2.17). This is expected because we know the line Kukric44369_131 was screened by Dr. Fu in the previouse study as having a long grain fill period under heat stress.

Plants that had the HV9W03-1596R allele for the Vrn-D3-KASP marker had an estimated increase in test weight SSI at 18 ASM 0.0259 and plants that had the TX04M410164 allele for the same trait had an increase in test weight SSI at 19 ASM and 20 ASM of 0.0599 and 0.0344 respectively. Plants that had the TX04M410164 allele for the Vrn-D3-KASP marker had an estimated increase in yield SSI (18 ASM *a*=0.00725, 19 ASM *a*=0.0414, and 20 ASM *a*=0.0256), flowering time SSI (18 ASM *a*=0.0404 and 19 ASM *a*=0.118), and physiological maturity SSI (18 ASM *a*=0.0126 and 19 ASM *a*=0.0674). Plants that had the HV9W03-1596R

allele for the wMAS00026 marker for *Ppd-D1* gene had an estimated increase in SSI for test weight at 20 ASM of 0.0807, yield at all locations (0.00646, 0.0489, 0.0214 for 18 ASM, 19 ASM, and 20 ASM respectively), flowering time (0.0372 and 0.146 at 18 ASM and 19 ASM respectively), and physiological maturity (0.0114 and 0.0745 at 18 ASM and 19 ASM respectively). Plants that had the TX04M410164 allele for the wMAS00026 marker had an estimated increase in SSI for kernel diameter at 18 ASM only (0.0124) and test weight at 18 ASM only (0.0319). Only plants that had the TX04M410164 allele for the BS_060270_51 marker showed an estimated increase in SSI for kernel diameter at 20 ASM (0.148) and for test weight at 18 ASM (0.0311). Plants that had the HV9W03-1596R allele for the Kukric44369_131 marker had an estimated increase in SSI for grain fill period at 18 ASM and 19 ASM (0.0152 and 0.109 respectively), and for physiological maturity at 19 ASM (0.033). Plants that had the TX04M410164 allele for the Kukric44369_131 marker had an estimated increase in SSI for kernel weight at 20 ASM (0.0832) (Table 2.18).

The best combination of alleles is to have the TX04M410164 allele for *Vrn-D3* and the HV9W03-1596R allele *Ppd-D1* because that combination resulted in the highest yield. This allele combination also resulted in the latest maturing lines and lowest test weights at every location (Table 2.20). One explanation for this is that the population as a whole was early maturing. I would hypothesise that if this population was segregating for aditional flowering time genes that made the population have a broader range in flowering time, we would see the earliest and latest maturing lines suffer lower yields and the medium early and medium maturity lines yield the highest. If we saw a broader range of maturity, maybe we would also see a greater effect from the two Chr 1B heat tolerance markers.

Conclusions

The Kukric44369_131 marker allele from HV9W03-1596R provided effective heat stress tollerance in our RIL population by means of lengthening the grain fill period by extending the physiological maturity time, and also by means of increasing grain yield while under terminal heat stress. The BS_060270_51 marker allele from HV9W03-1596R provided effective heat stress tollerance in our RIL population by way of increased grain weight under terminal heat stress.

References

Al-Khatib, K., & Paulsen, G. M. (1999). High-temperature effects on photosynthetic processes in temperate and tropical cereals. *Crop Science*, *39*(1), 119–125. https://doi.org/10.2135/cropsci1999.0011183X003900010019x

Altenbach, S. B., DuPont, F. M., Kothari, K. M., Chan, R., Johnson, E. L., & Lieu, D. (2003). Temperature, water and fertilizer influence the timing of key events during grain development in a US spring wheat. *Journal of Cereal Science*, *37*(1), 9–20. https://doi.org/10.1006/jcrs.2002.0483

Avni, R., Nave, M., Barad, O., Baruch, K., Twardziok, S. O., Gundlach, H., … Distelfeld, A. (2017). Wild emmer genome architecture and diversity elucidate wheat evolution and domestication. *Science*, *357*(6346), 93–97. https://doi.org/10.1126/science.aan0032

Balla, K., Bencze, S., Janda, T., & Veisz, O. (2009). Analysis of heat stress tolerance in winter wheat. https://doi.org/10.1556/AAgr.57.2009.4.6

Barkley, A., Tack, J., Nalley, L. L., Bergtold, J., Bowden, R., & Fritz, A. (2014). Weather, disease, and wheat breeding effects on Kansas wheat varietal yields, 1985 to 2011. *Agronomy Journal*, *106*(1), 227–235. https://doi.org/10.2134/agronj2013.0388

Barnabás, B., Jäger, K., & Fehér, A. (2008). The effect of drought and heat stress on reproductive processes in cereals. *Plant, Cell and Environment*, *31*(1), 11–38. https://doi.org/10.1111/j.1365-3040.2007.01727.x

Bennett, D., Reynolds, M., Mullan, D., Izanloo, A., Kuchel, H., Langridge, P., & Schnurbusch, T. (2012). Detection of two major grain yield QTL in bread wheat (Triticum aestivum L.) under heat, drought and high yield potential environments. *Theoretical and Applied Genetics*, *125*(7), 1473–1485. https://doi.org/10.1007/s00122-012-1927-2

Bergkamp, B., Impa, S. M., Asebedo, A. R., Fritz, A. K., & Jagadish, S. V. K. (2018). Prominent winter wheat varieties response to post-flowering heat stress under controlled chambers and field based heat tents. *Field Crops Research*, *222*(September 2017), 143–152. https://doi.org/10.1016/j.fcr.2018.03.009

Bernacchi, C. J., Portis, A. R., Nakano, H., Von Caemmerer, S., & Long, S. P. (2002). Temperature response of mesophyll conductance. Implications for the determination of Rubisco enzyme kinetics and for limitations to photosynthesis in vivo. *Plant Physiology*, *130*(4), 1992–1998. https://doi.org/10.1104/pp.008250

Bheemanahalli, R., Sunoj, V. S. J., Saripalli, G., Prasad, P. V. V., Balyan, H. S., Gupta, P. K., … Jagadish, S. V. K. (2019). Quantifying the impact of heat stress on pollen germination, seed set, and grain filling in spring wheat. *Crop Science*, *59*(2), 684–696. https://doi.org/10.2135/cropsci2018.05.0292

Blum, A., Klueva, N., & Nguyen, H. T. (2001). Wheat cellular thermotolerance is related to yield under heat stress. *Euphytica*, *117*(2), 117–123. https://doi.org/10.1023/A:1004083305905

Blum, A., Shpiler, L., Golan, G., & Mayer, J. (1989). Yield stability and canopy temperature of wheat genotypes under drought-stress. *Field Crops Research*, *22*(4), 289–296. https://doi.org/10.1016/0378-4290(89)90028-2

Borrás, L., Slafer, G. A., & Otegui, M. E. (2004). Seed dry weight response to source-sink manipulations in wheat, maize and soybean: A quantitative reappraisal. *Field Crops Research*, *86*(2–3), 131–146. https://doi.org/10.1016/j.fcr.2003.08.002

Calderini, D. F., Savin, R., Abeledo, L. G., Reynolds, M. P., & Slafer, G. A. (2001). The importance of the period immediately preceding anthesis for grain weight determination in wheat. *Euphytica*, *119*(1–2), 199–204. https://doi.org/10.1023/A:1017597923568

Chaves, M. M., Maroco, J. P., & Pereira, J. S. (2003). Understanding plant responses to drought - From genes to the whole plant. *Functional Plant Biology*, Vol. 30, pp. 239–264. https://doi.org/10.1071/FP02076

Chen, Y., Carver, B. F., Wang, S., Cao, S., & Yan, L. (2010). Genetic regulation of developmental phases in winter wheat. *Molecular Breeding*, *26*(4), 573–582. https://doi.org/10.1007/s11032-010-9392-6

Cruppe, G., DeWolf, E., Jaenisch, B. R., Andersen Onofre, K., Valent, B., Fritz, A. K., & Lollato, R. P. (2021). Experimental and producer-reported data quantify the value of foliar fungicide to winter wheat and its dependency on genotype and environment in the U.S. central Great Plains. *Field Crops Research*, *273*. https://doi.org/10.1016/J.FCR.2021.108300

Dvorak, J., & Akhunov, E. D. (2005). Tempos of gene locus deletions and duplications and their relationship to recombination rate during diploid and polyploid evolution in the Aegilops-Triticum alliance. *Genetics*, *171*(1), 323–332. https://doi.org/10.1534/genetics.105.041632

Eckardt, N. A. (2010). Evolution of domesticated bread wheat. *Plant Cell*, *22*(4), 993. https://doi.org/10.1105/tpc.110.220410

Ehleringer, J. R., & Dawson, T. E. (1992, December 1). Water uptake by plants: perspectives from stable isotope composition. *Plant, Cell & Environment*, Vol. 15, pp. 1073–1082. https://doi.org/10.1111/j.1365-3040.1992.tb01657.x

FAOSTAT. (2021). Retrieved February 16, 2021, from http://www.fao.org/faostat/en/#data/QC

Fischer, R. A. (1985). Number of kernels in wheat crops and the influence of solar radiation and temperature. *The Journal of Agricultural Science*, *105*(2), 447–461. https://doi.org/10.1017/S0021859600056495

Fischer, R. A., & Maurer, R. (1978). Drought resistance in spring wheat cultivars. I. Grain yield responses. *Australian Journal of Agricultural Research*, *29*(5), 897–912. https://doi.org/10.1071/AR9780897

Fitter, A., & Hay, R. K. M. (2002). *Environmental physiology of plants*. 367.

Food and Agriculture Organization of the United Nations. (2017). The Future of Food and Agriculture. *Food and Agriculture Organization of the United Nations*, (November), 1–52.

Fu, J., Bowden, R. L., Jagadish, S. V. K., & Gill, B. S. (2023). Genetic variation for terminal heat stress tolerance in winter wheat. *Crop Science*, *57*(5), 2626–2632. https://doi.org/10.2135/cropsci2016.12.0978

Giordano, N., Sadras, V. O., Correndo, A. A., & Lollato, R. P. (2024). Cultivar-specific phenotypic plasticity of yield and grain protein concentration in response to nitrogen in winter wheat. *Field Crops Research*, *306*, 109202. https://doi.org/10.1016/J.FCR.2023.109202

González-Schain, N., Dreni, L., Lawas, L. M. F., Galbiati, M., Colombo, L., Heuer, S., … Kater, M. M. (2016). Genome-wide transcriptome analysis during anthesis reveals new insights into the molecular basis of heat stress responses in tolerant and sensitive rice varieties. *Plant and Cell Physiology*, *57*(1), 57–68. https://doi.org/10.1093/pcp/pcv174

Grassini, P., Eskridge, K. M., & Cassman, K. G. (2013). ARTICLE Distinguishing between yield advances and yield plateaus in historical crop production trends. *Nature Communications*, *4*. https://doi.org/10.1038/ncomms3918

Graybosch, R. A., & Peterson, C. J. (2010). Genetic improvement in winter wheat yields in the Great Plains of North America, 1959-2008. *Crop Science*, *50*(5), 1882–1890. https://doi.org/10.2135/cropsci2009.11.0685

Heun, M., Schäfer-Pregl, R., Klawan, D., Castagna, R., Accerbi, M., Borghi, B., & Salamini, F. (1997). Site of einkorn wheat domestication identified by DNA fingerprinting. *Science*, *278*(5341), 1312–1314. https://doi.org/10.1126/science.278.5341.1312

Huang, S., Sirikhachornkit, A., Su, X., Faris, J., Gill, B., Haselkorn, R., & Gornicki, P. (2002). Genes encoding plastid acetyl-CoA carboxylase and 3-phosphoglycerate kinase of the Triticum/Aegilops complex and the evolutionary history of polyploid wheat. *Proceedings of the National Academy of Sciences of the United States of America*, *99*(12), 8133–8138. https://doi.org/10.1073/pnas.072223799

Jaenisch, B. R., de Oliveira Silva, A., DeWolf, E., Ruiz-Diaz, D. A., & Lollato, R. P. (2019). Plant population and fungicide economically reduced winter wheat yield gap in kansas. *Agronomy Journal*, *111*(2), 650–665. https://doi.org/10.2134/agronj2018.03.0223

Jaenisch, B. R., Munaro, L. B., Jagadish, S. V. K., & Lollato, R. P. (2022). Modulation of Wheat

Yield Components in Response to Management Intensification to Reduce Yield Gaps. *Frontiers in Plant Science*, *13*(May), 1–18. https://doi.org/10.3389/fpls.2022.772232

Kansas Mesonet, 2017: Kansas Mesonet Historical Data. (n.d.). Retrieved October 8, 2020, from https://mesonet.k-state.edu/weather/historical/#

Kim, J., Slafer, G. A., & Savin, R. (2021). Are portable polyethylene tents reliable for imposing heat treatments in field-grown wheat? *Field Crops Research*, *271*(January), 108206. https://doi.org/10.1016/j.fcr.2021.108206

Kleinsasser, A. (2019). 2019 in Review. In *Spotter Newsletter*. https://doi.org/10.1016/s1365-6937(19)30334-x

Knapp, M. (2019). Climate Office - Kansas weather highlights for 2018. Retrieved December 16, 2023, from https://climate.k-state.edu/news/stories/2019/01/weather_highlights/

Korzun, V., Röder, M. S., Ganal, M. W., Worland, A. J., & Law, C. N. (1998). Genetic analysis of the dwarfing gene (Rht8) in wheat. Part I. Molecular mapping of Rht8 on the short arm of chromosome 2D of bread wheat (Triticum aestivum L.). *Theoretical and Applied Genetics*, *96*(8), 1104–1109. https://doi.org/10.1007/s001220050845

Kumari, M., Pudake, R. N., Singh, V. P., & Joshi, A. K. (2013). Association of staygreen trait with canopy temperature depression and yield traits under terminal heat stress in wheat (Triticum aestivum L.). *Euphytica*, *190*(1), 87–97. https://doi.org/10.1007/s10681-012-0780-3

Levitt, J. (1972). Physiological Adaptations: Responses of Plants to Environmental Stresses. *Academic Press, New York*, *xiv*, 698. https://doi.org/10.1126/science.177.4051.786.a

Li, G., Boontung, R., Powers, C., Belamkar, V., Huang, T., Miao, F., … Yan, L. (2017). Genetic basis of the very short life cycle of "Apogee" wheat. *BMC Genomics*, *18*(1), 1–12. https://doi.org/10.1186/s12864-017-4239-8

Lobell, D. B., Schlenker, W., & Costa-Roberts, J. (2011). Climate trends and global crop production since 1980. *Science*, *333*(6042), 616–620. https://doi.org/10.1126/science.1204531

Lollato, R. P., Bavia, G. P., Perin, V., Knapp, M., Santos, E. A., Patrignani, A., & DeWolf, E. D. (2020). Climate-risk assessment for winter wheat using long-term weather data. *Agronomy Journal*, *112*(3), 2132–2151. https://doi.org/10.1002/agj2.20168

Lollato, R. P., Edwards, J. T., & Ochsner, T. E. (2017). Meteorological limits to winter wheat productivity in the U.S. southern Great Plains. *Field Crops Research*, *203*, 212–226. https://doi.org/10.1016/j.fcr.2016.12.014

Lopes, M. S., & Reynolds, M. P. (2012). Stay-green in spring wheat can be determined by spectral reflectance measurements (normalized difference vegetation methylation and chromatin patterning index) independently from phenology. *Journal of Experimental Botany*, *63*(10), 3789–3798. https://doi.org/10.1093/jxb/ers071

Mason, R. E., Mondal, S., Beecher, F. W., Pacheco, A., Jampala, B., Ibrahim, A. M. H., & Hays, D. B. (2010). QTL associated with heat susceptibility index in wheat (Triticum aestivum L.)

under short-term reproductive stage heat stress. *Euphytica*, *174*(3), 423–436. https://doi.org/10.1007/s10681-010-0151-x

Morgan, J. M. (2003). Osmoregulation and Water Stress in Higher Plants. *Https://Doi.Org/10.1146/Annurev.Pp.35.060184.001503*, *35*(1), 299–319. https://doi.org/10.1146/ANNUREV.PP.35.060184.001503

Munaro, L. B., Hefley, T. J., DeWolf, E., Haley, S., Fritz, A. K., Zhang, G., … Lollato, R. P. (2020). Exploring long-term variety performance trials to improve environment-specific genotype × management recommendations: A case-study for winter wheat. *Field Crops Research*, *255*(January). https://doi.org/10.1016/j.fcr.2020.107848

Nations, U. (n.d.). Population. Retrieved March 1, 2021, from un.org website: https://www.un.org/en/global-issues/population

Nawaz, A., Farooq, M., Cheema, S. A., & Wahid, A. (2013). Differential response of wheat cultivars to terminal heat stress. *International Journal of Agriculture and Biology*, *15*(6), 1354–1358.

NAWG. (2024). Wheat Production by Region. Retrieved February 4, 2024, from https://wheatworld.org/wheat-production-regions/

Özkan, H., Brandolini, A., Schäfer-Pregl, R., & Salamini, F. (2002, October 1). AFLP analysis of a collection of tetraploid wheats indicates the origin of Emmer and hard wheat domestication in Southeast Turkey [2]. *Molecular Biology and Evolution*, Vol. 19, pp. 1797–1801. https://doi.org/10.1093/oxfordjournals.molbev.a004002

Paliwal, R., Röder, M. S., Kumar, U., Srivastava, J. P., & Joshi, A. K. (2012). QTL mapping of terminal heat tolerance in hexaploid wheat (T. aestivum L.). *Theoretical and Applied Genetics*, *125*(3), 561–575. https://doi.org/10.1007/s00122-012-1853-3

Patrignani, A., Lollato, R. P., Ochsner, T. E., Godsey, C. B., & Edwards, J. T. (2014). Yield gap and production gap of rainfed winter wheat in the Southern great plains. *Agronomy Journal*, *106*(4), 1329–1339. https://doi.org/10.2134/AGRONJ14.0011

Pinto, R. S., Reynolds, M. P., Mathews, K. L., McIntyre, C. L., Olivares-Villegas, J. J., & Chapman, S. C. (2010). Heat and drought adaptive QTL in a wheat population designed to minimize confounding agronomic effects. *Theoretical and Applied Genetics*, *121*(6), 1001–1021. https://doi.org/10.1007/s00122-010-1351-4

Porter, J. R., & Gawith, M. (1999, January 1). Temperatures and the growth and development of wheat: A review. *European Journal of Agronomy*, Vol. 10, pp. 23–36. https://doi.org/10.1016/S1161-0301(98)00047-1

Prasad, P. V. V., & Djanaguiraman, M. (2014). Response of floret fertility and individual grain weight of wheat to high temperature stress: Sensitive stages and thresholds for temperature and duration. *Functional Plant Biology*, *41*(12), 1261–1269. https://doi.org/10.1071/FP14061

Ray, D. K., Mueller, N. D., West, P. C., & Foley, J. A. (2013). Yield Trends Are Insufficient to Double Global Crop Production by 2050. *PLoS ONE*, *8*(6), 66428.

https://doi.org/10.1371/journal.pone.0066428

Reddy, S. K., Liu, S., Rudd, J. C., Xue, Q., Payton, P., Finlayson, S. A., … Lu, N. (2014). Physiology and transcriptomics of water-deficit stress responses in wheat cultivars TAM 111 and TAM 112. In *Journal of Plant Physiology* (Vol. 171). https://doi.org/10.1016/j.jplph.2014.05.005

Reynolds, M. P., Quilligan, E., Aggarwal, P. K., Bansal, K. C., Cavalieri, A. J., Chapman, S. C., … Yadav, O. P. (2016, March 1). An integrated approach to maintaining cereal productivity under climate change. *Global Food Security*, Vol. 8, pp. 9–18. https://doi.org/10.1016/j.gfs.2016.02.002

Ross, T., Lott, N., & Center, N. C. D. (2003). A climatology of 1980-2003 extreme weather and climate events. In *National Climatic Data Center Technical Report No. 2003-01*. Retrieved from http://www.ncdc.noaa.gov/ol/reports/billionz.html

Sadras, V. O., Giordano, N., Correndo, A., Cossani, C. M., Ferreyra, J. M., Caviglia, O. P., … Lollato, R. P. (2022). Temperature-Driven Developmental Modulation of Yield Response to Nitrogen in Wheat and Maize. *Frontiers in Agronomy*, *4*, 903340. https://doi.org/10.3389/FAGRO.2022.903340/BIBTEX

Saini, H. S., Sedgley, M., & Aspinall, D. (1984). Developmental anatomy in wheat of male sterility induced by heat stress, water deficit or abscisic acid. *Australian Journal of Plant Physiology*, *11*(4), 243–253. https://doi.org/10.1071/PP9840243

Sciarresi, C., Patrignani, A., Soltani, A., Sinclair, T., & Lollato, R. P. (2019). Plant traits to increase winter wheat yield in semiarid and subhumid environments. *Agronomy Journal*, *111*(4), 1728–1740. https://doi.org/10.2134/agronj2018.12.0766

Shewry, P. R., & Hey, S. J. (2015). The contribution of wheat to human diet and health. *Food and Energy Security*, Vol. 4, pp. 178–202. https://doi.org/10.1002/FES3.64

Slafer, G. A., García, G. A., Serrago, R. A., & Miralles, D. J. (2022). Physiological drivers of responses of grains per m2 to environmental and genetic factors in wheat. *Field Crops Research*, *285*(March). https://doi.org/10.1016/j.fcr.2022.108593

Slafer, G. A., Savin, R., & Sadras, V. O. (2014). Coarse and fine regulation of wheat yield components in response to genotype and environment. *Field Crops Research*, *157*, 71–83. https://doi.org/10.1016/j.fcr.2013.12.004

Tack, J., Barkley, A., & Nalley, L. L. (2015). Effect of warming temperatures on US wheat yields. *Proceedings of the National Academy of Sciences of the United States of America*, *112*(22), 6931–6936. https://doi.org/10.1073/pnas.1415181112

Talukder, A. S. M. H. M., McDonald, G. K., & Gill, G. S. (2014). Effect of short-term heat stress prior to flowering and early grain set on the grain yield of wheat. *Field Crops Research*, *160*, 54–63. https://doi.org/10.1016/j.fcr.2014.01.013

Talukder, S. K., Babar, M. A., Vijayalakshmi, K., Poland, J., Prasad, P. V. V., Bowden, R., & Fritz, A. (2014). Mapping QTL for the traits associated with heat tolerance in wheat (Triticum aestivum L.). *BMC Genetics*, *15*(1), 97. https://doi.org/10.1186/s12863-014-0097-

Team}, {R Core. (2022). *R: A Language and Environment for Statistical Computing*. Retrieved from https://www.r-project.org/

U.S. National Association of Wheat Growers. (2019). Wheat Facts | National Association of Wheat Growers. Retrieved January 20, 2021, from https://www.wheatworld.org/wheat-101/wheat-facts/

UNIDO. (2018). Indicator 2.4.1: Proportion of agricultural area under productive and sustainable agriculture. Retrieved from https://unstats.un.org/sdgs/metadata/?Text=&Goal=&Target=2.4

USDA-NASS. (2023). USDA/NASS QuickStats. Retrieved February 3, 2024, from National Agricultural Statistics Service website: https://quickstats.nass.usda.gov/

USDA ERS. (2018). USDA ERS - Wheat Data. Retrieved December 11, 2023, from https://www.ers.usda.gov/data-products/wheat-data/

Verma, V., Foulkes, M. J., Worland, A. J., Sylvester-Bradley, R., Caligari, P. D. S., & Snape, J. W. (2004). Mapping quantitative trait loci for flag leaf senescence as a yield determinant in winter wheat under optimal and drought-stressed environments. *Euphytica*, *135*(3), 255–263. https://doi.org/10.1023/B:EUPH.0000013255.31618.14

Vijayalakshmi, K., Fritz, A. K., Paulsen, G. M., Bai, G., Pandravada, S., & Gill, B. S. (2010). Modeling and mapping QTL for senescence-related traits in winter wheat under high temperature. *Molecular Breeding*, *26*(2), 163–175. https://doi.org/10.1007/s11032-009-9366-8

Villareal, R. L., Bañuelos, O., Mujeeb-Kazi, A., & Rajaram, S. (1998). Agronomic performance of chromosomes 1B and T1BL.1RS near-isolines in the spring bread wheat Seri M82. *Euphytica*, *103*(2), 195–202. https://doi.org/10.1023/A:1018392002909

Wang, S., Wong, D., Forrest, K., Allen, A., Chao, S., Huang, B. E., … Akhunov, E. (2014). Characterization of polyploid wheat genomic diversity using a high-density 90 000 single nucleotide polymorphism array. *Plant Biotechnology Journal*, *12*(6), 787–796. https://doi.org/10.1111/pbi.12183

Wei, T., & Simko, V. (2021). *R package "corrplot": Visualization of a Correlation Matrix*. Retrieved from https://github.com/taiyun/corrplot

Yang, J., Sears, R. G., Gill, B. S., & Paulsen, G. M. (2002). Quantitative and molecular characterization of heat tolerance in hexaploid wheat. *Euphytica*, *126*(2), 275–282. https://doi.org/10.1023/A:1016350509689

Zhao, H., Zhang, L., Kirkham, M. B., Welch, S. M., Nielsen-Gammon, J. W., Bai, G., … Lin, X. (2022). U.S. winter wheat yield loss attributed to compound hot-dry-windy events. *Nature Communications*, *13*(1). https://doi.org/10.1038/s41467-022-34947-6

Appendix A - Supplemental Information

Appendix A Table A. 1 Response of BLUPs by location to marker alleles estimated by regression analysis across all environments and all traits. Slope is expressed as the effect of the HV9W03-1596R allele. Kukric44369, BS_060270, wMAS, and Vrn-D3 are shortened and represent Kukric44369_131, BS_060270_51, wMAS00026, Vrn-D3-KASP respectively. Linear model estimates are on top and the p-values are directly below where *, **, *** indicate significance at $P < 0.05$, 0.01, 0.001, respectively; ns, non-significant.

		Estimated slope								
Marker	Loc	Kernel diameter	Kernel hardness	Kernel weight	Test weight	Grain yield	Plant height	Flowering time	Grain fill period	Physiological maturity
Vrn-D3	18_ASM	1.45E-02	-2.56E-01	4.03E-01	6.09E+00	-3.89E+01	-1.86E-01	-5.20E-01	2.87E-02	-4.21E-01
Vrn-D3	18_ASM	**	ns	***	***	***	ns	***	ns	***
Vrn-D3	18_McP	1.05E-02	-1.09E+00	3.62E-01	1.27E+00	-6.73E+01	-1.38E-01			
Vrn-D3	18_McP	*	***	***	ns	***	ns			
Vrn-D3	18_SUM	1.32E-02	-5.76E-01	4.01E-01	3.45E+00	-5.62E+01	-2.23E-02			
Vrn-D3	18_SUM	**	**	***	**	***	ns			
Vrn-D3	19_ASM	1.77E-02	-1.05E+00	5.23E-01	1.69E+00	-7.81E+01	-1.03E-01	-7.02E-01	-2.59E-03	-6.11E-01
Vrn-D3	19_ASM	***	***	***	*	***	ns	***	ns	***
Vrn-D3	19_HUM	1.81E-02	-1.28E+00	5.22E-01	3.27E+00	-8.43E+01	-1.55E-01			
Vrn-D3	19_HUM	***	***	***	***	***	ns			
Vrn-D3	19_SUM	8.59E-03	2.23E-01	3.49E-01	3.63E+00	-5.23E+01	-1.64E-01			
Vrn-D3	19_SUM	Ns	ns	***	***	***	ns			
Vrn-D3	20_ASM	7.43E-03	-5.45E-01	2.80E-01	1.74E+00	-7.33E+01	-2.28E-01	-2.16E-01	-2.74E-02	-2.26E-01
Vrn-D3	20_ASM	Ns	*	**	*	***	ns	***	ns	***
Vrn-D3	20_HUM	2.02E-02	-1.03E+00	5.02E-01	5.45E+00	-5.57E+01				
Vrn-D3	20_HUM	***	***	***	***	*				
Vrn-D3	20_KGM	1.43E-02	-2.06E-01	3.88E-01	3.21E+00	-6.84E+01				
Vrn-D3	20_KGM	***	ns	***	***	***				
Vrn-D3	20_SUM	1.14E-02	-6.38E-01	4.02E-01	3.63E+00	-6.39E+01				

Vrn-D3	20_SUM	*	**	***	***	***				
Vrn-D3	HYD	1.39E-02	-6.37E-01	4.25E-01	2.87E+00	-4.71E+01	-2.27E-02			
Vrn-D3	HYD	***	***	***	***	***	ns			
BS_060270	18_ASM	4.67E-03	2.46E-02	1.70E-02	4.57E+00	-1.45E+01	1.15E-01	-4.49E-03	-6.53E-02	-8.89E-02
BS_060270	18_ASM	Ns	ns	ns	**	ns	ns	ns	ns	ns
BS_060270	18_McP	5.18E-03	-3.88E-02	1.91E-02	2.84E+00	-2.74E+01	1.42E-01			
BS_060270	18_McP	Ns	ns	ns	**	ns	ns			
BS_060270	18_SUM	4.41E-03	6.51E-01	-5.50E-03	3.89E+00	-2.31E+01	1.87E-01			
BS_060270	18_SUM	Ns	***	ns	**	ns	ns			
BS_060270	19_ASM	-1.27E-03	3.41E-01	-1.77E-01	-4.50E-01	-2.28E+01	2.48E-01	9.66E-02	-6.57E-02	-1.08E-02
BS_060270	19_ASM	Ns	ns	ns	ns	ns	ns	ns	ns	ns
BS_060270	19_HUM	2.39E-03	-1.77E-01	-1.14E-01	3.16E-01	-3.56E+01	1.58E-01			
BS_060270	19_HUM	Ns	ns	ns	ns	*	ns			
BS_060270	19_SUM	5.08E-03	6.37E-01	-5.42E-02	1.07E+00	-3.14E+01	1.67E-01			
BS_060270	19_SUM	Ns	**	ns	ns	*	ns			
BS_060270	20_ASM	-2.71E-03	5.42E-01	-1.80E-01	-1.33E-01	-2.33E+01	2.35E-01	5.06E-02	-5.08E-02	-2.97E-02
BS_060270	20_ASM	Ns	*	ns	ns	ns	ns	ns	ns	ns
BS_060270	20_HUM	9.00E-03	4.97E-01	3.68E-02	3.47E+00	5.66E+00				
BS_060270	20_HUM	*	*	ns	***	ns				
BS_060270	20_KGM	2.68E-03	1.26E-01	-8.20E-02	8.34E-01	-2.23E+01				
BS_060270	20_KGM	Ns	ns	ns	ns	ns				
BS_060270	20_SUM	6.07E-03	1.29E-01	-5.04E-02	1.21E+00	-2.64E+01				
BS_060270	20_SUM	Ns	ns	ns	ns	ns				
BS_060270	HYD	3.44E-03	-1.05E-01	-1.08E-01	-2.84E-03	-2.05E+01	6.95E-03			
BS_060270	HYD	Ns	ns	ns	ns	*	ns			
Kukric44369	18_ASM	-8.61E-04	-6.89E-01	1.66E-02	1.19E+00	1.63E+01	1.51E-01	1.11E-01	-1.34E-01	-7.71E-02
Kukric44369	18_ASM	Ns	**	ns	ns	ns	ns	ns	**	ns
Kukric44369	18_McP	-2.24E-03	-6.27E-01	-5.85E-02	2.13E-01	2.64E+01	1.67E-01			
Kukric44369	18_McP	Ns	**	ns	ns	ns	ns			

Kukric44369	18_SUM	-1.57E-03	-7.25E-01	-3.47E-02	3.12E-01	2.78E+01	4.85E-02			
Kukric44369	18_SUM	Ns	***	ns	ns	*	ns			
Kukric44369	19_ASM	-1.63E-03	-4.82E-01	-1.37E-02	6.47E-01	2.52E+01	1.81E-01	7.25E-02	-1.70E-01	-1.61E-01
Kukric44369	19_ASM	Ns	*	ns	ns	ns	ns	ns	**	*
Kukric44369	19_HUM	-2.99E-03	-3.20E-01	-6.49E-02	2.08E-01	3.02E+01	1.63E-01			
Kukric44369	19_HUM	Ns	ns	ns	ns	*	ns			
Kukric44369	19_SUM	-1.71E-03	-6.96E-01	-2.29E-02	2.09E-01	1.45E+01	1.20E-01			
Kukric44369	19_SUM	Ns	***	ns	ns	ns	ns			
Kukric44369	20_ASM	-7.92E-04	-4.07E-01	8.39E-03	4.25E-01	2.18E+01	1.81E-01	1.71E-02	1.11E-02	3.19E-02
Kukric44369	20_ASM	Ns	ns	ns	ns	ns	ns	ns	ns	ns
Kukric44369	20_HUM	-1.37E-03	-2.15E-01	-5.20E-03	1.17E+00	5.90E+00				
Kukric44369	20_HUM	Ns	ns	ns	ns	ns				
Kukric44369	20_KGM	-1.87E-03	-3.18E-01	-2.05E-02	5.74E-01	2.22E+01				
Kukric44369	20_KGM	Ns	ns	ns	ns	ns				
Kukric44369	20_SUM	-5.60E-04	-3.88E-01	-1.06E-02	1.02E+00	2.86E+01				
Kukric44369	20_SUM	Ns	ns	ns	ns	ns				
Kukric44369	HYD	-2.01E-03	-2.25E-01	-5.59E-02	5.03E-01	1.96E+01	2.41E-02			
Kukric44369	HYD	Ns	ns	ns	ns	ns	ns			
wMAS	18_ASM	-1.88E-02	-6.38E-01	-2.72E-01	-5.93E+00	3.40E+01	1.45E+00	6.29E-01	-1.19E-01	3.91E-01
wMAS	18_ASM	***	**	**	***	**	***	***	*	***
wMAS	18_McP	-1.25E-02	7.06E-01	-2.14E-01	1.94E-01	7.86E+01	1.37E+00			
wMAS	18_McP	**	***	*	ns	***	***			
wMAS	18_SUM	-1.46E-02	8.19E-02	-2.44E-01	-2.03E+00	5.22E+01	1.23E+00			
wMAS	18_SUM	**	ns	*	ns	***	***			
wMAS	19_ASM	-1.74E-02	6.40E-01	-2.69E-01	-8.70E-01	8.41E+01	1.42E+00	9.59E-01	-1.34E-01	6.40E-01
wMAS	19_ASM	***	**	*	ns	***	***	***	*	***
wMAS	19_HUM	-1.49E-02	6.79E-01	-2.37E-01	-1.31E+00	8.79E+01	1.37E+00			
wMAS	19_HUM	***	**	*	ns	***	***			
wMAS	19_SUM	-1.27E-02	-8.64E-01	-2.40E-01	-3.76E+00	4.16E+01	1.44E+00			

wMAS	19_SUM	**	***	*	***	**	***			
wMAS	20_ASM	-8.75E-03	3.93E-01	-1.18E-01	8.72E-01	6.40E+01	1.40E+00	3.57E-01	-7.70E-02	2.14E-01
wMAS	20_ASM	*	ns	ns	ns	***	***	***	*	***
wMAS	20_HUM	-1.85E-02	7.32E-01	-3.18E-01	-2.23E+00	3.81E+01				
wMAS	20_HUM	***	***	***	*	ns				
wMAS	20_KGM	-1.95E-02	3.08E-01	-3.22E-01	-2.46E+00	5.20E+01				
wMAS	20_KGM	***	ns	***	**	**				
wMAS	20_SUM	-1.51E-02	7.04E-01	-2.69E-01	-1.97E+00	5.98E+01				
wMAS	20_SUM	***	**	**	*	***				
wMAS	HYD	-1.60E-02	6.44E-01	-2.86E-01	-1.60E+00	4.32E+01	1.63E-01			
wMAS	HYD	***	***	**	*	***	***			

Appendix A Table A. 2 Response of stress sensitivity indices by location to marker alleles estimated by regression analysis across all environments in which stress sensitivity was > 0.02. Slope is expressed as the effect of the HV9W03-1596R allele. Linear model estimates are on top and the p-values are directly below where *, **, *** indicate significance at P < 0.05, 0.01, 0.001, respectively; ns, non-significant.

		Estimated slope								
Marker	Location	Kernel diameter	Kernel hardness	Kernel weight	Test weight	Grain yield	Plant height	Flowering time	Grain fill period	Physiological maturity
Vrn-D3	18_ASM	-6.47E-03	-2.36E-02	-1.17E-02	-2.59E-02	7.25E-03	2.04E-02	4.04E-02	-5.06E-03	1.26E-02
Vrn-D3	18_ASM	Ns	ns	*	***	*	ns	***	ns	***
Vrn-D3	19_ASM	1.56E-01	7.95E-02	-1.93E-01	5.99E-02	4.14E-02	1.43E-02	1.18E-01	-1.31E-02	6.74E-02
Vrn-D3	19_ASM	Ns	**	ns	*	***	ns	***	ns	***
Vrn-D3	20_ASM	-9.07E+00	-5.43E-02	5.94E-02	3.44E-02	2.56E-02	3.46E-02			
Vrn-D3	20_ASM	Ns	ns	ns	*	***	ns			
Vrn-D3	20_HUM	-3.38E-02	4.44E-02	-2.80E-02	-4.75E-02	1.58E-02				
Vrn-D3	20_HUM	Ns	**	ns	***	ns				
Vrn-D3	18_McP	9.73E-03	2.09E-01	2.94E-03	3.61E-02	2.46E-02	6.32E-03			

Vrn-D3	18_McP	Ns	*	ns	ns	**	ns				
Vrn-D3	18_SUM	-6.62E-04	2.46E-02	-6.90E-03	-1.15E-02	1.70E-02	1.01E-03				
Vrn-D3	18_SUM	Ns	ns	ns	ns	**	ns				
Vrn-D3	19_SUM	3.01E-02	-4.13E-02	5.69E-03	-1.82E-02	1.24E-02	3.13E-02				
Vrn-D3	19_SUM	Ns	**	ns	ns	ns	ns				
BS_060270	18_ASM	-3.93E-03	-1.16E-02	-1.00E-02	-3.11E-02	2.13E-03	-1.33E-02	7.52E-03	3.16E-03	3.91E-03	
BS_060270	18_ASM	Ns	ns	ns	***	ns	ns	ns	ns	ns	
BS_060270	19_ASM	-2.82E-01	-7.60E-02	2.02E-01	2.58E-02	6.18E-03	-4.06E-02	-1.15E-02	1.03E-02	-3.12E-03	
BS_060270	19_ASM	Ns	**	ns	ns	ns	ns	ns	ns	ns	
BS_060270	20_ASM	-1.48E+01	-8.52E-02	7.64E-02	4.13E-03	6.10E-03	-3.78E-02				
BS_060270	20_ASM	*	ns	ns	ns	ns	ns				
BS_060270	20_HUM	-5.12E-02	-4.99E-02	-4.56E-02	-5.94E-02	-1.67E-02					
BS_060270	20_HUM	*	***	**	***	ns					
BS_060270	18_McP	-8.97E-03	-3.10E-02	-2.19E-02	-7.70E-02	7.65E-03	-6.71E-03				
BS_060270	18_McP	Ns	ns	*	***	ns	ns				
BS_060270	18_SUM	-8.00E-03	4.60E-01	-1.33E-02	-5.19E-02	6.46E-03	-1.11E-02				
BS_060270	18_SUM	Ns	***	ns	***	ns	ns				
BS_060270	19_SUM	-2.01E-02	-5.36E-02	-1.51E-02	-2.07E-02	1.07E-02	-3.47E-02				
BS_060270	19_SUM	Ns	***	ns	ns	ns	ns				
Kukric44369	18_ASM	-1.58E-03	4.26E-02	-5.64E-03	-5.00E-03	-3.15E-03	-1.56E-02	-1.16E-02	1.52E-02	6.52E-03	
Kukric44369	18_ASM	Ns	*	ns	ns	ns	ns	ns	**	ns	
Kukric44369	19_ASM	2.79E-01	6.16E-02	-2.95E-01	-8.65E-03	-8.84E-03	-2.67E-02	-1.33E-02	1.09E-01	3.30E-02	
Kukric44369	19_ASM	Ns	*	ns	ns	ns	ns	ns	**	**	
Kukric44369	20_ASM	9.10E+00	-2.26E-02	-8.32E-02	2.06E-03	-5.69E-03	-2.59E-02				
Kukric44369	20_ASM	Ns	ns	*	ns	ns	ns				
Kukric44369	20_HUM	2.35E-02	1.70E-02	4.54E-03	-9.88E-03	-3.53E-03					
Kukric44369	20_HUM	Ns	ns	ns	ns	ns					
Kukric44369	18_McP	3.37E-03	1.47E-01	-1.73E-04	-6.30E-03	-8.13E-03	-7.99E-03				
Kukric44369	18_McP	Ns	ns	ns	ns	ns	ns				

Kukric44369	18_SUM	7.17E-04	-2.97E-01	-5.14E-03	2.15E-03	-9.82E-03	-2.15E-03			
Kukric44369	18_SUM	Ns	*	ns	ns	ns	ns			
Kukric44369	19_SUM	6.50E-03	3.87E-02	1.05E-04	7.16E-03	-1.51E-03	-2.08E-02			
Kukric44369	19_SUM	Ns	*	ns	ns	ns	ns			
wMAS	18_ASM	1.24E-02	1.06E-01	8.32E-03	3.19E-02	-6.46E-03	-1.58E-01	-3.72E-02	7.09E-03	-1.14E-02
wMAS	18_ASM	*	***	ns	***	*	***	***	ns	**
wMAS	19_ASM	-2.34E-01	-1.55E-02	1.32E-01	-3.89E-02	-4.89E-02	-2.12E-01	-1.46E-01	3.63E-02	-7.45E-02
wMAS	19_ASM	Ns	ns	ns	ns	***	***	***	ns	***
wMAS	20_ASM	4.47E+00	1.22E-01	-3.71E-02	-8.07E-02	-2.14E-02	-2.05E-01			
wMAS	20_ASM	Ns	ns	ns	***	***	***			
wMAS	20_HUM	-6.69E-03	-3.44E-02	6.76E-04	1.20E-02	-1.27E-03				
wMAS	20_HUM	Ns	*	ns	ns	ns				
wMAS	18_McP	-8.42E-03	-2.89E-02	-8.84E-03	-4.66E-02	-3.38E-02	-6.30E-02			
wMAS	18_McP	Ns	ns	ns	*	***	***			
wMAS	18_SUM	1.08E-02	-2.91E-01	9.37E-03	8.49E-03	-1.51E-02	-6.68E-02			
wMAS	18_SUM	ns	*	ns	ns	**	***			
wMAS	19_SUM	-3.63E-02	7.08E-02	-1.78E-02	3.87E-02	-7.61E-03	-2.76E-01			
wMAS	19_SUM	ns	***	ns	**	ns	***			